UNIVERSITÀ DEGLI STUDI DI SALERNO

UNIVERSITY OF SALERNO
Department of Pharmacy

PhD Program
in **Drug Discovery and Development**

**XXXVIII** Cycle

# PhD Thesis

# *Possible uses of cystic fibrosis drugs in protein processing in the ER*

PhD Candidate

Dott. *Adele Serra*

Supervisor

Prof. *Silvia Franceschelli*

Co-supervisor

Prof. *Maria Pascale*

PhD program coordinator: Prof. *Alessandra Tosco*

# Abstract

Proteins are essential for cellular function, and their correct folding within the ER is crucial for maintaining cell homeostasis. When protein quality control fails, misfolded proteins accumulate, trigger ER stress, and activate the Unfolded Protein Response (UPR), which can ultimately lead to cell death. This condition underlies several conformational disorders, including cystic fibrosis (CF), caused by mutations in the CFTR gene. CF therapy has been revolutionized by modulators, particularly correctors, which improve the amount and stability of misfolded CFTR at the plasma membrane. However, their precise mechanism of action in the cellular environment remains unclear, and a direct binding to CFTR has not been demonstrated. On this basis, we hypothesized that CFTR correctors may exert broader cytoprotective effects and could be repurposed for diseases characterized by impaired protein processing in the ER. We first investigated Lumacaftor (VX-809), the first clinically approved corrector, in lung adenocarcinoma and melanoma cell models in which ER stress was induced by thapsigargin, a SERCA inhibitor that disrupts ER $Ca^{2+}$ homeostasis. VX-809 significantly modulated key ER stress-related pathways, including UPR signaling, apoptosis, oxidative stress, and inflammation. Considering the high burden and limited therapeutic options of neurodegenerative diseases, we then tested VX-809 in a neuroblastoma model commonly used to study these disorders and confirmed a broad protective effect against ER stress. Since the corrector currently used in clinical practice is Elexacaftor (VX-445), we next performed a direct comparison by repeating the full *in vitro* panel in lung adenocarcinoma and neuroblastoma cells. Functional proteomic analyses in neuroblastoma cells revealed that VX-445 largely recapitulates and extends VX-809 effects, with a prominent role in the regulation of $Ca^{2+}$ homeostasis and oxidative stress.

Finally, by assessing mitochondrial apoptosis, membrane potential, oxidative stress, and calcium handling, we showed that VX-445 also modulates all these mitochondrial processes, indicating a specific mitochondrial-directed action. On the basis of the results obtained, it is well-founded to hypothesize that the correctors investigated in this thesis could also be employed for the treatment of other diseases associated with altered proteostasis in the ER.

# Index

# Chapter I
# General Introduction

## 1.1 Description of the structure and main functions of the endoplasmic reticulum (ER)

### *1.1.1 Structural organization of the ER*

It took over 50 years for the scientific community to "rediscover" the endoplasmic reticulum (ER). Although the structure of the ER was first described by Emilio Veratti in 1092, it was the studies of George Palade and Keith Porter that captured the structural complexities of this fundamental organelle organized with a thin tubular network present in the cytoplasm. Advances in microscopy techniques have, over time, revealed that the ER is composed of a single continuous membrane that forms a network containing multiple domains with different structures and functions. The ER as a whole is classically divided into three distinct domains, namely the nuclear envelope (NE), the ER sheets, and the ER tubules. The latter two structures, collectively known as the “peripheral ER,” are intertwined in a dynamic and interconvertible network, but are maintained and regulated differently from the proteins that shape the ER (Wang *et al.,* 2022).

The peripheral ER consists of an interconnected network composed of two membrane domains with distinctly different shapes: flat cisternae sheets and reticulated tubules. Specifically, an ER sheet contains a lumen positioned between two flattened, opposing double membrane layers, and the luminal distance between these layers is maintained at approximately 50 nm in animal cells. These sheets have low membrane curvature, except at the edges, where the lipid bilayer folds back on itself. The tubules, which emerge from the nuclear envelope (NE) and cisterna sheets, form a reticulated structure connecting all ER domains. These tubules are highly dynamic, continuously

forming and reorganizing. They interconnect mainly at three-way junctions, generating a loosely polygonal network that extends throughout the cytoplasm. Although they share some characteristics with cisternae, the main difference lies in the geometry of the surface: tubules have a highly curved surface, while cisternae are largely flat. As a result, tubules have a higher surface-to-volume ratio, making them more suitable for surface-dependent functions. In contrast, sheets provide a more favorable environment for luminal processes. The reticulated morphology of the ER allows its membranes to reach various cellular regions while preserving space for the traffic of other organelles (Friedman & Voeltz, 2011).

### *1.1.2 ER Morphological diversity and specialized domains.*

For a long time, the relationship between the complex structure of the ER and its various functions remained unknown, as did the contribution of ER defects to human diseases. Early electron microscope studies led to the hypothesis that the sheets and tubules of the ER might perform distinct functions. Observations revealed that the former tended to be “rough,” that is covered with ribosomes, while the latter were mostly devoid of ribosomes and therefore considered “smooth.” Then, at the ultrastructural level, this organization translates into two types of ER: smooth (SER) and rough (RER) (Chen *et al.,* 2013). Sheets represent the principal site for the translation, translocation, post-translational modification, and folding of both integral membrane and secretory proteins. It is plausible that their relatively flat membranes provide more stable platforms than tubules, thereby offering enhanced support for the large, membrane-bound polysomes required for protein synthesis. In contrast, the functions of tubules are less well understood, but they are hypothesized to be the primary sites of lipid synthesis and signaling between the ER and other organelles.

The ratio of sheets to tubules varies across cell types, reflecting the specific functional demands placed upon ER architecture. For instance, cells with high secretory capacity, such as pancreatic cells, display stacked layers of ribosome-coated sheets, whereas cells with limited protein secretion, like neurons, contain an extensive tubular network. Moreover, within the ER, there

are specialized regions known as ER exit sites (ERES), defined by their unique role in the assembly of COPII vesicles that mediate ER-to-Golgi trafficking. Morphologically, ERES appear as ribosome-free regions within the network of RERs, consisting of vesicular-tubular membrane aggregates that remain continuous with the reticulum membrane. However, current knowledge regarding their biogenesis and organization remains limited. Contact sites between the ER and other cellular organelles are essential; indeed, it interacts with mitochondria, the Golgi apparatus, endosomes, lysosomes, peroxisomes, and the plasma membrane to facilitate the transfer of lipids and intracellular signals. Interactions with the cytoskeleton also play a critical role in its dynamics and spatial distribution (Chen *et al.,* 2013).

### *1.1.3 Overview of ER functions*

The ER is a specialized organelle that exerts a pivotal role in maintaining cellular homeostasis. Its principal functions encompass protein synthesis and trafficking, proper protein folding, lipid biosynthesis, calcium ($Ca^{2+}$) storage, and the regulation of redox balance (Walter *et al.,* 2025). In the following paragraph, particular attention will be devoted on a selection of the principal functions of the ER, providing a more detailed examination of their cellular relevance.

#### *1.1.3.1 Protein synthesis and chaperone networks in the ER*

Among the multiple functions of the ER, the primary one is the synthesis of membrane and secretory proteins. A variety of specialized proteins and complexes, collectively referred to as chaperones, assist in ensuring proper protein folding and enhance the overall efficiency of this process. These include heat shock proteins (Hsp70s) and the Hsp60 chaperone family (Cao *et al.,* 2021).

Co-translational translocation across the ER membrane generally requires an N-terminal signal sequence. Once this sequence emerges from the ribosomal exit tunnel, it is recognized in the cytosol by the signal recognition particle (SRP), which transiently halts translation to maintain the nascent chain in a translocation-competent state. Translation resumes only after SRP binds

to its receptor on the ER membrane, allowing the ribosome-nascent chain complex (RNC) to dock onto the Sec61 translocon, the channel that mediates insertion into or translocation across the membrane. In secretory proteins, the signal peptide (SP) is cleaved by the signal peptidase complex (SPC), whereas uncleaved signal sequences anchor proteins within the membrane. Once the polypeptide enters the ER lumen through Sec61, its folding is assisted by resident chaperones and folding enzymes.

Two major chaperone systems are BiP and the calnexin (CNX)/calreticulin (CRT) cycle. BiP functions in association with its ERdj co-chaperones and the nucleotide exchange factors Sil1 and Grp170, the latter also acting as a chaperone in its own right. Specifically, BiP cooperates with ERdj1 and ERdj2 during ribosome recruitment and translocation, with ERdj3 and ERdj6 during protein folding, and with ERdj4 and ERdj5 in ER-associated degradation of misfolded proteins. Properly folded proteins exit the ER and are transported to the Golgi apparatus for further processing and delivery to their final destinations, whereas misfolded proteins are retrotranslocated to the cytosol for proteasomal degradation.

Additional folding factors include Grp94, which assists in folding proteins handed off by BiP; peptidyl-prolyl isomerases (PPIases), which catalyze cis-trans isomerization of X-Pro peptide bonds; and protein disulfide isomerases (PDIs), which mediate the formation, reduction, and rearrangement of disulfide bonds. Several of these factors bind $Ca^{2+}$, an ion essential for ER homeostasis and protein folding, as many resident chaperones in the ER are calcium-dependent (Ellgaard *et al.,* 2016).

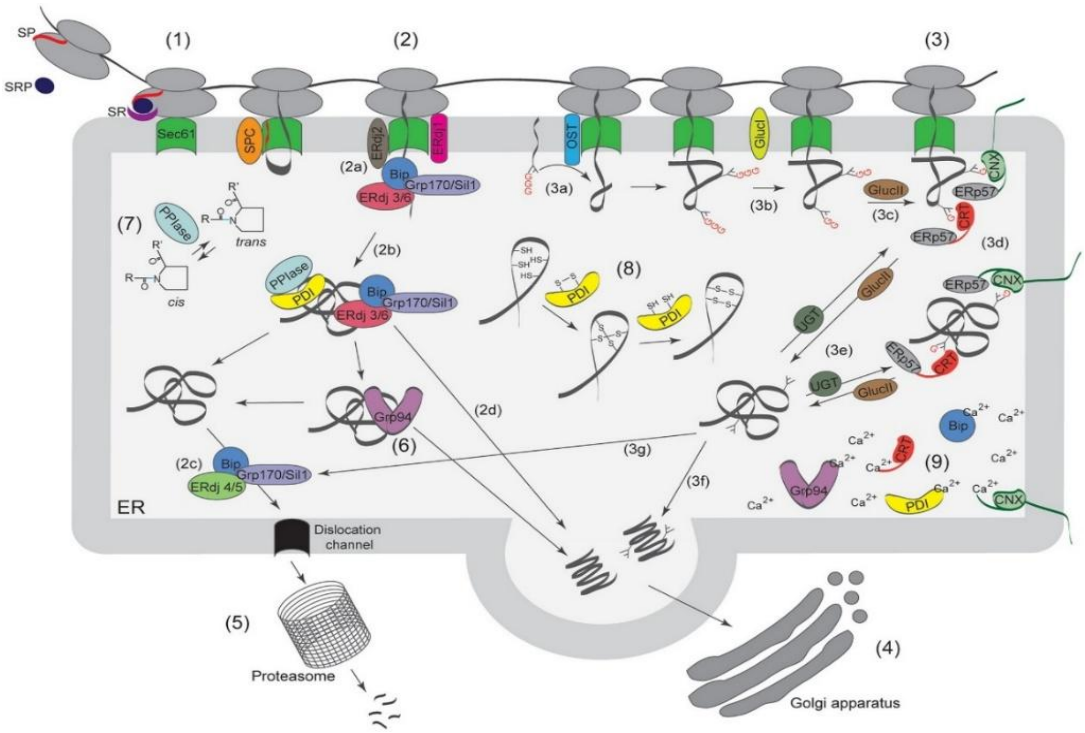


**Figure 1**: *Protein maturation and quality control in the ER, encompassing folding, chaperone activity, disulfide bond regulation, the calnexin/calreticulin cycle, ER-associated degradation, and $Ca^{2+}$-dependent processes (Ellgaard et al., 2016).*

### *1.1.3.2 ER-quality control and export of properly folded proteins*

Closely linked to its synthetic function, the ER has also become highly specialized in quality control processes aimed at preventing the accumulation of aberrant proteins. ER quality control operates at multiple levels, universally relying on the molecular recognition of defective protein states, considering features such as hydrophobic patch exposure, protein aggregation, and glycan trimming. Collectively, these pathways constitute a network that ensures efficient degradation of target substrates. Among the canonical mechanisms are ER-associated degradation (ERAD), which extracts proteins from the ER lumen or membrane for proteasomal degradation, and ER-phagosis, a specialized form of autophagy that eliminates ER portions containing aggregated proteins for lysosomal destruction. Additional specialized quality control pathways monitor the accuracy of post-translational targeting to organelles, assess folding states during the early phases of synthesis, and degrade orphan subunits of multicomponent complexes (Phillips *et al.,* 2020).

By contrast, correctly folded luminal and membrane proteins exit the ER through specialized domains known as ER exit sites (ERES). These subdomains are highly organized and dynamic structures dedicated to protein export, capable of undergoing both structural and functional remodeling in response to cellular demands. ERES are distributed throughout the ER network, and the transfer of proteins to the Golgi apparatus depends on microtubule-based transport mediated by the dynein/dynactin motor complex. As previously noted, two coat protein complexes, COPI and COPII, play complementary roles in shaping their architecture and supporting their function. COPII induces membrane curvature, regulates cargo selection, and remains associated with ERES after export, whereas COPI and Rab1 accompany the cargo upon its release from the site (Perkins *et al.,* 2021).

#### *1.1.3.3 ER as a central hub for lipid biogenesis and storage*

The ER plays a central role in lipid biosynthesis, which occurs predominantly at membrane contact sites (MCSs) with other organelles, particularly within the tubular ER network. These specialized regions enable the production of phospholipids, sterols, and neutral lipids, as well as the formation of lipid droplets that bud directly from the ER membrane. Lipid transport to other organelles and the plasma membrane is mediated through both vesicular and non-vesicular mechanisms, involving lipid transfer proteins located at these MCSs (Perkins *et al.,* 2021). The ER maintains lipid homeostasis to meet cellular demands, a function essential for other organelles that rely on it for the supply of key fatty acids.

Glycerophospholipids, sphingolipids, cholesterol, and fatty acids (FAs) are the major components of biological membranes. In particular, the ER membrane is mainly composed of glycerophospholipids, in particular phosphatidylcholine (PC), phosphatidylethanolamine (PE), phosphatidylinositol (PI), and phosphatidylserine (PS). Within the ER, the principal phospholipids, including PC, PE, PS, PI, and phosphatidylglycerol (PG), are synthesized through two major pathways: the Kennedy pathway, responsible for the de novo synthesis of PC and PE, and the cytidine diphosphate-diacylglycerol (CDP-DAG) pathway, which primarily produces

PS, PI, and PG. When lipids accumulate excessively in the ER, disrupting its homeostasis, they are detoxified through conversion into neutral lipids, such as cholesterol esters (CEs) or triacylglycerols (TGs), which are safely stored in lipid droplets (LDs). These neutral lipids thus serve as a molecular reservoir, providing material for membrane biogenesis when required or functioning as an energy source for cellular and tissue metabolism (Celik *et al.,* 2023).

*1.1.3.4 Calcium homeostasis in ER function and crosstalk*

Among the many functions attributed to the endoplasmic reticulum (ER), regulation of calcium ion ($Ca^{2+}$) storage and mobilization is fundamental. $Ca^{2+}$ acts as a versatile second messenger whose intracellular concentration affects not only ER activity but also downstream processes such as mitochondrial metabolism and apoptosis. Several ER-resident chaperones, including calnexin, calreticulin, and protein disulfide isomerases, are $Ca^{2+}$-dependent, and their folding activity relies directly on luminal levels. Tight control of $Ca^{2+}$ is crucial for cellular integrity, as its imbalance promotes the accumulation of misfolded proteins, thereby triggering ER stress and activating the unfolded protein response (UPR), a pathway designed to restore homeostasis or, if unsuccessful, induce cell death (Perkins *et al.,* 2021). The UPR pathway will be discussed in the following sections.

$Ca^{2+}$ release from the ER is mediated by membrane channels, primarily ryanodine receptors (RyRs) and inositol 1,4,5-trisphosphate receptors ($IP_3Rs$), which respond to intracellular cues. The ER also interacts functionally with other organelles, and $Ca^{2+}$ regulation is a central mechanism in this cross-talk. Mitochondria are strategically positioned near $IP_3$, allowing rapid $Ca^{2+}$ uptake. Calcium is essential for sustaining mitochondrial functions such as ATP synthesis and redox balance. This transfer is facilitated by a multiprotein complex linking ER-bound $IP_3Rs$ with the voltage-dependent anion channel 1 (VDAC1) on the outer mitochondrial membrane. Key players include Grp75, which bridges the two components, and mitofusin 2, proposed to contribute to ER–mitochondria tethering and calcium transport, though its role remains debated (Filadi *et al.,* 2018). These contact sites are critical for calcium balance.

When ER $Ca^{2+}$ stores are depleted, cells initiate compensatory uptake of extracellular $Ca^{2+}$ to restore luminal levels. This process relies on the interaction between STIM1, a $Ca^{2+}$-sensitive ER transmembrane protein, and Orai1, a plasma membrane $Ca^{2+}$ channel. Upon depletion, STIM1 relocates to membrane sites, where it binds Orai1 to form a functional complex. Activation of Orai1 drives $Ca^{2+}$ entry into the cytosol, a process known as store-operated calcium entry (SOCE) (Saint-Martin Willer *et al.,* 2024). Cytosolic $Ca^{2+}$ is then pumped back into the ER by ATP-dependent sarco/endoplasmic $Ca^{2+}$ ATPases (SERCAs), restoring luminal concentrations. These mechanisms highlight how ER interactions with mitochondria and the plasma membrane are essential for regulating both $Ca^{2+}$ release and replenishment, underscoring the central role of this ion in cellular health (Perkins *et al.,* 2021).

## 1.2 ER Stress: triggers and responses

### *1.2.1 Principal factors inducing ER Stress*

The life of living organisms is based on maintaining homeostasis. The concept of “stress” indicates a deviation from this stable state. The homeostatic condition requires that any substantial imbalance, from physical-chemical changes to molecular damage, be counterbalanced or corrected. To maintain functional fidelity, cells use stress surveillance mechanisms that detect operational disturbances and help restore balance. These mechanisms trigger resolution measures in relation to the extent of the disturbance, allowing for lasting adaptation to the ongoing low-grade load. However, such mechanisms can also function as switches: if stress exceeds mitigation capacity and damage becomes irreparable, they shift their signaling from adaptation to cellular elimination (Figure 2a).

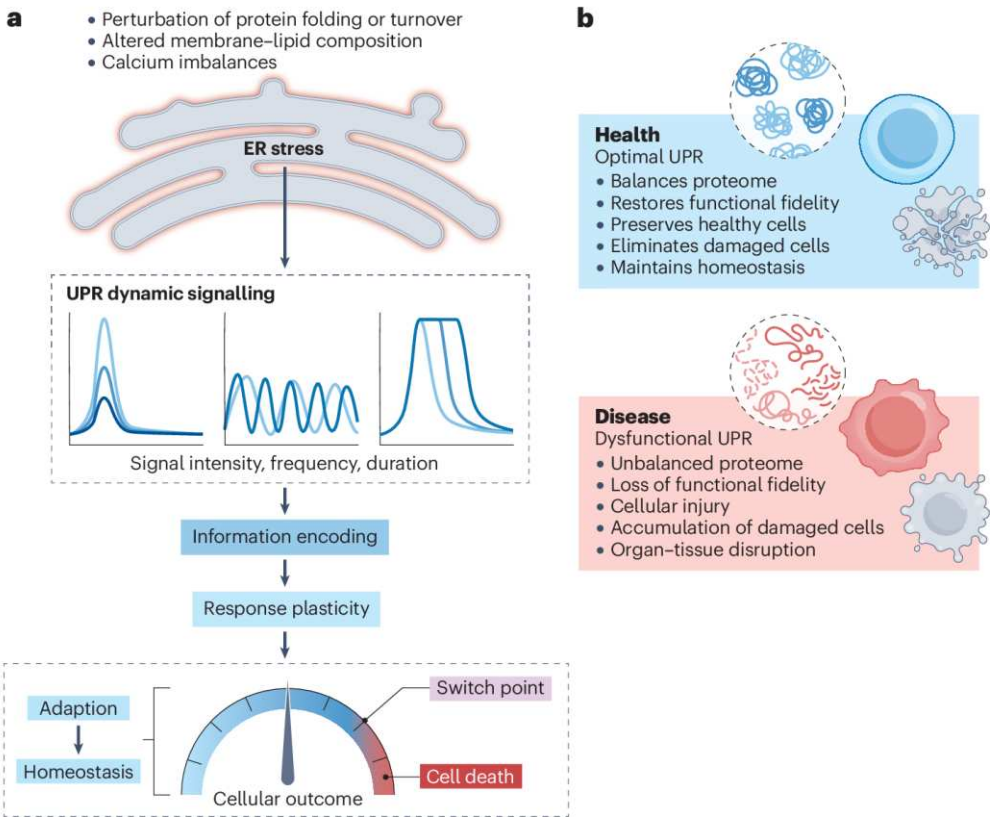


**Figure 2**: *(a) ER stress triggers the UPR which adjusts proteostasis through adaptive signalling. Depending on stress severity, the UPR promotes recovery or, if homeostasis cannot be restored, switches to apoptosis. (b) Proper UPR signalling preserves cellular function, while dysregulation contributes to disease.*

Distinct cell types have different homeostatic ranges within which stress can be resolved and outside of which cell death occurs. Aging and disease compress or reconfigure this range, leading to a loss of resilience (Acosta-Alvear *et al.,* 2025). Under physiological conditions, the ER's highly specialized quality control system strictly monitors protein biogenesis and maturation to ensure proper conformational folding. When proteins fail to fold correctly, chaperone molecules detect these anomalies, ubiquitinate them, and transfer them into the cytoplasm, where they are subsequently directed to the ERAD pathway for elimination by the 26S proteasome.

A wide range of perturbations can compromise ER homeostasis, including glycosylation inhibition, disulfide bond breakage, intracellular hypoxia, pH fluctuations, accumulation of damaged DNA, redox imbalance, autophagy defects, energy depletion, nutritional excess or deficiency, folding anomalies, elevated protein synthesis, and disturbances in $Ca^{2+}$ homeostasis. Among

these, calcium fluctuations, both overload and depletion, are particularly relevant. The ER acts as the main calcium reservoir, and its acute release initiates multiple cellular responses, including signaling pathways leading to cell death. Moreover, alterations in ER $Ca^{2+}$ levels can severely impair protein folding, due to the fact that many of the chaperones residing in the ER are calcium-dependent, thereby aggravating organelle stress (Cao *et al.,* 2021).

In response to such stimuli, cells activate a cascade of adaptive mechanisms to ensure survival under adverse conditions, reflecting the strategies of cellular adaptation to internal environmental changes and giving rise to the condition known as ER stress (Zhang *et al.,* 2024). ER stress represents the cellular response to various internal and external disturbances that compromise organelle function. It encompasses several adaptive pathways, including the ER overload response (EOR), the sterol regulatory element cascade response (SRECR), and, most prominently, the unfolded protein response (UPR) (Cao *et al.,* 2021). Among these, the UPR constitutes the most prevalent and essential pathway, activated primarily by the accumulation of misfolded proteins within the ER lumen. This compensatory system is mediated by a complex network of intracellular signaling cascades that collectively aim to restore ER homeostasis. In addition to promoting the degradation of misfolded proteins, the UPR also drives ER expansion and enhances its folding capacity, thereby ensuring organelle stability (Zhang *et al.,* 2024).

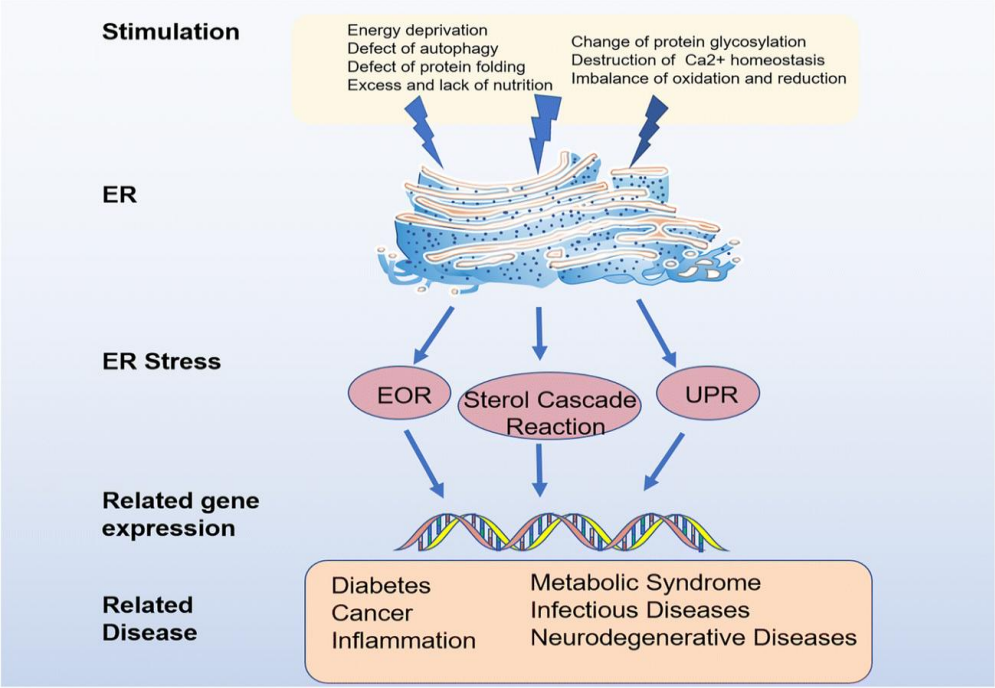


**Figure 3**: *Cellular pathways activated during ER stress. Accumulation of unfolded or misfolded proteins triggers adaptive responses such as EOR, the sterol-regulated cascade, and the UPR. Failure of these mechanisms can lead to pathological conditions including metabolic, inflammatory, infectious, and neurodegenerative diseases (Cao et al., 2021).*

### *1.2.2 Endoplasmic reticulum overload response (EOR)*

EOR is triggered by excessive accumulation of correctly folded proteins within the ER lumen, contrary to UPR. This accumulation triggers the EOR response, which induces the nuclear transcription factor NF-κB, whose downstream gene expression supports the cell's adaptive defense processes. It has been hypothesized that EOR may involve alterations in calcium storage and release, as well as the generation of reactive oxygen species (ROS) during periods of ER stress. However, the precise molecular pathways underlying this response remain unclear.

The primary goal of EOR is to restore the ER's ability to process proteins, reestablish redox balance, and maintain calcium homeostasis, thereby promoting cellular resilience under adverse conditions. However, if damage to the ER becomes irreparable, the cell initiates programmed death pathways, such as apoptosis (Cao *et al.,* 2021).

### *1.2.3 Sterol regulatory element cascade response (SRECR)*

Sterol cascade regulation occurs through the consumption of cholesterol, which is an important component of the cell membrane and is synthesized in the endoplasmic reticulum. Cholesterol consumption leads to the proteolysis of the membrane-bound transcription factor sterol regulatory element-binding protein (SREBP), and this process requires the SREBP cleavage-activating protein (SCAP), both of which are proteins present in the ER membrane. After SREBP cleavage, an active transcription factor is released that not only activates the expression of genes necessary for cholesterol absorption and biosynthesis, but also the synthesis and absorption of fatty acids. SREBPs are related to ER stress, inflammation, autophagy, and apoptosis, as well as participating in the pathogenic processes of many diseases such as obesity, non-alcoholic fatty liver disease, chronic kidney disease, and cancer (Shimano & Sato, 2017).

### *1.2.4. Unfolding Protein Response (UPR)*

#### *1.2.4.1 Sensors, chaperones and adaptive responses*

Cellular functional fidelity requires proteome homeostasis, or proteostasis, which aging and disease disrupt. Eukaryotic cells maintain proteostasis through compartmentalized but integrated stress surveillance mechanisms. These include the heat shock response in the cytosol, the DNA damage repair response (DDR) in the nucleus, other systems in the mitochondria, in the Golgi apparatus, in peroxisomes and lysosomes and the response to misfolded proteins (UPR) in the ER, so evolution has equipped the ER with its own stress surveillance system.

The UPR is a dynamic signaling network that detects disturbances in the ER in protein folding and turnover, membrane lipid composition, or calcium concentration and integrates this information to remodel the cell's transcriptome and regulate ER capacity according to demand or, if homeostasis cannot be restored, to induce apoptotic cell death. It should be emphasized that the concepts of ER stress and UPR activation are often confused, but they are distinct: the former denotes a deviation from the optimal, the latter the measures taken in response (Acosta-Alvear *et al.,* 2025).

There are two main mechanisms through which the UPR restores ER homeostasis and alleviates stress (Figure 2a): on the one hand, by upregulating ER chaperones to support protein folding, and on the other, by reducing the ER protein load through translational inhibition and degradation of improperly folded proteins. This modulation of chaperone expression enhances the clearance of misfolded (mutant or unfolded) proteins while simultaneously decreasing the synthesis of new protein molecules, thereby relieving ER burden. Studies have shown that the ubiquitin–proteasome system (UPS), E3 ubiquitin ligases, and deubiquitinases (DUBs) are closely linked to ER stress (Walter *et al.,* 2025).

The ER hosts several chaperones of particular relevance, including GRP78/BiP, calnexin, calreticulin, and oxidoreductases (protein disulfide isomerase family). These chaperones strengthen the folding capacity of the ER, helping to reduce the load of unfolded proteins. BiP is the major ER chaperone and serves as the primary sensor for UPR activation. Calnexin and calreticulin act as quality control chaperones, binding misfolded glycoproteins and enabling their refolding within the ER.

In addition to chaperones, three transmembrane proteins play a crucial role as UPR mediators: inositol-requiring enzyme 1 (IRE1), protein kinase R (PKR)-like endoplasmic reticulum kinase (PERK), and activating transcription factor 6 (ATF6) (Mori, 2024). Under normal conditions, BiP naturally associates with these proteins, keeping them inactive. Conversely, when protein folding is disrupted and misfolded proteins accumulate in the ER lumen, a stress signal is initiated. This signal promotes the dissociation of BiP from IRE1, PERK, and ATF6, thereby activating them and triggering a cascade of downstream events. BiP/GRP78 (immunoglobulin heavy chain-binding protein/glucose-regulated protein of molecular weight 78 kDa) is one of the most highly expressed ER resident chaperones and is a member of the heat-shock protein (Hsp70) family. BiP is localized to the ER through an N-terminal cleaved signal peptide and a C-terminal ER retention motif (KDEL). The C-terminal domain of BiP binds to exposed hydrophobic patches on protein folding intermediates with rather low substrate specificity. The N-terminal domain of BiP functions as a

peptide-dependent ATPase that uses ATP hydrolysis to promote a conformational change in the C-terminal region that promotes high-affinity peptide binding. Upon exchange of ATP for bound ADP, BiP reverts to the low-affinity peptide-binding state. In this way, the cell couples substrate binding and release with the expenditure of cellular energy. Stress signals induce further responses such as increased chaperone expression, activation of protein degradation pathways, reduced protein translation, and inflammation, in an attempt to mitigate ER stress. However, if the adaptive response fails, the cell ultimately undergoes apoptosis.

A

B

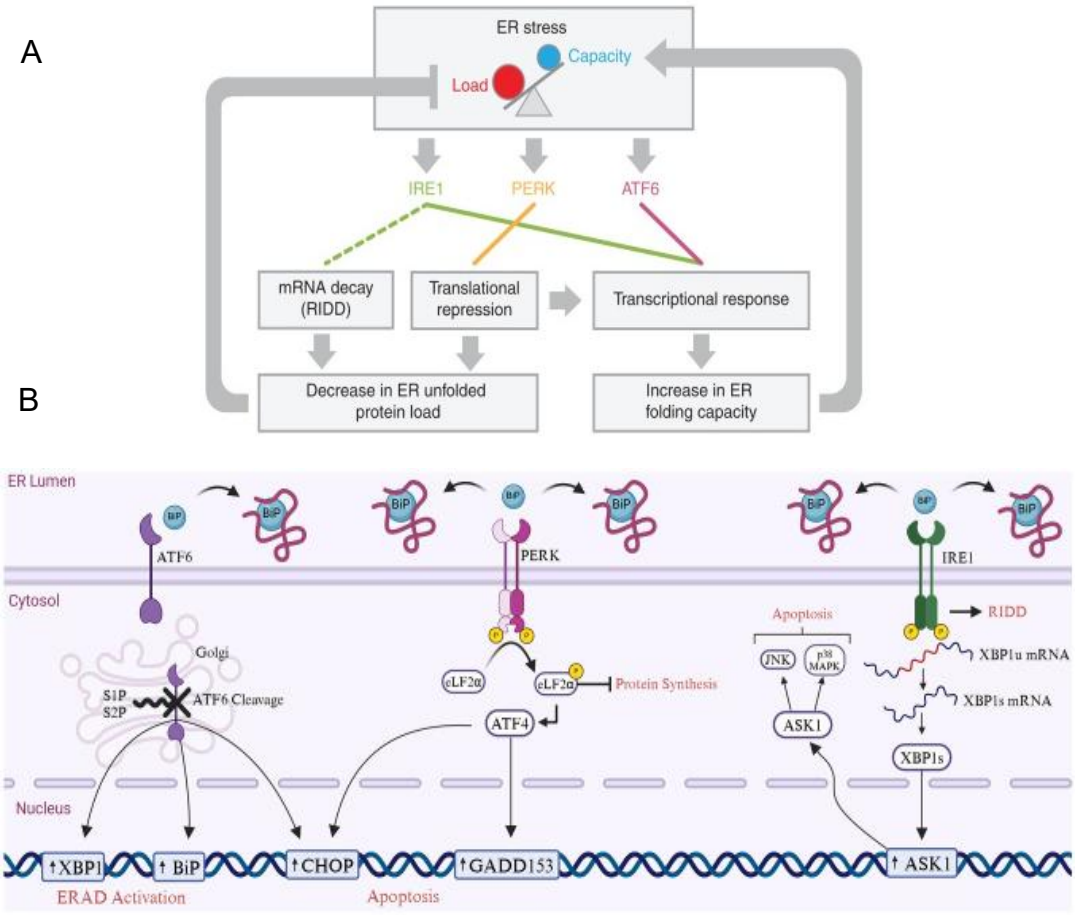


**Figure 4:** *Overview of the mammalian UPR. (A) The UPR signalling network is mediated by three main transducers, IRE1, PERK, and ATF6, each driving distinct adaptive responses to maintain ER proteostasis (Preissler & Ron, 2019),(B) Schematic representation of the UPR pathways activated during ER stress condition. The figure highlights the mechanism of the three major signaling arms. Activation of these pathways leads to adaptive responses, including ERAD, regulation of protein synthesis, and induction of apoptosis (Ghemrawi et al., 2025).*

*1.2.4.2 IRE1*

IRE1 is known to be the most conserved branch of the UPR. From yeast to humans, it has been preserved as a type I ER transmembrane protein, containing two cytoplasmic catalytic domains: (i) a serine/threonine kinase domain and (ii) a C-terminal endoribonuclease (RNase) domain. In mammals, two isoforms of IRE1 exist: IRE1α and IRE1β, with most UPR research focusing on IRE1α (Ghemrawi *et al.,* 2025). Under ER stress conditions, BiP dissociation promotes IRE1 homodimerization and autophosphorylation, thereby initiating the stress response. This process is followed by the cleavage and activation of X-box binding protein 1 (XBP1), which exerts strong control over the transcription of ER chaperones, lipid biogenesis, and ER-associated degradation (ERAD) components, facilitating both folding and degradation of misfolded proteins. In addition, XBP1 also exhibits non-specific endonuclease activity toward nucleic acids, resulting in the rapid degradation of ER-associated mRNAs. This occurs through modulation of the IRE1-dependent decay (RIDD) process, ultimately reducing protein synthesis and alleviating stress (Preissler & Ron, 2019).

The cytosolic domain of activated IRE1, under prolonged ER stress, interacts with tumor necrosis factor receptor–associated factor 2 (TRAF2). The IRE1–TRAF2 complex activates ASK1 and subsequently p38 mitogen-activated protein kinase (p38 MAPK), leading to the activation of the JNK pathway. Activation of the ASK1–JNK axis induced by ER stress triggers apoptosis. Moreover, several pro-apoptotic BCL-2 family members, including BAX and BAK, interact with IRE1 and enhance its RNase/kinase activity, thereby promoting XBP1 mRNA splicing, transcriptional activation of XBP1 target genes, JNK phosphorylation, and apoptosis. These findings suggest that IRE1, together with associated factors, may play a key role in apoptosis during severe or prolonged ER stress (Siwecka *et al.,* 2021).

*1.2.4.3 PERK*

PERK is a type I ER transmembrane protein with serine/threonine kinase activity in its C-terminal cytosolic domain, and it recognizes the accumulation

of misfolded proteins through its N-terminal luminal domain, like IRE1. Similar to the previous sensor, BiP dissociation triggers PERK activation, leading to oligomerization and autophosphorylation.

Activated PERK phosphorylates eIF2α at Ser51, resulting in global attenuation of protein translation to reduce the load of nascent proteins entering the ER. However, not all proteins are affected by this block: Indeed, this phosphorylation promotes the specific translation of ATF4 by altering the reading frame of its mRNA. ATF4 in turn activates the transcription of numerous genes involved in the functional UPR, including those associated with amino acid metabolism, redox homeostasis, and apoptosis. When survival signals fail, ATF4 induces the expression of CHOP (also known as GADD153), a potent pro-apoptotic factor under ER stress conditions. CHOP belongs to the C/EBP family of bZIP transcription factors and upregulates several pro-apoptotic mediators, including GADD34, Death receptor 5 (DR5), Tribbles-related protein 3 (Trb3), Bim, and PUMA (p53 upregulated modulator of apoptosis). GADD34 plays a key role in regulating the stress response: CHOP-mediated induction of GADD34 promotes eIF2α dephosphorylation, ultimately allowing recovery from translational attenuation. Therefore, the PERK-eIF2α-ATF4 pathway is implicated in dual biological functions, mediating both survival and apoptosis (Singh *et al.,* 2024).

*1.2.4.4 ATF6*

Among the three ER stress sensors, ATF6 shows the greatest divergence. It is a transcription factor containing a basic leucine zipper (bZIP) domain and a type II ER transmembrane protein. In mammals, two ATF6 genes are known, ATF6α and ATF6β, both ubiquitously expressed, although the former displays higher transcriptional activity. ATF6 activation in response to ER stress leads to outcomes similar to those of IRE1-XBP1 transcriptional activation; however, unlike IRE1 and PERK, ATF6 differs significantly in primary amino acid sequence, domain architecture, and mode of action. Under basal conditions, ATF6 resides in the ER bound to BiP. Upon accumulation of misfolded proteins, BiP dissociates from ATF6, enabling its interaction with these proteins. ATF6 then translocates from the ER to the Golgi apparatus, where it

is processed by Site-1 protease (S1P) and Site-2 protease (S2P) in the luminal and transmembrane domains, respectively. As a result, the N-terminal fragment of ATF6 containing the bZIP domain translocates to the nucleus and induces several UPR target genes, including ER chaperones (BiP, PDI, GRP94) and XBP1, which in turn activates ERAD components (Singh *et al.,* 2024).

### *1.2.5 Cells fate regulated by UPR response*

It is well established that, under cellular stress, two principal adaptive strategies safeguard ER function. First, protein synthesis is attenuated via PERK activation, triggering a downstream cascade that includes RIDD, which degrades mRNAs encoding ER-targeted proteins. In parallel, ER stress induces autophagy to clear damaged ER regions and misfolded protein aggregates, thereby supporting repair. Second, the synthesis of proteins essential for ERAD, phospholipid production, chaperone-assisted folding, amino acid metabolism, and redox control is upregulated (Fusakio *et al.,* 2016). When protein misfolding is sustained or excessive and UPR-driven compensation fails, cell death ensues. Chronic ER stress engages both caspase-dependent apoptosis and caspase-independent necrosis, with CHOP, activated downstream of PERK, serving as a key regulator. CHOP upregulates pro-apoptotic genes (BIM, TRB3, DR5, PUMA) while repressing BCL-2, thereby promoting apoptosis under ER stress (Fusakio *et al.,* 2016).

Oxidative stress is central to this process. Beyond modulating CHOP, PERK facilitates ROS signaling between the ER and mitochondria. Extensive evidence links ER stress, oxidative stress, and apoptosis, indicating that misfolded-protein buildup and disruption of ER redox homeostasis culminate in CHOP-dependent cell death. Chronic stress also perturbs ER calcium balance: diverse stressors deplete ER $Ca^{2+}$ and cause cytosolic $Ca^{2+}$ overload despite the strict regulation mediated by ER calcium receptor like ryanodine receptors (RyR) and inositol 1,4,5-trisphosphate receptors (InsP3R). Elevated cytosolic $Ca^{2+}$ can drive apoptosis via aberrant activation of calpain or the phosphatase calcineurin, activation of ER-resident caspases such as caspase-4, or by inducing mitochondrial dysfunction (Pecoraro *et al.,* 2021).

Alternatively, IRE1α can promote apoptosis by activating MAPK pathways that engage BCL-2 family members and/or RIDD. Given these opposing outcomes of ER stress, clarifying how UPR sensors tune their signaling outputs is essential to understand the mechanisms that govern divergent cell fates (Liu *et al.,* 2024).

## 1.3 Functional dialogue between ER and Mitochondria: physical connections and crosstalk in cell fate

Mitochondria are double-membrane organelles commonly known as the cell's powerhouses, as they are primarily responsible for producing most of the cell's ATP through oxidative phosphorylation. However, energy generation represents only a small fraction of their multifaceted roles. These highly dynamic organelles serve as central hubs that coordinate a wide range of cellular processes, including metabolism, muscle contraction, neurotransmitter release, antioxidant defense, signal transduction, autophagy, and programmed cell death (Ma *et al,* 2020). Far from being static entities, mitochondria continuously remodel their structure through fission and fusion events, allowing them to adapt to environmental cues and cellular stress. Through these mechanisms, they can support both essential survival functions and pathways leading to cell death, depending on the physiological or pathological context (Modesti *et al.,* 2021)

### *1.3.1 The ER–Mitochondria Interface: Physical Layout*

The ER is the largest membrane-bound organelle in eukaryotic cells and functions as a central communication hub, establishing contact with all major organelles, including mitochondria, the Golgi apparatus, endosomes, lysosomes, peroxisomes, and the plasma membrane. ER-Membrane contact (EMCSs) act as molecular bridges that enhance communication and coordination among membrane-associated organelles with specialized cellular functions. EMCSs are highly dynamic structures, typically spanning 10–80 nm, that form between the smooth ER and the outer mitochondrial membrane. These regions are stabilized by specific tethering proteins, allowing close interaction between the two organelles without actual membrane fusion. The

critical importance of these sites is further underscored by the fact that MCS alterations have emerged as a hallmark of a wide range of diseases, including lysosomal storage disorders, neurodegeneration, and cancer. Despite this growing recognition, the full biological significance of MCSs is only beginning to emerge in its complexity (Sassano *et al.,* 2022).

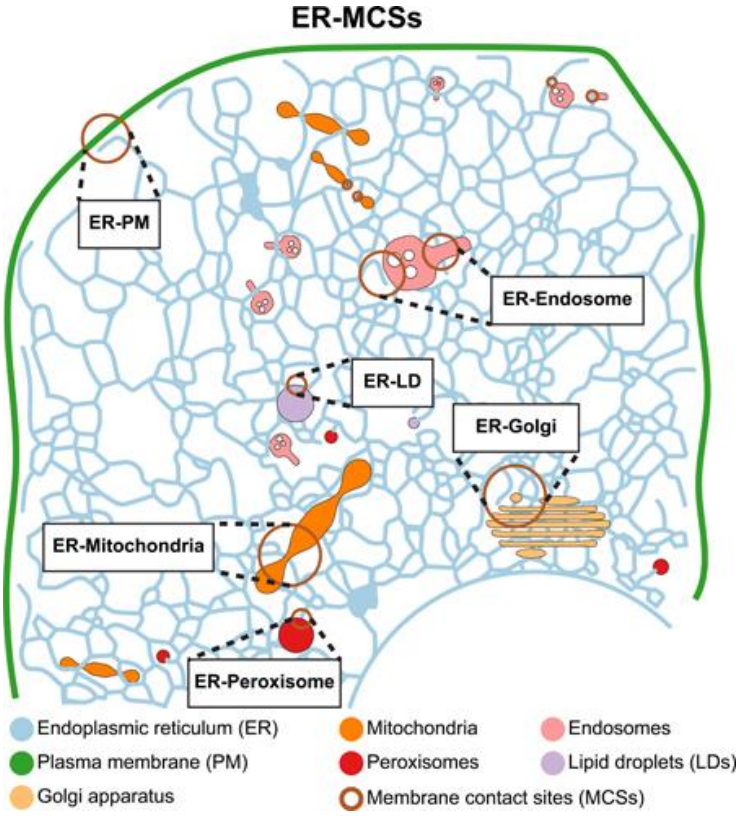


**Figure 5:** *ER membrane contacts sites (MCSs) with other organelles and the plasma membrane (PM) (Wu et al., 2018).*

A close physical association between mitochondria and the ER had been proposed as early as the 1970s. Nevertheless, mitochondria-associated membranes (MAMs) were only firmly established as a distinct biochemical entity in 1990, when Jean Vance, using cell fractionation, isolated a membrane fraction defined as a biochemical contact site between the ER and mitochondria. The physical coupling between the two organelles is sustained by distinct tethering proteins located on both the ER and the outer mitochondrial membrane (OMM) (Fernandes *et al.,* 2023). 634 proteins were identified on the ER and 137 proteins on mitochondria and 68 of these proteins overlapped with MAM when comparing them (Hung *et al.,* 2017). MAMs gained increasing attention as a critical microdomain essential for

maintaining cellular homeostasis. These sites represent a cholesterol-rich microdomain, functionally similar to lipid rafts, where numerous proteins involved in lipid metabolism, transport, and calcium regulation are concentrated. MAMs are highly dynamic structures that recruit specific proteins to regulate their organization and function according to the cell's metabolic state. These specialized domains facilitate direct communication between the ER and mitochondria, influencing a wide range of cellular processes, including $Ca^{2+}$ signalling, energy and lipid metabolism, organelle dynamics, ER stress and oxidative stress responses, inflammation, apoptosis, and autophagy.

### *1.3.2 MAMs and relationship with UPR's sensors*

Several studies suggest that MAMs are critical subcellular hubs for proteostasis (Watanabe *&* Yamanaka, 2025). During the early phase of the UPR, MAMs undergo dynamic assembly, a response generally viewed as pro-survival and linked to enhanced mitochondrial $Ca^{2+}$ uptake and improved respiratory activity. Consistent with this, key UPR sensors such as PERK and IRE1α have been localized to MAMs (Jia *et al.,* 2024). GRP78/BiP, an ER-resident chaperone, localizes to the ER lumen and is enriched at MAMs. BiP is widely regarded as a master regulator of the UPR: it promotes proper protein folding, limits aggregate accumulation within the ER, and its upregulation serves as a hallmark of ER stress that modulates UPR activation. Within MAMs, IRE1α can accumulate and, depending on context, drive either adaptive survival or apoptosis through effects on mitochondrial $Ca^{2+}$ handling. IRE1α also acts as a scaffold that governs the positioning of inositol 1,4,5-trisphosphate receptors (IP3Rs) at MAMs (Carreras-Sureda *et al.,* 2019).

PERK is likewise abundant at MAMs. It forms complexes with MAM-resident proteins such as the sigma-1 receptor (S1R) and mitofusin-2 (MFN2), supporting MAM assembly and stabilizing ER–mitochondria coupling (Mao *et al.,* 2022). Upon ER stress, BiP dissociates from PERK's luminal domain, enabling PERK activation. Activated PERK phosphorylates eIF2α and engages the nuclear factor erythroid 2-related factor 2 (NRF2) pathway, thereby helping maintain redox homeostasis and promoting cell survival during

the early phases of ER stress (Jia *et al.,* 2024). Beside to the classic UPR mechanism, PERK can facilitate signal exchanges through MAMs. In particular, PERK showed a direct role in ER-mitochondria contact sites. Indeed, through functional studies and subcellular fractionation, it was confirmed that PERK is an integral member of MAMs, a study on the genetic ablation of PERK in MEF cells caused an interruption of MAMs and led to greater protection from apoptosis caused by agents that simultaneously mobilize Ca2+ and induce ER stress through ROS.

### *1.3.3 UPRmt: a mitochondria-specific unfolded protein response*

As with ER, where the UPR counters the buildup of misfolded proteins, mitochondria mount a mitochondrial unfolded protein response (mtUPR), a transcriptional program that preserves homeostasis. mtUPR is triggered by proteotoxic stress (D'Amico *et al.,* 2017) to curb cytosolic protein synthesis and clear mislocalized mitochondrial proteins that cannot be imported. Analogous to ER stress process like the ubiquitin–proteasome system (UPS) and mitophagy support mitochondrial proteostasis via the protein quality control (PQC) network, with chaperones and proteases coordinating protein folding, assembly, and degradation. mtUPR signaling has been most deeply characterized in invertebrates, where the cascades differ substantially from those in mammals; nevertheless, the response is evolutionarily conserved, as shown by specific genetic markers in engineered mouse models and in humans. In mammals, recent work and bioinformatic analyses indicate epigenetic regulation by histone H3 lysine-27 (H3K27) demethylases and induction of multiple chaperones (CHOP, TRAP1, mtHSP70, and the HSP60–MSP10 multimer) and proteases (ClpP, YME1L1, LONP1). However, the upstream regulation mechanisms for these pathways remain incompletely defined.

Mitochondrial stress activates mtUPR both directly, through mitochondrial DNA (mtDNA) alteration-induced imbalances among mitochondrial oxidative phosphorylation system (OXPHOS) complexes, and indirectly via activating ATF4 and ATF5 (Molenaars *et al.,* 2020).

## 1.4 Mitochondrial Ca2+ Handling

$Ca^{2+}$ is a key intracellular second messenger that drives signaling across a broad range of biological processes. Its steady state is maintained by an intricate network of channels, pumps, and exchangers. Within this framework, mitochondria tune cellular $Ca^{2+}$ by coordinating both uptake and release. As a result, mitochondrial $Ca^{2+}$ ($mCa^{2+}$) has a dual impact: it supports essential physiology such as ATP production and regulation of mitochondrial metabolism, while also contributing to pathophysiological programs including cell death and the progression and metastasis of cancer. Accordingly, disturbances in $mCa^{2+}$ pathways or mutations in $Ca^{2+}$ transporters can affect cellular activities throughout the cell. Dysregulated $mCa^{2+}$ signaling is, in fact, widely linked to disease states, including cancer, neurological disorders, and cardiovascular diseases (Modesti *et al.,* 2021).

Increases in cytoplasmic calcium $(Ca^{2+})c$ are a ubiquitous signaling mechanism that governs virtually every aspect of cellular function. The mitochondrial role in shaping cytosolic Ca2+ signals has become clearer with the discovery that subsets of mitochondria lie in close proximity to $Ca^{2+}$ channels on the ER, the sarcoplasmic reticulum (SR), and the plasma membrane. This arrangement allows these organelles to act as strategic sensors and preferential responders to fluctuations in local Ca2+ flux (Cartes-Saavedra *et al.,* 2025).

In particular, MAMs, described above, are specialized microdomains that transfer Ca2+ from the ER to mitochondria. Inositol 1,4,5-trisphosphate receptor (IP3R)-mediated release of Ca2+ from the ER, elevates $(Ca^{2+})c$ at ER-mitochondria contact sites, thereby promoting mitochondrial $Ca^{2+}$ uptake. The ER sigma-1 receptor (Sigma1R) localizes to MAMs and interacts with the chaperone BiP to stabilize IP3R, prolonging inter-organelle Ca2+ signaling. $Ca^{2+}$ ions enter mitochondria through the voltage-dependent anion-selective channel (VDAC) and the mitochondrial calcium uniporter (MCU), situated on the outer mitochondrial membrane (OMM) and inner mitochondrial membrane (IMM), respectively, and then accumulate in the matrix. The 75-kDa glucose-regulated protein (GRP75) facilitates $Ca^{2+}$ transfer within MAMs by bridging

ER IP3R to mitochondrial VDAC. Consequently, MAMs tune mitochondrial Ca2+ levels and play major roles in oxidative phosphorylation, reactive oxygen species (ROS) generation, and downstream signaling. Moreover, ER-mitochondria Ca2+ transfer regulates apoptosis, as excessive matrix Ca2+ can trigger opening of the mitochondrial permeability transition pore (mPTP) and the release of pro-apoptotic factors, such as cytochrome c, into the cytosol (Fernandes *et al.,* 2023).

### 1.5 The Mitochondrion as a Hub of Oxidative Stress

Mitochondria-derived ROS generated by the electron transport chain (ETC) constitute the principal cellular source of ROS. The ETC comprises a series of complexes embedded in the mitochondrial inner membrane that receive reducing equivalents from NADH or FADH2 and transfer electrons to molecular oxygen, yielding H2O and, concomitantly, ROS (Zhao *et al.,* 2019). Complex I and Complex III are the main mitochondrial sites of ROS generation. Mitochondria both produce and detoxify ROS, making oxidative stress their chief vulnerability and fueling a vicious cycle with metabolic dysfunction, mitochondrial DNA (mtDNA) damage, altered mitochondrial dynamics, and dysregulated mitophagy. Under physiological conditions, mitochondrial ROS production is balanced by intracellular antioxidant systems; however, this equilibrium is easily disrupted by pathological factors such as radiation, hypoxia, cytokines, hyperlipidemia, and hyperglycemia, leading to ROS accumulation, heightened oxidative stress, cellular injury, and diseases including cancer, cardiovascular, neurological, and respiratory disorders.

For example, in tumorigenesis, excessive ROS promotes progression by accelerating DNA damage and reshaping the tumor microenvironment (Cheung *et al.,* 2022). Oxidative stress also perturbs the equilibrium between mitochondrial fusion and fission, typically shifting it toward fission. When ROS increase, the synthesis of fusion-related proteins is inhibited, promoting fission, which in turn can further amplify ROS production and aggravate mitochondrial dysfunction. Finally, mitochondrial DNA (mtDNA), which carries unique genetic information and resides predominantly in the matrix, can be damaged by oxidative stress directly or indirectly. Compared with nuclear DNA, mtDNA is

closer to the primary sites of ROS production and is therefore more susceptible to oxidative attack, resulting in lesions and mutations; a common oxidative lesion is 8-oxo-7,8-dihydroguanine (8-oxoG). Under oxidative stress, ROS can also interfere with mtDNA replication and repair mechanisms (Xu *et al.,* 2025).

### 1.6 Mitochondrion and its key role in the apoptotic process

Mitochondria, regulate energy production, sustain cellular activities, coordinate metabolic pathways and, paradoxically, determine cell fate. Numerous studies identify them as convergence points for multiple death-inducing pathways, activating the diverse mechanisms underlying programmed cell death, both apoptotic and non-apoptotic. It follows that dysfunction of these pathways over time leads to, or contributes to, a range of disorders, including neurodegenerative, cardiovascular, and metabolic diseases. Accordingly, therapeutic strategies centred on mitochondria-associated programmed cell death show considerable promise, opening new avenues for treatment (Nguyen *et al.,* 2023)

Apoptosis is a rapid, stimulus-driven program essential for physiological homeostasis across virtually all organs; morphologically, cellular changes culminate in the formation of apoptotic bodies that are engulfed by resident phagocytes (Chipuk *et al.,* 2021). The core signaling machinery centers on cysteine-aspartate proteases (caspases), activated by proteolytic processing triggered by pro-apoptotic cues. About 14 mammalian caspases are known, grouped as effectors (caspase-3, -6, -7), initiators (caspase-2, -8, -9, -10), and inflammatory caspases. The effector and initiator set cooperate: once initiator caspases -8/-9/-10 are engaged by upstream adaptors, effector caspases -3/-7 cleave specific substrates. In contrast, inflammatory caspases drive cytokine signaling and other programmed cell death (PCD) modes, such as pyroptosis.

Cytochrome c (Cyt c) is a heme protein synthesized as an apoprotein in the cytoplasm and then imported into mitochondria, specifically the intermembrane and intracristae spaces, where it functions as a hub of the respiratory chain (Giacomello *et al.,* 2021). Upon activation, Cyt c is released into the cytosol, where it allosterically activates and oligomerizes Apoptotic protease-activating

factor 1 (APAF1) to assemble the apoptosome, which in turn activates caspase-9 and propagates apoptotic signaling.

Another major regulatory axis is the B-cell lymphoma 2 (Bcl-2) family (~25 cytosolic proteins), partitioned into three groups: multidomain pro-apoptotic proteins (Bax, Bak), BH3-only pro-apoptotic proteins (tBid, Bad, NOXA, PUMA, Bim), and anti-apoptotic proteins (Bcl-2, Bcl-xL). Anti-apoptotic members primarily counter pro-apoptotic factors to preserve mitochondrial membrane integrity. Basally, Bak is mitochondrial and Bax is cytosolic; upon activation, Bax inserts into the outer mitochondrial membrane (OMM), partners with Bak, and BH3-only proteins engage their hydrophobic groove to activate them, driving marked OMM conformational changes.

As shown in Figure 6, apoptosis is initiated through two principal routes: the extrinsic and the intrinsic pathways. The extrinsic (death-receptor) pathway is triggered when extracellular ligands bind transmembrane death receptors (Fas, tumor necrosis factor (TNF), or TNF-related apoptosis-inducing ligand (TRAIL)), leading to recruitment of Fas-associated death domain (FADD) and activation of initiator caspase-8. Through caspase-8, this pathway intersects the intrinsic route by activating the BH3-only protein Bid, an amplifier of apoptosis. The intrinsic (mitochondrial/Bcl-2–regulated) pathway is driven by irreversible mitochondrial outer membrane permeabilization (MOMP), caused either by pore formation mediated by Bax/Bak or following mitochondrial permeability transition (MPT) upon opening of the mitochondrial permeability transition pore (mPTP) (Nguyen *et al.,* 2023).

A growing body of evidence indicates that the integrity of the outer mitochondrial membrane (OMM) is a key determinant of cell survival or death; specifically, the mitochondrial outer membrane permeabilization (MOMP), drives apoptosis in primed cells and is classified into caspase-dependent and caspase-independent forms (Amanakis & Murphy, 2020). External (growth-factor withdrawal, cytotoxic insults) and internal cues (ROS, DNA damage, hypoxia) activate BH3-only proteins that, via two distinct mechanisms, drive MOMP. In the caspase-dependent route, MOMP releases Cyt c culminating in cellular dismantling). Notably, Cyt c’s positioning within inner mitochondrial

membrane (IMM) cristae does not favor rapid release; pro-apoptotic Bcl-2 family members, especially Bim and Bak, remodel cristae and widen pores to enable bulk Cyt c efflux from the intermembrane space (IMS), ensuring robust caspase activation (Bock & Tait, 2020). A second caspase-dependent mechanism centers on $Ca^{2+}$ dysregulation: impaired control of $Ca^{2+}$ exchange via the VDAC leads to matrix $Ca^{2+}$ overload and opening of the mitochondrial permeability transition pore (mPTP). Opening is further promoted by ROS, inorganic phosphate, low pH, ATP depletion, the membrane lipid milieu, and inter-organelle communication. This aspect highlights the essential correlation between calcium homeostasis, mitochondria and apoptosis.

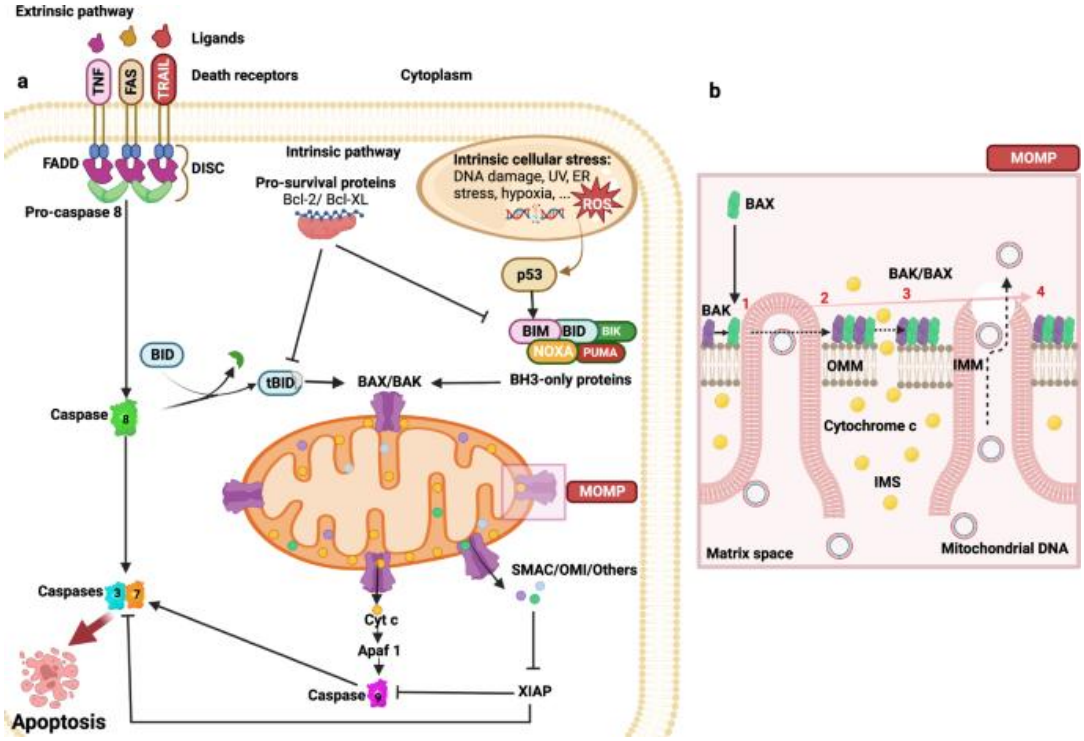


**Figure 6**: *Apoptosis: Extrinsic/Intrinsic Pathways & Mitochondria. a) Extrinsic: TNF, FAS, and TRAIL activate caspase-8. Intrinsic: cellular stresses activate BH3-only proteins, inhibit Bcl-2, and activate Bax/Bak, leading to MOMP and release of Cyt c that binds Apaf1 to form the apoptosome, activating caspase-9 and then caspase-3/-7. The caspase inhibitor XIAP is blocked by proteins such as SMAC, promoting apoptosis. Caspase-8 links the two pathways via Bid/tBid. b) Bax/Bak: at rest, Bax is cytosolic and Bak is mitochondrial. During apoptosis, BH3-only proteins activate Bax/Bak, which accumulate on the OMM, dimerize/oligomerize to form pores, releasing Cyt c and other IMS proteins. Over time, micropores permit IMM protrusion, herniation, and rupture, ultimately releasing mtDNA (Nguyen et al., 2023).*

## 1.7 From ER Stress to human disease

Studies identifying ER stress as a key factor in a wide spectrum of human diseases are steadily increasing. Among the most relevant conditions are cardiovascular diseases (CVDs), neurodegenerative disorders, metabolic and autoimmune pathologies, fibrotic diseases, viral infections, and cancer. Although these disorders may appear heterogeneous, they share a unifying feature: the presence of intra- and/or extracellular conditions that impair proper protein folding, leading to their accumulation within the ER and triggering stress responses. Given that ER stress and the consequent activation of the UPR can culminate in cell death, it is not surprising that all conditions promoting enhanced protein misfolding or a diminished ability of the ER to manage unfolded proteins may ultimately result in disease (Liu *et al.,* 2024)

Although endoplasmic reticulum stress is implicated in a wide range of diseases, this thesis will focus exclusively on those conditions that play a central role within the specific context under investigation.

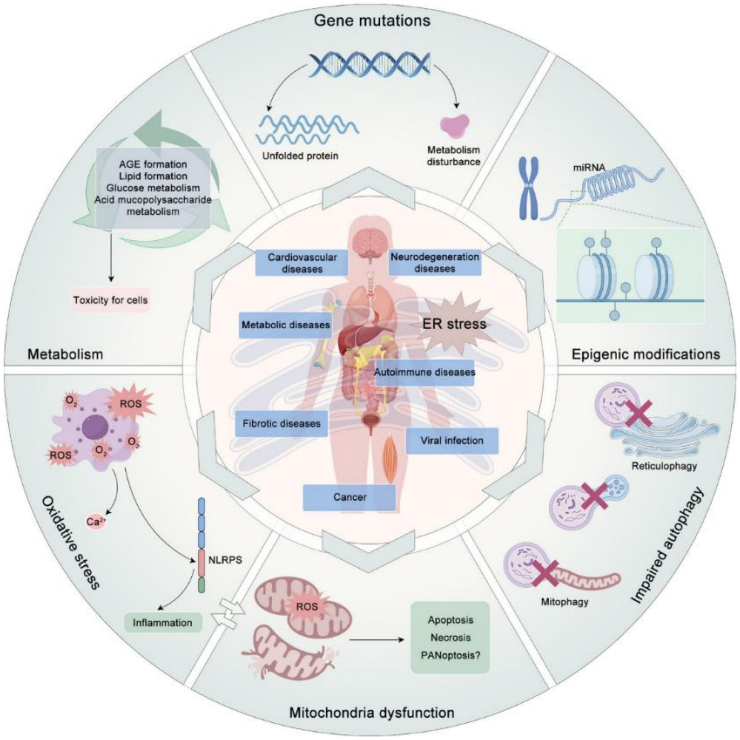


**Figure 7:** *Outline of the potential role of ER stress in disease pathogenesis. ER stress is implicated in many human diseases through mechanisms including genetic and epigenetic alterations, defective autophagy, oxidative stress, mitochondrial dysfunction and metabolic imbalance (adapted from Chen et al.,2023).*

### *1.7.1 ER-stress and neurodegenerative disease*

#### *1.7.1.1 Contribution of the UPR signaling branches to neurodegenerative Processes*

The ER plays a crucial role in the etiology of various neurodegenerative and neuroinflammatory disorders. Because the brain has a high demand for protein synthesis, it is particularly vulnerable to ER dysfunction, which can contribute to the onset of conditions such as Alzheimer's disease (AD), Parkinson's disease (PD), Huntington's disease (HD), and amyotrophic lateral sclerosis (ALS) (Hasan *et al.,* 2024). These disorders are characterized by cognitive and motor decline, and post-mortem samples from affected patients show elevated ER stress and UPR activation markers (Gami-Patel *et al.,* 2021) along with pathological protein aggregates, including amyloid-β and tau in AD, α-synuclein in PD, polyglutamine in HD, SOD1, FUS, and TDP43 in ALS, and Lewy bodies in Lewy body dementia. Mechanistic studies indicate that UPR sensors and ER stress exert context-dependent roles in neurodegeneration. For instance, IRE1 deletion in the murine nervous system accelerates age-related decline (Cabral-Miranda *et al.,* 2022), while IRE1 promotes pathology in HD and PD models (Yan *et al.,* 2019). Conversely, transgenic IRE1 expression protects against AD (Duran-Aniotz *et al.,* 2017), and XBP1 deletion protects against ALS, PD, and HD (Valdés *et al.,* 2014) although neuronal XBP1 overexpression induces seizures (Wang *et al.,* 2023). These examples highlight the context-dependent functions of XBP1 across neurodegenerative disorders, being protective in some cases but detrimental in others (Liu *et al.*, 2024). Despite significant advances, this remains a challenging area due to its complexity.

Like IRE1, PERK also shows context-dependent effects. Preclinical studies demonstrated that PERK deletion in dopaminergic neurons causes motor and cognitive impairment, as does genetic reduction of eIF2α phosphorylation (Longo et al., 2021). PERK haploinsufficiency worsens ALS, whereas GADD34 mitigates it (Wang *et al.,* 2014; Ghadge *et al.,* 2020). Moreover, CHOP deletion attenuated PD has been observed (Colla *et al.,* 2012). Although these findings suggest a neuroprotective role for the PERK-eIF2α

pathway, other studies report the opposite: Costa-Mattioli *&* Walter (2020) showed that sustained eIF2α phosphorylation and eIF2B insufficiency impair cognition. Additional studies revealed that pharmacological inhibition of PERK restores memory deficits after experimental traumatic brain injury, pointing to eIF2B/phospho-eIF2α modulation as a promising therapeutic strategy.

By contrast, the role of ATF6 in neurodegeneration has been less explored. In AD, ATF6 dysregulation has been reported: although generally considered neuroprotective, reduced ATF6 expression impairs stress responses, promotes amyloid beta (Aβ) and tau accumulation, and contributes to neurodegeneration (Ghemrawi *&* Khair, 2020). This suggests that proper ATF6 function is essential to sustain cellular health and counteract ER stress-mediated damage. In dopaminergic neurons, basal BiP levels are reduced in ATF6α KO mice, which also display increased sensitivity to PD-induced neurotoxins (Egawa *et al.,* 2011). In HD models, ATF6 activity is suppressed, contributing to disease pathogenesis (Naranjo *et al.,* 2016). These findings underscore the importance of the ATF6 pathway in maintaining proteostasis in specific neuronal subsets. Further studies are needed to assess the therapeutic potential of targeting this UPR branch in neurodegenerative diseases (Liu *et al.,* 2024).

*1.7.1.2 Role of calcium imbalance and oxidative stress in neurodegeneration*

As previously mentioned, together with altered protein folding and misfolded protein accumulation, factors such as altered redox balance and calcium homeostasis are among the main triggers of ER stress. Redox homeostasis plays a critical role in both normal cellular function and in disorders of the human central nervous system, highlighting the close link between ER stress and neurodegeneration. Excessive ROS production contributes to oxidative stress, a key feature of aging and many degenerative diseases, including neurodegenerative disorders. Oxidative stress has been strongly associated with Aβ proteinopathy in Alzheimer's disease (AD) and α-synuclein proteinopathy in Parkinson's disease (PD) (Goldsteins *et al.,* 2022).

Disruption of calcium (Ca2+) homeostasis in neurons is a hallmark of neurodegenerative diseases (Shiga *et al.,* 2024). Calcium plays a crucial role in numerous intracellular processes, acting as a second messenger; therefore, its concentration is kept extremely low by actively transporting cytoplasmic calcium out of the cell or storing it within the ER or mitochondria.

In AD, $Ca^{2+}$ dyshomeostasis with increased cytoplasmic levels leads to ER stress and neuronal death, further worsening the disease. Several mechanisms have been described: extracellular Aβ oligomers induce $Ca^{2+}$ influx through NMDARs and voltage-gated calcium channels (VGCCs) on the plasma membrane, thereby raising cytoplasmic $Ca^{2+}$ levels and altering ER $Ca^{2+}$ homeostasis. Consistently, treatment of mature hippocampal neurons with Aβ oligomers resulted in cytosolic $Ca^{2+}$ imbalance, ER dysfunction, and ER stress–mediated apoptosis (Costa *et al.,* 2012). Moreover, Aβ oligomers and presenilin mutations trigger $Ca^{2+}$ dyshomeostasis by promoting ER $Ca^{2+}$ release through ryanodine receptors (RyRs) and inositol 1,4,5-trisphosphate receptors ($IP_3Rs$).

Similarly, in PD, α-synuclein oligomers at the plasma membrane form $Ca^{2+}$-permeable pores, allowing calcium entry that drives pathological changes and cell death. In addition, PD-associated genes such as BST1, ITPKB, and PLA2G6 have been implicated in the regulation of ER $Ca^{2+}$ levels. Mutant proteins causing ALS, HD, and prion diseases also increase $Ca^{2+}$ influx and disrupt ER $Ca^{2+}$ balance, ultimately leading to excitotoxicity and ER stress in affected neurons (Kim *et al.,* 2022).

### *1.7.2 ER-stress and cancer: a brief overview*

The development of cancer is driven by a range of elements within the tumor microenvironment (TME), such as hypoxia, pH instability, ROS, and various metabolic by-products. In this framework, the ER coordinates adaptive mechanisms in response to these stimuli, supporting persistent tumor expansion.

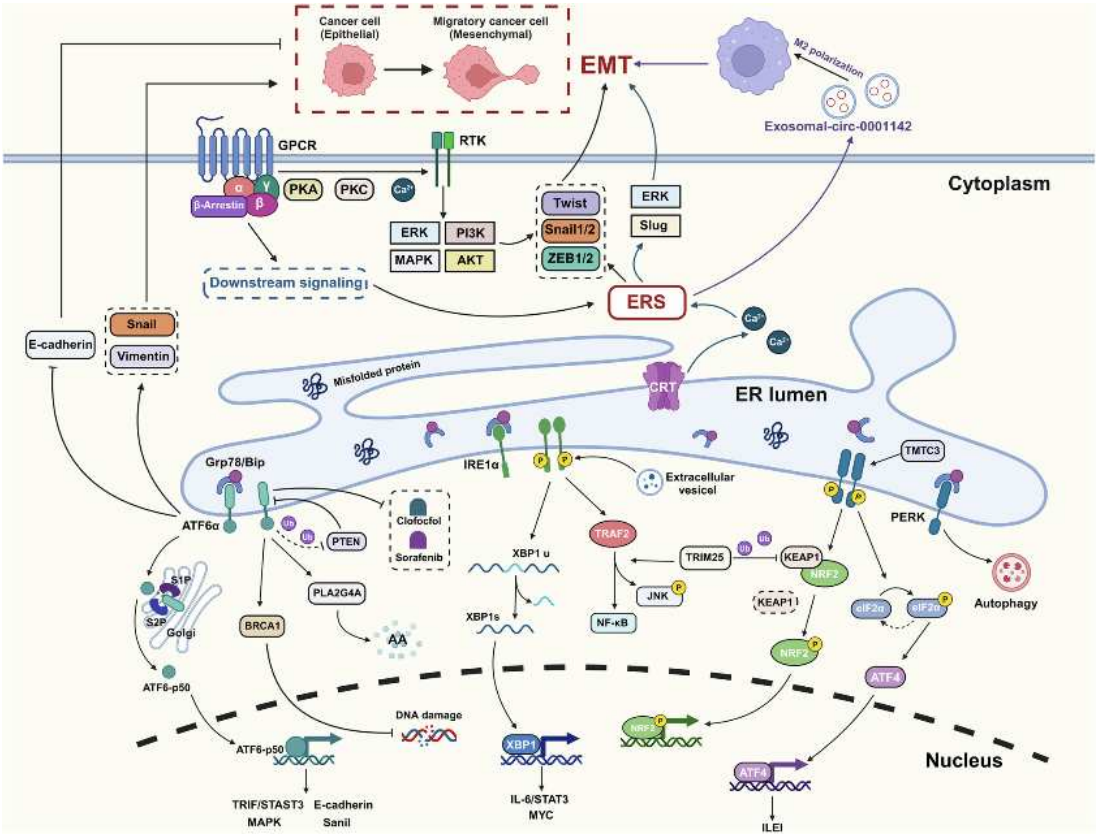


**Figure 8:** *The role of ERS in tumor progression. ER stress contributes to tumor growth by regulating cell proliferation through multiple pathways, including IRE1/XBP1/IL-6/STAT3, IRE1/TRAF2/NF-κB, PERK/NRF2, PERK/eIF2α/ATF4, and ATF6/STAT3. It also promotes metastasis, mainly by driving epithelial-mesenchymal transition (EMT) in tumor cells and by influencing the polarization of tumor-associated macrophages (Zhang et al., 2024).*

Recent evidence highlights the pivotal role of ER-stress in cancer biology, influencing tumor development and progression. The uncontrolled growth of cancer cells is supported, in part, by ER Stress which facilitates their proliferation (Hanahan D, 2022). For instance, in melanoma, UPR activation promotes tumor growth through the IL-6/STAT3 pathway (Chen & Zhang, 2017). Similarly, the IRE1-XBP1 axis amplifies MYC-driven oncogenesis in breast and urothelial cancers (Zhao *et al.,* 2018), while tumor-derived extracellular vesicles activate IRE1α, inducing malignant transformation in bladder cancer (Wu *et al.,* 2019). The oncogenic potential of IRE1α is linked to its phosphatase domain, which, in response to stress, recruits TRAF2, thereby triggering JNK and NF-κB activation.

In contrast, the PERK arm of the UPR exhibits tumor-suppressive activity, particularly in breast cancer, where it limits cell proliferation, although the underlying mechanisms remain unclear. Elevated ATF6α expression has been associated with prostate cancer progression via modulation of arachidonic acid metabolism through the ATF6α-PLA2G4A axis (Zhao *et al.,* 2022) and with enhanced BRCA-1 expression, supporting DNA damage evasion in colon cancer (Benedetti *et al.,* 2022). Moreover, ATF6 promotes cervical cancer cell proliferation through MAPK signaling (Liu *et al.,* 2020).

## 1.8 ER-stress and cystic fibrosis

### *1.8.1 General background on cystic fibrosis*

Cystic fibrosis (CF) is among the most prevalent and life-threatening inherited autosomal recessive disorders, affecting around 40,000 individuals in the United States and an estimated 105,000 across 94 countries, with the highest incidence observed in Caucasian populations (Wang *et al.,* 2025). The identification of the gene encoding the cystic fibrosis transmembrane conductance regulator (CFTR) in 1989 marked a turning point in clarifying the link between CF and its associated protein product. Although CF is a systemic disorder affecting multiple organs, including the lungs, pancreas, sweat glands, and gastrointestinal tract, pulmonary complications remain the leading cause of morbidity and mortality. Impaired CFTR function causes dehydration of the airway surface liquid, making the respiratory tract highly vulnerable to persistent infections and contributing to a broad spectrum of lung manifestations (Saint-Criq *&* Gray, 2017).

### *1.8.2 CFTR protein: function and structure and its folding process*

The CFTR protein is expressed in the apical membranes of polarized epithelial cells in the sweat ducts, pancreatic duct, intestines, biliary tree, and vas deferens, and a few non-epithelial containing tissues such as erythrocytes, cardiac myocytes, immune cells such as macrophages, and smooth muscle (Anwar *et all.,* 2024). CFTR operates primarily as an anion channel important in maintaining proper functions of the lung, pancreas, and intestine (Zhang et all., 2018). CFTR primarily mediates the transport of chloride and bicarbonate

anions, but it also contributes to the movement of other ions and modulates the activity of various ion transporters, most remarkably via the epithelial sodium channel (ENaC) present in the respiratory tracts and others, including calcium-activated chloride channels (CaCC), outward rectifying chloride channels (ORCC), the renal outer medullar K+ (ROMK) channels, and the sodium/proton exchanger NHE3, and an aquaporin channel (Anwar *et all.,* 2024 ). Belonging to the ATP-binding cassette (ABC) transporter family, as shown by Figure 10, CFTR comprises two membrane-spanning domains (TMDs, also referred to as MSDs), each containing six transmembrane helices (TM1–TM6 in TMD1/MSD1; TM7–TM12 in TMD2/MSD2), along with two intracellular loops (ICL1 and ICL2 for TMD1, ICL3 and ICL4 for TMD2). The cytoplasmic region features two nucleotide-binding domains (NBDs) and a regulatory (R) domain that harbors consensus sites for phosphorylation by protein kinase A (PKA) and protein kinase C (PKC) (Figure 9).

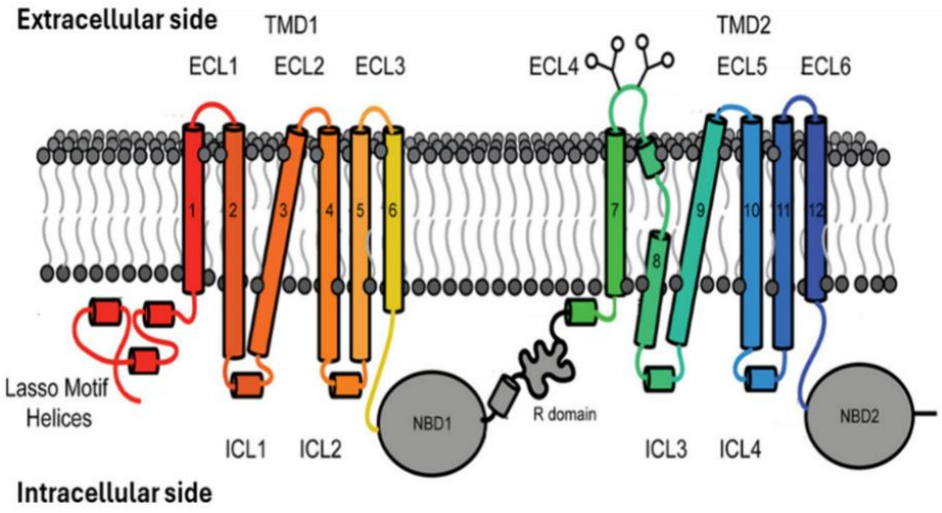


**Figure 9:** *Human CFTR's overall structure. elements constituting the CFTR protein are: the two membrane-spanning domains (MSD) or transmembrane domains (TMD), two cytosolic nucleotide-binding domains (NBDs) or nucleotide-binding folds (NBFs), and one regulatory domain (R), which contains consensual phosphorylation sites of PKA and PKC (Wang et all., 2025).*

CFTR functions uniquely among ABC transporters as a passive anion channel. Unique unstructured regions such as the regulatory insertion region and regulatory domain are found in no other ABC transporters and likely give

CFTR its passive anion channel properties (Hwang *et all.,* 2018). CFTR activity is tightly regulated through cAMP-mediated PKA-dependent phosphorylation of the R domain and ATP binding at the NBDs, allowing it to function primarily as an anion-conducting channel. Structural data from the ATP-bound human CFTR (Zhang *et all.,* 2018) indicate that phosphorylation by PKA repositions the R domain away from the NBD interface, facilitating the conformational shifts required for channel opening (Wang *et al.,* 2025)

Due to its complex topology, CFTR undergoes an elaborate folding process that is tightly controlled by proteostasis regulators located both at the membrane and within the cytosol. The protein is synthesized and inserted into the ER membrane, where it folds through coordinated co- and post-translational events. This process is monitored at several stages by heat shock proteins, co-chaperones, and lectin-interacting chaperones. The ubiquitin E3 ligase system also plays a pivotal role, targeting misfolded CFTR for degradation via the proteasome, autophagy-related pathways, or lysosomal recycling associated with the plasma membrane (PM). Once CFTR achieves its native conformation and undergoes initial glycosylation within the ER, it is transported through the Golgi apparatus for further glycosylation, ultimately reaching the PM (Figure 10) (McDonald *et all.,* 2023).

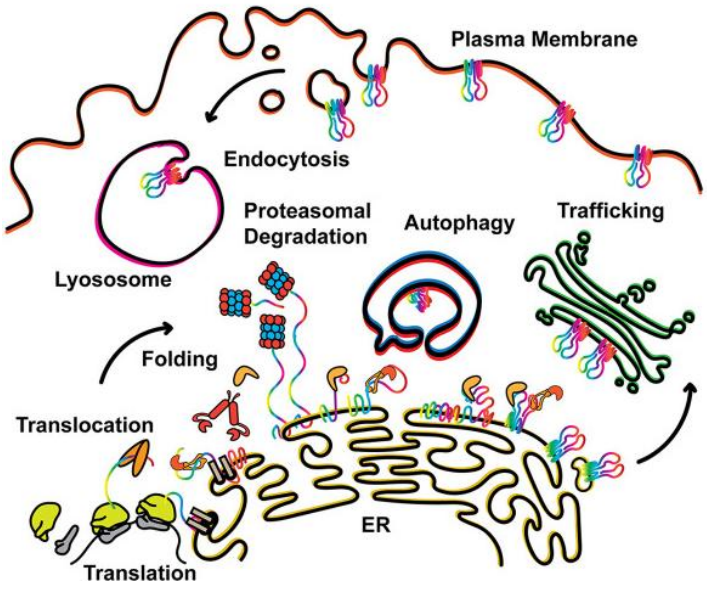


**Figure 10:** *CFTR proteostasis begins with translation of the CFTR polypeptide and its translocation into the ER membrane. Molecular chaperones and cochaperones assist folding or direct misfolded CFTR to proteasomal degradation or autophagy.*

*Properly folded CFTR is trafficked through the Golgi to the plasma membrane, where it undergoes peripheral quality control (PQC), endocytosis, and eventual lysosomal degradation (McDonald et al., 2023).*

### *1.8.3 Classification of the major mutations causing CF*

It is now well established that mutations in the CFTR gene are the underlying cause of CF. Among them, the most common variant, known as F508del or Phe508del, is thought to have originated in a population known as the *Bell Beaker people* about 5,000 years ago (Farrell *et al.,* 2018). This mutation results in the loss of a phenylalanine at position 508 in the 1480 amino acid CFTR sequence, leading to defective folding and impairing protein synthesis, maturation, and function.

More than a thousand CFTR mutations have been identified, though not all are pathogenic. Approximately one thousand are considered disease-causing because they disrupt CFTR production, function, or both. These mutations have been systematically divided into seven classes:

- Class I: nonsense mutations introducing premature stop codons, which completely abolish CFTR synthesis; found in about 10% of patients.
- Class II: the most prevalent group, including the F508del variant. Nearly 90% of CF patients carry at least one F508del allele, and about half are homozygous. These mutations destabilize the protein, causing it to be misfolded and prematurely degraded by the proteostasis network. As a result, only small amounts of mature, functional CFTR reach the plasma membrane, leading to defective ion transport across epithelial tissues.
- Classes III and IV: associated with functional impairments. The protein reaches the cell surface but fails to respond adequately to cAMP-dependent activation (Class III, e.g., G551D and S1251N) or shows reduced conductance (Class IV).

- Classes V, VI, and VII: rare variants that reduce the total number of CFTR proteins at the cell surface. This decrease may result from RNA splicing defects, reduced membrane stability, or complete absence of mRNA (Wang *et al.,* 2025).

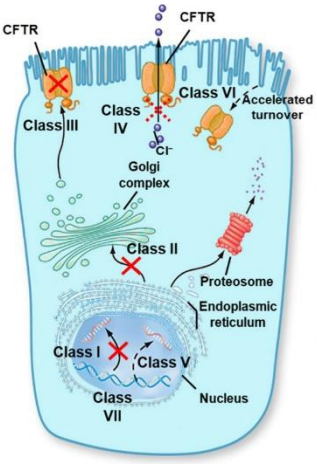


| | Class I | Class II | Class III | Class IV | Class V | Class VI | Class VII |
|---|---|---|---|---|---|---|---|
| **CFTR Defect** | No Functional CFTR Protein | CFTR Trafficking Defect | Impaired CFTR Gating | Decreased CFTR Channel Conductance | Reduced Synthesis of CFTR Protein | Decreased CFTR Stability | No CFTR mRNA |
| **Types of CFTR Mutations** | Nonsense; Frameshift; Canonical Splice | Missense | Missense | Missense | Splice Site Mutation; Missense | Missense | Splice Site Mutation |
| **Known CFTR Mutations** | W1282X G542X R553X | F508del N1303K R560T | G551D G551S G1349D | R117H R334W R117C | A455E 3272-26A→G 3849+10kbC→T | Q1412X rF508del 4326delTC | 1717-1G→A Dele2,3(21kb) |
| **Required Therapy** | Rescue Synthesis of CFTR | Rescue Trafficking of CFTR | Restore CFTR Channel Activity | Restore CFTR Channel Activity | Correct Splicing | Promote CFTR Stability | Not possible to Rescue |

**Figure 11:** *Schematic representation and classification of CFTR protein mutation classes (Wang et all., 2025).*

### *1.8.4 Pharmacological strategies in CF therapy*

CF presents with varying degrees of severity, ranging from mild to severe, depending on the specific mutation involved. Over time, a number of diagnostic tools have been developed to assess both the presence and the extent of the disease, with the sweat chloride test being the earliest and most established method (Green *et al.,* 2024). Although CF was initially considered an untreatable condition, significant progress has since been achieved in both its therapeutic management and clinical outcomes.

Traditional treatment for cystic fibrosis relied on a set of supportive therapeutic strategies designed to alleviate symptoms, prevent or lessen complications, and improve overall disease management. The pharmacological regimen typically included a range of antibiotics and anti-inflammatory drugs, mucolytics, bronchodilators, corticosteroids for nasal polyps, as well as pancreatic and digestive enzymes, alongside vitamin and mineral supplementation. The treatment plan was closely tailored and regularly

adjusted through routine clinical evaluations, given the need for continuous monitoring to effectively control symptoms and minimize the progression of complications. Beyond medications and supplements, patients were also required to perform daily airway clearance procedures, which significantly affected their quality of life.Significant progress has been made over the years in elucidating the function of the CFTR gene and identifying therapeutic strategies to address the molecular defects caused by its most frequent mutations. These advances have led to the development of innovative treatments involving small-molecule CFTR modulators, which act at multiple points along the pathogenic cascade responsible for CF, aiming to restore proper channel activity. Based on the nature of the defect they are designed to repair, modulators fall into distinct categories.

Potentiators, for example, are compounds that enhance the gating function or ion conductance of defective CFTR channels by increasing their open probability at the cell surface; correctors, on the other hand, assist in the proper folding and intracellular trafficking of misfolded CFTR proteins, promoting their delivery to the plasma membrane. The class of CFTR modulators also includes a group of compounds known as amplifiers, which function by increasing the amount of immature CFTR protein within the cell. More recently, a new category of CFTR modulators has emerged, aimed at stabilizing the nucleotide-binding domain (NBD). These stabilizers are currently under development and are intended to be used in combination with complementary modulators to restore CFTR activity in individuals carrying the F508del mutation (Wang *et all.,* 2025). Among modulators there are also the read-through drugs that treat mutations that form in frame premature stop codons. This academic work focuses on CFTR correctors.

## 1.9 CFTR Correctors: types, mechanisms and clinical translation

### *1.9.1 Mechanistic categorization of CFTR Corrector types*

As previously noted, correctors are specifically developed to address CFTR mutations associated with protein processing defects, most notably F508del. These compounds interact with the mutant CFTR, promoting proper folding

within the ER and facilitating its subsequent maturation. This mechanism enhances CFTR trafficking to the plasma membrane, reduces its premature degradation, and increases the density of functional channels at the cell surface. By these means, correctors are particularly well suited to act synergistically with other modulators, thereby contributing to the restoration of CFTR function and the amelioration of CF-related pathological defects. The classification of correctors considers three main types based on different aspects of CFTR folding and stability (Okiyoneda *et al.,* 2013):

- **Type 1** correctors: stabilize the interface between NBD1 and MSD. By binding to hydrophobic pockets within MSD1, they support the early stages of CFTR folding, thereby reducing premature degradation and increasing the probability of successful trafficking to the plasma membrane. Lumacaftor (VX-809) and Tezacaftor (VX-661) are representative compounds of this class.
- **Type 2** correctors: act primarily on NBD2 and its interactions with MSD interfaces. They enhance CFTR domain assembly, reinforce the overall structural integrity of the protein, and facilitate its maturation and subsequent transport to the plasma membrane. Corr4a serves as a notable example of this group.
- **Type 3** correctors: are designed to directly stabilize NBD1 and promote its interactions with other CFTR domains. The small molecule Elexacaftor (VX-445) belongs to this category (Baroni D, 2025).

This thesis places particular emphasis on the study of VX-809 and VX-445.

correctors

### *1.9.2 Brief history of discovery and current therapeutic combination strategies*

The history of correctors includes, among its fundamental milestones, the identification of VRT-325, a quinazoline compound discovered through HTS. Although effective in increasing the expression of mature F508del-CFTR at the plasma membrane (Van Goor *et al.,* 2006), it lacked specificity and, at high concentrations, even inhibited protein function (Kim Chiaw *et al.,* 2010).

Despite subsequent improvements, efficacy remained limited, thereby prompting the development of Lumacaftor (VX-809), which exhibited markedly greater activity (Van Goor *et al.,* 2011). Vertex Pharmaceuticals, a biotechnology company recognized as a leader in CF research, played a pioneering role in the development of the first small-molecule CFTR modulators (Wang *et all.,* 2025). The evidence that single correctors alone are generally insufficient to fully restore CFTR expression prompted the design of combination therapies aimed at achieving synergistic functional rescue.

Then, in 2015 **Orkambi** that is Lumacaftor, VX-809, in combination with the potentiator ivacaftor (VX-770), became the first corrector approved by both the FDA and the EMA for cystic fibrosis patients aged 12 years and older carrying at least one copy of the F508del mutation.

Its success represented a pivotal milestone in CFTR modulator research, paving the way for next-generation correctors. Over time, additional HTS campaigns have been conducted to identify more potent and effective molecules. In parallel, research increasingly focused on modulators suitable for inclusion in triple-combination regimens, a strategic approach aimed at amplifying the functional rescue of CFTR. For this reason, Veit and colleagues made significant progress in this direction by screening a library of approximately 600,000 compounds, which led to the isolation and characterization of novel correctors (Veit *et al.,* 2020).

Through extensive HTS studies, structure-activity relationship (SAR) analyses, and chemical optimization aimed at improving safety, efficacy, and pharmacokinetic profile, Vertex Pharmaceuticals developed Elexacaftor (VX-445), which emerged as a potent third-generation corrector. VX-445 has shown strong synergistic activity in combination with Tezacaftor and Ivacaftor, significantly enhancing the functional expression of F508del-CFTR. This triple therapy, marketed as **Trikafta** in the United States and **Kaftrio** in Europe, was first approved by the FDA in 2019 and subsequently by the EMA in 2020 for patients aged 12 years and older carrying at least one F508del allele, following excellent clinical trial outcomes. Treatment improved key indicators of lung function, such as forced expiratory volume in one second (FEV1), and

significantly reduced both pulmonary exacerbations and sweat chloride levels (Baroni D., 2025).

### *1.9.3 Comparative analysis of the correctors VX-445 and VX-809*

#### *1.9.3.1 Mechanistic insights and binding sites of correctors*

Early studies on the mechanisms of action and binding sites of VX-809 suggested that the corrector directly interacted with F508del-CFTR or with proteins involved in its synthesis or degradation (Van Goor *et al.,* 2011). Subsequent investigations using truncated mutants and isolated CFTR domains revealed that VX-809 primarily increases the stability of MSD1, indicating this domain as its main binding site (Loo *et al.,* 2013). Later work clarified that VX-809 stabilizes MSD1 during the early stages of CFTR folding (He *et al.,* 2013). Additional studies highlighted a dual role, as VX-809 not only facilitates co-translational folding of the mutant protein but also stabilizes CFTR at the plasma membrane, thereby enhancing its function (Eckford *et al.,* 2014). In the following years, growing evidence consistently confirmed MSD1 as the principal binding site of VX-809. A crucial advance came from Fiedorczuk and Chen (2022), who, through cryo-EM structural analysis of human CFTR in complex with these molecules, demonstrated that VX-809 binds directly to a hydrophobic pocket within MSD1, further validating this domain as the main binding site (Fiedorczuk & Chen, 2022).

Given the therapeutic relevance of VX-445, numerous research groups have focused on elucidating its mechanism of action and identifying its binding site on CFTR (Baroni D., 2025). The work of Veit *et al* (2020) marked a key step in this direction, demonstrating that VX-445 synergistically enhances the processing of F508del-CFTR in human bronchial epithelial cells when combined with type I or type II correctors. The authors concluded that VX-445 functions as a type III corrector by directly stabilizing NBD1. Another major challenge has been the identification of VX-445 binding sites on CFTR, requiring advanced techniques such as cryo-electron microscopy (cryo-EM), molecular docking, and sophisticated biochemical approaches. Baatallah et al. identified two potential binding sites: one on MSD1 and another shared with

VX-809 on NBD1. Simultaneous binding of both correctors to MSD1 was shown to enhance the allosteric interaction between MSD1 and NBD1, providing a mechanistic explanation for the increased CFTR rescue observed when VX-445 is combined with other correctors (Baatallah *et al.,* 2021).

## 1.10 From preliminary data to thesis scope

### *1.10.1 VX-809 provided the first evidence of activity in the absence of target protein overexpression*

As previously described, numerous studies in the literature have investigated the binding site of correctors on the CFTR target protein. Indeed, CF remains a rare disease, yet knowledge about its molecular basis has significantly increased over time. However, several considerations need to be addressed. One is that most of these studies, even when employing state-of-the-art technologies, focus primarily on the interaction between specific protein domains and the pharmacological molecule under investigation.

These works aim to identify the binding site of correctors on CFTR (Amico *et al.,* 2019; Bardin *et al.,* 2021; Fiedorczuk *&* Chen, 2022) without fully accounting for the remarkable complexity of the cell and the multiple protein partners with which these drugs may interact, potentially influencing pathways with cell-wide effects. Another important point is that, despite the exponential increase in knowledge on correctors, their exact mechanism of action has not yet been fully elucidated (Baroni D, 2025).

A particularly interesting observation was reported by Pecoraro et al. (2021) in a study conducted on human adenocarcinomic alveolar basal epithelial cells (A549), stably expressing either wild-type (wt) CFTR or ΔF508-CFTR, regarding the synergistic anti-inflammatory activity between the corrector VX-809 and Matrine, a quinolizidine alkaloid (Zhang *et al.,* 2018; Huang *&* Xin, 2018) known to modulate the activity of molecular chaperones within the cell. The study demonstrated not only a synergistic anti-inflammatory effect of VX-809 in combination with Matrine, but also that this association enhanced the maturation of the mutant CFTR protein (Basile *et al.,* 2012).

During the experiments, tests were also performed on A549 cells, where no overexpression of either wtCFTR or ΔF508-CFTR is present. As showed in the Figure 13, the experiment revealed the unanticipated ability of Lumacaftor to attenuate apoptosis under basal CFTR expression. This observation suggested that the corrector may exert its activity through a broader mechanism of action, potentially mediated by an additional protein partner involved in its anti-apoptotic effect.

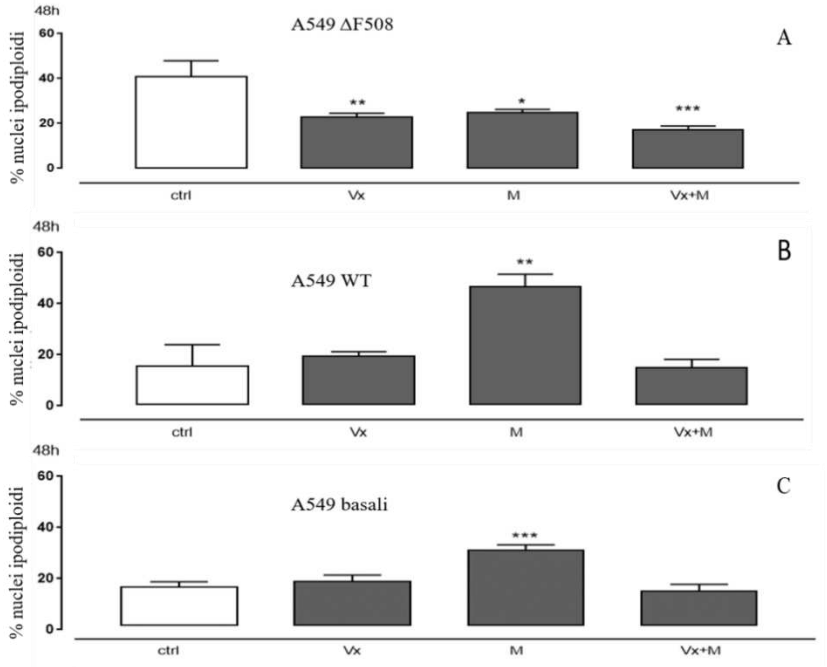


**Figure 12**: *VX-809 attenuates apoptotic processes even under basal conditions of CFTR expression. A549 cells overexpressing mutated CFTR (A), wtCFTR (B), or basal CFTR levels were treated with VX-809 (2 μM) and Matrine (300 μM) for 48 h. Cells were then stained with propidium iodide, and nuclear fluorescence was analyzed by flow cytometry. Data are presented as mean ± S.E.M. of the percentage of hypodiploid nuclei from at least three independent experiments, each performed in duplicate. Statistical significance was assessed using the Mann-Whitney U test. *p < 0.5, **p < 0.05, and ***p < 0.001 vs. non-treated cells*.

### *1.10.2 Aim of the thesis*

*General goal*

Considering that CF correctors were originally developed to promote the correct folding of misfolded CFTR protein within the ER, thereby increasing the amount of functional protein at its target sites; recognizing that the precise

mechanism of action of these compounds remains only partially elucidated; Recognizing that most studies in the literature focus on the interaction of isolated CFTR domains with small molecules rather than on drug-protein interactions within the complex cellular environment; and in light of evidence indicating that these correctors are neither strictly selective nor exclusively specific for CFTR, but may also act on other transporters within the same family; the overall objective of this thesis is to evaluate, through *in vitro* studies, the possibly ability of CF correctors to assist the cell in processing proteins within the ER, thereby alleviating the conditions of ER stress that cause cell death and ultimately contributing to the prospect of a potential new therapeutic indication.

# Chapter II

# *Material and Methods*

## 2.1 Cell Culture

A549 (adenocarcinomic human alveolar basal epithelial) and A375 (malignant melanoma) cells were routinely maintained in 100 mm sterile Petri dishes, whereas SH-SY5Y (human neuroblastoma; CL0208, Elabscience, Houston, TX, USA) and MO3.13 (immortalized human–human hybrid oligodendrocytes; 4410, CELLutions Biosystems, Burlington, Ontario, Canada) cells were cultured in 75 cm² sterile flasks. A549 and SH-SY5Y cells were grown in DMEM/F12 (Euroclone, Pero (MI), Italy), while MO3.13 cells were maintained in DMEM (Euroclone). A375 cells were cultured in DMEM supplemented with glutamine (2 mM). All media were supplemented with 10% fetal bovine serum (FBS; Euroclone), 100 U/mL penicillin, and 100 µg/mL streptomycin. Cells were kept at 37 °C in a humidified atmosphere with 5% $CO_2$, routinely subcultured weekly, and used for experiments at <80% confluence.

## 2.2 Experimental Protocol

Cells were seeded and allowed to adhere for 24 h. To induce ER stress, cells were pretreated with Thapsigargin (TG, 300 nM) (Sigma-Aldrich, St. Louis, MO, USA) for the time points indicated for each assay.TG primarily inhibits the ER calcium pump, depleting ER calcium stores and thereby disrupting the protein folding process. This leads to accumulation of unfolded proteins within the ER, triggering ER stress (Kurekova *et al.,* 2025). After TG removal, fresh medium was added with or without the corrector(s). Depending on the assay, cells were treated with VX-809 (2 µM; S1565, Selleckchem, Houston, TX, USA) and/or VX-445 (3 µM; S8851, Selleckchem) for 24 h. Cells

were then collected and lysates harvested 24 h post-treatment for both VX-treated and TG-treated conditions.

### 2.3 Protein extraction and Western Blotting assay

A459, A375 and MO3.13 (7 × $10^5$ cells/plate) and SH-SY5Y (1× $10^6$ cells/plate) were seeded in 100 mm tissue culture plates and after 24h were treated as described in the experimental protocol. Total proteins were extracted from cells by freeze/thawing in RIPA buffer (20 mM Tris-HCl pH 7.5, 1 mM EGTA, 150 mM NaCl, 1 mM Na2EDTA, 1% sodium deoxycholate, 1× protease and phosphatase inhibitor cocktail, and 2% IGEPAL instead 1% for A549 and A375 cells) for 30 min. Then, cells were centrifuged at 14,000 rpm for 15 min at 4 °C. Protein concentration was analyzed by a Bradford assay and 60 µg of protein were run on 8–10% acrylamide gel and separated by SDS-PAGE, under denaturing conditions, and transferred to nitrocellulose membranes using a minigel apparatus (Bio-Rad Laboratories, Richmond, BC, Canada). Blots were then blocked in Tris-buffered saline, containing 5% nonfat dry milk for 1h at room temperature, and incubated overnight with specific primary antibodies at 4 °C using Actin, GAPDH or Tubulin as a loading control (Table ). After washes in PBS/0.1% Tween, the right secondary antibody (Table) was added for 1 h at room temperature. The immunoreactive protein bands were detected with enhanced chemiluminescence (ECL) reagents and blot imaging (LAS 4000; GE Healthcare, Milan, Italy). Western blotting imaging data were quantified using ImageJ software Version 1.54j.

**Table 1:** *Antibodies used for Western blot analysis*

| Primary Antibody | Supplier | Catalog no. |
|---|---|---|
| **anti-ATF4** | Proteintech | 10835-1-AP |
| **anti-ATF6** | Cell Signaling | 658805 |
| **anti-CHOP** | OriGene | TA802218 |
| **anti-PERK** | Cell Signaling | 3192 |
| **anti-GRP78/BiP** | Cell Signaling | 3177 |
| **anti-SODIII** | Santa Cruz Biotechnology | sc-271170 |
| **anti-IKKα** | Santa Cruz Biotechnology | sc-7606 |
| **anti-NF-κB** | Thermo Fisher Scientific | MA5-15181 |
| **anti-SERCAII** | Santa Cruz Biotechnology | sc-376235 |
| **anti-cytochrome c** | Proteintech | 66264-1-Ig |

| | | |
|---|---|---|
| **anti-IRE1** | Proteintech | 28164-1-AP |
| **anti-Bcl-2** | Santa Cruz Biotechnology | sc-7382 |
| **anti-actin** | OriGene | TA811000 |
| **anti-GAPDH** | Santa Cruz Biotechnology | sc-32233 |
| **anti-tubulin** | Santa Cruz Biotechnology | sc-5286 |
| **Secondary Antibody** | | |
| **anti-rabbit** | Bethyl Laboratories | A120-101P |
| **anti-mouse** | Bethyl Laboratories | A90-137P |

### 2.4 Analysis of Intracellular Calcium Signaling

Intracellular calcium concentrations were analyzed using the fluorescent indicator dye Fura 2-AM bought from Sigma-Aldrich (St. Louis, MO, USA). It is the membrane-permeant acetoxymethyl ester form of Fura 2. For the assay, $3\times10^4$ cells/plate were seeded in 24-well tissue culture plates and treated as described above. After treatment period, cells were washed with phosphate buffered saline (PBS) and resuspended in 1 mL of Hank's balanced salt solution (HBSS) containing 5 μM Fura 2-AM for 45 min. Afterwards, cells were washed with the same buffer to remove excess Fura 2-AM and incubated in calcium-free HBSS/0.5 mM EGTA buffer for 15 min to push Fura 2-AM hydrolysis into its active-dye form, Fura 2. Then, cells were transferred to the spectrofluorometer (Perkin-Elmer LS-55, Milano (MI), Italy). Depending on the subcellular compartment of interest, different pharmacological agents were employed: thapsigargin (1 nM) to assess ER calcium stores, ionomycin (1 μM), a calcium ionophore that permeabilizes biological membranes and is widely used to mobilize total intracellular calcium reserves, and carbonyl cyanide m-chlorophenylhydrazone (CCCP; 5 μM), a protonophore that dissipates the mitochondrial membrane potential and thereby promotes mitochondrial calcium release/depletion. All reagents were purchased from Sigma-Aldrich (St. Louis, MO, USA) and were applied by adding the appropriate concentration of each compound directly to the cuvette in calcium-free HBSS supplemented with 0.5 mM EGTA. The excitation wavelength was alternated between 340 and 380 nm, and emission fluorescence was recorded at 515 nm. The ratio of fluorescence intensity of 340/380 nm (F340/F380) was strictly related to intracellular free calcium, as previously reported. The results were

expressed as the delta (Δ) of the Thapsigargin-induced or Ionomycin or CCCP-induced increase in the basal fluorescence ratio (F340/F380 nm).

### 2.5 Hypodiploid DNA Detection

SH-SY5Y and MO3.13 cells ($8 \times 10^4$ cells/well) and $2.5 \times 10^3$ cells/well for A375 and A549 cells were plated in a 24-well plate and allowed to grow for 24h and treated following the experimental protocol. After two PBS washes, cells were resuspended in 500 µL of 0.1% sodium citrate buffer, 0.1% Triton X-100, and 50 µg/mL of propidium iodide (PI) purchased from Sigma-Aldrich (St. Louis, MO, USA). The cells were then incubated for 30 min at 4 °C in the dark to analyze the DNA content. By applying Cell Quest software, flow cytofluorometry was used to analyze PI-stained cells. The study of cellular debris was stopped by raising the scatter threshold, and the logarithmic scale was used to record the amount of DNA in the nucleus. The percentage of the hypodiploid region is used to represent the results.

### 2.6 Evaluation of Intracellular and Mitochondrial ROS Release

Cytosolic and mitochondrial ROS generation was assessed using a 24-well plates where SH-SY5Y and MO3.13 ($8 \times 10^4$ cells/well), A549 and A375 ($2.5 \times 10^3$ cells/well) were seeded and treated according to the experimental protocol. For cytosolic ROS, cells were harvested after treatment and washed twice with PBS, then incubated in PBS containing 2′,7′-dichlorofluorescein diacetate (H2DCF-DA; 10 µM) at 37 °C for 30 minutes in the dark. H2DCF-DA was purchased from Sigma-Aldrich (St. Louis, MO, USA). Cell fluorescence was then measured using fluorescence-activated cell sorting (FACSscan; Becton–Dickinson) and analyzed with Cell Quest software version 4.1. With regard to mitochondrial ROS, changes in O2− production were assessed using mitochondrial superoxide fluorescent indicators MitoSOX Red (M36008; Invitrogen, ThermoFisher, Waltham, MA, USA). Cells were incubated with MitoSOX Red (2.5 µM) for 15 minutes in the dark at 37°C, followed by washing. The fluorogenic dye MitoSOX Red is used to detect superoxide very specifically in the mitochondria of living cells. Once in the mitochondria, it is oxidized by superoxide and produces red fluorescence, which is measured by

flow cytometry (FACScan; BD Biosciences, San Jose, CA, USA) and analyzed with the same software above.

### 2.7 Flow Cytometry Assay to evaluate an intracellular target

Protein expressions (anti-caspase 4, COXII, pSTAT3 and ikBα, cyt c) were analyzed by fluorescence-activated cell sorting (FACSscan; Becton-Dickinson, Franklin Lakes, NJ, USA). SH-SY5Y ($8 \times 10^4$ cells/well), A549 and A375 ($5 \times 10^4$ cells) cell lines were grown on a 24-well plate allowed to adhere for 24h, and then treated as described above. Next, cells were mechanically harvested and fixed in a solution containing 4% formaldehyde and PBS for 15 min. After washing, cells were blocked with 2% BSA and PBS with 0.1% sodium azide for an additional 20 min Then, cells were permeabilized with buffer containing Triton X-0.1%, 2% BSA, and PBS in the presence of 0.1% sodium azide for 30 min. Subsequently, the cells were incubated with primary antibodies: anti-COXII (sc-19999), anti-p-STAT3 (sc-8059), anti-IkB-α (sc-371), anti-caspase 4 (sc-1229) anti-Cytochrome c (66264-1-Ig), followed by Texas-Red conjugated secondary antibody (T6390) purchased from Thermo Fisher Scientific (Waltham, MA, USA). Finally, after being rinsed with fixation buffer, cells were detected using flow cytometry and examined using Cell Quest software (version 4.1). The values were reported as the percentage of positive cells.

### 2.8 Expression Proteomics

SH-SY5Y cells were seeded and then, after 24 hours of adhesion, pretreated with 300 nM TG for 2 hours. After washing off the TG, the cells were provided with fresh growth medium, either with or without Vx. After a 24-hour treatment period with corrector Vx-445 (3 μM), the cells were detached with trypsin and, after two washes with PBS, the pellet was subjected to functional proteomic analysis.

The obtained cell pellets were lysed in an ammonium bicarbonate (AmBic, 50 mM, pH 8.5) buffer comprising 8 M Urea, 0. 5% w/vol sodium deoxycholate and a protease inhibitor cocktail (1x final concentration). Lysis was achieved through sonication (Branson Digital Sonicator, 30% amplitude, on/off pulses of

9.9 seconds, total lysis time of 1 minute), followed by samples centrifugation at 21000 rcf at 18°C, for 20 minutes. The proteins concentration of the supernatants was evaluated through Bradford assay. Equal protein amounts (500 µg in 90 µl) were then submitted to an in-solution digestion protocol with a LysC/trypsin mixture, as reported in Morretta et al. (2022) study.

The obtained peptides mixtures where then dried under vacuum, dissolved in 5% FA and desalted through Sep-Pak C18 1 cc (50 mg) cartridges (Waters, Milford, MA, USA). Briefly, cartridges were activated flushing 3 mL of 100% CH3CN and then conditioned with 3 mL of 0.1% FA. Samples were then loaded, desalted flushing the cartridges with 3 mL of 0.1% FA and finally eluted flushing two times 500 µL of 80% CH3CN, 20% H2O, 0,1% FA. For the subsequent MS analysis, the peptides mixtures were dried under vacuum and re-dissolved in 10% FA. Subsequently, 1 µg of each digest was analysed through nano-UHPLC-MS/MS on a Tribrid Orbitrap Mass Spectrometer coupled to a Vanquish Neo UHPLC system (ThermoFisher Scientific, Bremen) equipped with an EASY-Spray PepMAPTM Neo C18 column (1500 bar, 2 µm, 100 Å, 75 µm × 750 mm, ThermoFisher Scientific, Bremen). Peptides elution was achieved at a flow rate of 300 nL/min with the following gradient: 0.1 min at 1% B, 0.1 min to 180.1 min to 45% B, 180.2 min to 99% B, then held at 99% B for 16 min and brought back to 1% B (A: H2O, 0.1% FA; B: 80% CH3CN, 20% H2O, 0.1% FA). The mass spectrometer was operated in data-dependent acquisition mode, with a cycle time of 1.5 sec. Full scan MS spectra were acquired in the Orbitrap with the following settings: scan range 375–1500 m/z, normalized full-scan automatic gain control (nAGC) target of 100% at 240000 resolution, maximum injection time of 50 ms. Precursors were isolated in the Quadrupole and MS2 spectra were generated with HCD (normalized collision energy of 30%) and acquired in the Ion Trap (rapid scan mode), with a nAGC target of 300%, and a maximum injection time of 20 ms. The obtained raw files were then analysed through *Proteome Discoverer* (version 3.1.0.638). Spectra were searched by Sequest against a reviewed Homo sapiens database (UP000005640, March 2024, gene count 20,656) using the following parameters: trypsin digestion; maximum of two missed cleavages; cysteine carboxyamidomethylation as fixed modification and methionine oxidization as

variable modification. Precursor mass and fragment mass tolerance were respectively set at 10 ppm and 0.6 Da. Label-free quantification was performed using both unique and razor peptides, and proteins abundances ratios were calculated through a pairwise ratio-based approach, corroborated by a background-based t-test.

### 2.9 Drug Affinity Responsive Target Stability (DARTS)

SH-SY5Y cell pellets were lysed in M-PER (Mammalian Protein Extraction Reagent, Thermo Scientific, Waltham, USA) supplied with a protease inhibitor cocktail (Gene-Spin, Milan, Italy), as reported by the manufacturer. The lysate was centrifuged at 10000 g for 10 min at 4°C, and Bradford assay (Bio-Rad, Hercules, USA) was used to determine proteins concentration of the obtained supernatant. Equal protein aliquots (80 µL at 3 µg/µL) were then incubated with DMSO or with increasing amounts of Vx-445 (final concentrations of 1 M, 10 M, and 100 M), for 1 hour at room temperature and under continuous shaking. Final DMSO amount was 1.7% vol/vol in each sample. Samples were then submitted to limited proteolysis (1:1000 w/w subtilisin to proteins ratio) for 30 minutes (25°C, 450 rpm), except for an aliquot of the DMSO-treated lysate, which was submitted to mock proteolysis. Subtilisin was then quenched with 1 mM phenylmethane-sulfonyl-fluoride (PMSF, Sigma Aldrich-Merck). This experiment was performed in triplicate.

Then, 20 µg of each sample were heated at 95°C in Laemmli buffer and proteins were separated through 1D-SDS-PAGE, on 4%-12% polyacrylamide gradient gels (CriterionTM XT Precast Gel, 4-12% Bis-Tris, Bio-Rad, Hercules, USA). The gels were Coomassie stained (Coomassie Brilliant Blue R-250, Bio-Rad, Hercules, USA), and gel bands were excised and submitted to an in situ tryptic digestion protocol. Peptides mixtures were then dryed ender vacuum and dissolved in 10% Formic acid (FA) for the subsequent nano-UHPLC-MS/MS analysis. 1 µL of each digest was analysed on an Orbitrap Q-Exactive Classic Mass Spectrometer coupled to an UltiMate 3000 Ultra-High Pressure Liquid Chromatography (UHPLC) system (ThermoFisher Scientific, Bremen), equipped with an EASY-Spray PepMAPTM RSLC C18 column (3 µm, 100 Å, 75 µm × 50 cm, ThermoFisher Scientific, Bremen).

Peptides elution was achieved at a flow rate of 300 nL/min with the following gradient: 1 min at 3% B, 1 min to 40 min to 28% B, 40 min to 41 min to 70% B, 41 min to 49 min at 70% B and 50 min back to 3% B until 60 min (A: 95% H2O, 5% CH3CN, 0.1% AcOH; B: 95% CH3CN, 5% H2O, 0.1% AcOH). The mass spectrometer was set in data-dependent acquisition mode. Full scan MS spectra were acquired as follows: scan range 375–1500 m/z, full-scan automatic gain control (AGC) target 3e6 at 70000 resolution, maximum injection time 50 ms. MS2 spectra were generated for up to 8 precursors (normalized collision energy of 28%) and the fragment ions acquired at a resolution of 17500, with an AGC target of 1e5 and a maximum injection time of 80 ms. The obtained raw files were analysed through Proteome Discoverer (version 2.4.1.15). MSPepSearch was used to perform a spectral library search (NIST Human Orbitrap HCD Library) with a mass tolerance of 10 ppm for MS1 and 0.02 Da for MS2. The target False Discovery Rate (FDR) was set to 1% (strict) and 5% (relaxed). Subsequently, MS/MS spectra were then also searched by Sequest against Swiss Prot Homo sapiens database, as follows: trypsin digestion; maximum of two missed cleavages; cysteine carbamidomethylation as fixed modification; methionine oxidization, protein N-terminal acetylation and/or demethylation as variable modifications; precursor mass tolerance of 10 ppm and fragment mass tolerance of 0.02 Da. *Label-free* quantification was performed on both unique and razor peptides, and a pairwise ratio-based approach was used to evaluate Vx-445 vs CTRL proteins abundances. For each calculated ratio, a background-based t-test was performed.

### 2.10 RNA Extraction and RT-PCR Protocol

For the RNA extraction, SH-SY5Y cells were seeded into 100 mm culture plates according to the experimental protocol. In accordance with the manufacturer's instructions, TRI reagent (T9424, Sigma-Aldrich, Darmstadt, Germany) was used to extract RNA of which 0.5 µg was retrotranscribed using the RevertAid First Strand cDNA synthesis kit (K1622). 2µl of cDNA were subjected to semiquantitative PCR using the following primers: 5′-C CTT CTG GGT AGA CCT CTG GGA G-3′ and 5′-A AAC AGA GTA GCA GCT CAG ACT

GC-3′. By staining 4% agarose gels with ethidium bromide and subjecting them to LAS 4000 (GE Healthcare, Chicago, IL, USA), fragments of 452 and 426 bps were found, which correspond to unspliced and spliced XBP1 mRNA.

### 2.11 ELISA assay

IL-6 levels in the supernatant of SH-SY5Y and A549 cell lines were determined using an Enzyme-Linked Immuno Sorbent Assay (ELISA). Both cells were seeded in 96-well plates (5.0 × 104 cells/well), left to attach for 24h, and processed as previously described. ELISA was performed using a commercially available kit. High-binding ELISA plates (Nunc®) were coated with the IL-6 capture antibody and incubated overnight at 4 °C. After four washes with 1× PBS containing 0.05% Tween-20, wells were blocked with ELISA diluent buffer (1×) for 1h at room temperature. Subsequently, 50 µL of samples and a seven-point serial dilution of the IL-6 standard were added to the wells, including a zero-point containing buffer alone, and incubated for 2h at room temperature. After four additional washes, 50 µL/well of HRP-conjugated detection antibody were added and the plate was incubated for 30 min at room temperature, followed by washing. Then, 50 µL of TMB substrate were added to each well and incubated for 15 min at room temperature, after which the reaction was stopped by adding 25 µL of 2 N $H_2SO_4$. Absorbance was measured at 450 nm using a microplate spectrophotometer (Multiskan Spectrum, Thermo Fisher), and IL-6 concentrations (pg/mL) were calculated from the standard curve generated in Excel.Cytokine release was expressed as pg/mL.

### 2.12 Detection of Nitric Oxide Levels

Nitric Oxide (NO) levels were assessed in SH-SY5Y and A549 cell lines (8 × 104 cells/well), which were seeded in 24-well plates and processed as indicated above. After being treated, the cells were then harvested, flushed with PBS twice, and then incubated in PBS with 4,5-diaminofluorescein diacetate (DAF-2DA; 10 µM) probe for 1 h in the dark (37 °C). Fluorescence-activated cell sorting (FACSscan; Becton-Dickinson, Franklin Lakes, NJ, USA)

was then used to measure the fluorescence of the cells, and Cell Quest software (version 4.1) was used to interpret the results.

### 2.13 Measurement of Mitochondrial Membrane Depolarization

To evaluate the mitochondrial membrane depolarization (ΔΨm), the fluorescent dye tetramethylrhodamine methyl ester (TMRE) was used that, due to its positive charge, penetrates and accumulates in the mitochondria in inverse proportion to the membrane potential. SH-SY5Y and MO3.13 cells (80× 104 cells/well into 24 well plate) were treated as described above, then the TMRE (150 nM) was added, and the plate was centrifuged at 1200 rpm for 5 min. Thereafter, cells were collected with staining buffer (PBS containing 0.1% Sodium Azide and 2% BSA). Cell fluorescence was evaluated via fluorescence-activated cell sorting and analyzed using Cell Quest software. Data are expressed as the % of positive TMRE cells.

### 2.14 Analytical Statistics

The software GraphPad Prism8 (GraphPad Software Inc., San Diego, CA, USA), commercially available, was used for data assessments and statistical analysis. The data are shown as the mean ± standard error of at least three distinct experiments that were carried out in technical triplicate. Statistical information was gathered using the non-parametric Mann–Whitney U technique between the experimental points. If the $p$ values fell between $<0.01$ and 0.05, the differences were regarded as significant.

# Chapter III

# *In vitro* study of VX-809's ability to reduce the ER-stress and to play a role in more general pathological processes.

## 3.1 Introduction

It is now well established that proteins represent an essential class of macromolecules for life, and the fundamental condition to ensure their proper function is the acquisition of an appropriate folding. The organelle most directly involved in protein synthesis and folding is the ER. When either exogenous or endogenous factors alter protein processing, a condition known as ER stress is triggered in the cell. Cellular stress induced by the abnormal accumulation of unfolded or misfolded proteins in the ER is emerging as a potential trigger of several human diseases (Hetz *et al.,* 2020).

Proteostasis control in the ER is also mediated by the UPR, which conveys information on the protein folding state to the nucleus and cytosol to regulate the cellular folding capacity or, in the case of chronic damage, induce programmed cell death by apoptosis. Numerous studies have demonstrated a connection between ER stress and other pathological states at both cellular and organismal level. ER stress and oxidative stress are closely linked events that impact cellular homeostasis and apoptosis. Moreover, through ROS production, ER stress induces mitochondrial dysfunction, a vital intracellular organelle, and further increases mitochondrial ROS production (Dandekar *et al.,* 2015). This aspect is particularly relevant, since mitochondrial dysfunction is associated with an ever-growing number of human diseases, including neurodegenerative disorders, cardiomyopathies, metabolic syndrome, cancer, and obesity (Jha & Morrison, 2018). Several studies have also demonstrated a connection between ER stress and the inflammatory response through

multiple mechanisms (Zhang & Kaufman, 2008), highlighting how ER stress represents a central process that triggers many other pathological mechanisms.

CF is one of the most common hereditary diseases, associated with mutations in the CFTR protein gene. Among the modern drugs used in CF treatment, Lumacaftor (VX-809) belongs to the category of correctors and was the first drug approved by the FDA for the treatment of patients homozygous for the F508del-CFTR mutation (Choong et al., 2022). Based on studies showing that the corrector VX-809 is not strictly specific for the CFTR protein (Amico et al., 2019; Bardin et al., 2021; Fiedorczuk & Chen, 2022), its ability to act as a corrector of the mutated CFTR channel could also extend to other misfolded proteins, thereby suggesting potential applications in additional pathologies.

The results described in this first chapter provide preliminary evidence that VX-809 may exert effects beyond the correction of its target protein folding, acting on ER stress associated with misfolded or unfolded proteins and thereby revealing a broader mechanism of action with potential off-label relevance.

## 3.2 Results

### *3.2.1 VX-809 Impacts the Unfolded Protein Response*

As previously described, multiple factors can disrupt the delicate equilibrium within the ER and induce stress conditions. When ER homeostasis is altered, proteins may fail to fold correctly and accumulate in this organelle, activating the UPR pathway which is a signaling system that detects misfolded proteins in the ER and coordinates a cellular response aimed at restoring protein homeostasis.

To test the hypothesis of VX-809 involvement in protein misfolding, we analyzed, through Western blotting, the activation of UPR signaling components, such as Grp78/BiP and ATF4, after inducing protein misfolding-ER stress, with TG, in A549 and A375 cell lines. Western blot analysis performed on both cell extracts showed a significant increase ($p < 0.005$) in

BiP expression following TG exposure, confirming the induction of ER stress. Conversely, pretreatment with Vx-809 markedly attenuated the TG-induced upregulation of BiP, with a statistically significant effect ($p < 0.05$) observed after 4 hours, as illustrated in Figure 14 (Panel A and B).

Within the UPR pathway, we also examined the modulation of ATF4 expression, a key transcription factor involved in the regulation of several essential genes (24). In this context as well, the corrector significantly reduced ATF4 expression at both experimental time points ($p < 0.005$), supporting its modulatory effect on ATF4 activation in A549 (Figure 14C) and A375 cells (Figure 14D). As further confirmation of the action of the VX-809 corrector on the UPR, further sensors on the A549 cell lines were evaluated.

In A549 cells, ATF6 levels significantly increased ($p < 0.001$) after TG pretreatment compared to control cells, confirming ER stress induction. Vx-809 treatment significantly reduced TG-induced ATF6 expression ($p < 0.05$) (Figure 14E).

PERK, becomes activated through phosphorylation once BiP dissociates from its luminal domain to bind misfolded proteins. To assess this activation, the phosphorylated form (p-PERK) was analyzed by Western blot in A549 cells. As shown in Figure 14F, PERK phosphorylation was identified by the characteristic band-shift due to the increased molecular weight following autophosphorylation (Amodio et al., 2019). As expected, the p-PERK form was absent in untreated and Vx-809-treated cells but appeared only after TG exposure. Notably, Vx-809 administration reduced the p-PERK band-shift after 4 h of TG pretreatment.

Finally, CHOP, a transcription factor strongly associated with the UPR, was analyzed. As shown in Figure 14G, Western blot results revealed a significant increase in CHOP levels ($p < 0.05$) in TG-treated cells compared to controls, confirming the occurrence of reticular stress. Vx-809 treatment decreased CHOP expression in our experimental model, indicating its ability to help restore ER homeostasis.

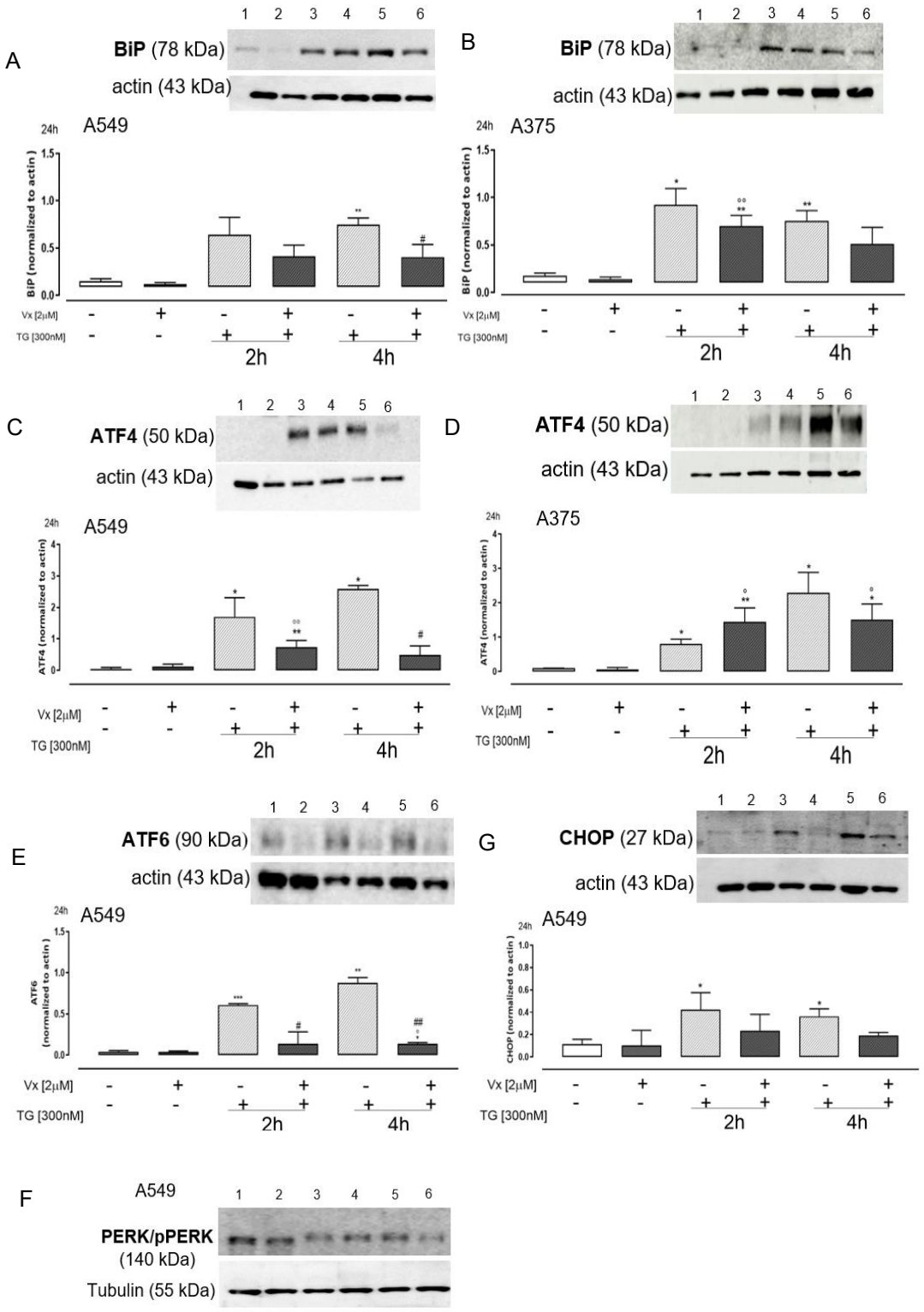


**Figure 14:** *Vx-809 modulates UPR activation. Western blot analysis: 1 = ctrl, 2 = Vx-809, 3 = TG for 2 h, 4 = Vx-809 after pre-treatment with TG for 2 h, 5 = TG for 4 h, 6 = Vx-809 after pre-treatment with TG for 4 h. Cells were pretreated with 300 nM TG for 2 or 4 h to induce ER stress. Subsequently, 2 μM of the corrector Vx-809 were administered for 24 h. BiP and ATF4 expressions on A549 (A,C) and on A375 (B,D) were detected by Western blot analysis. Were detected by Western blot analysis as well as ATF6 (E), PERK/pPERK (**F**), and CHOP (G) on A549 cells Actin protein expression was used as a loading control. Results are expressed as mean ± S.E.M.*

*from at least three independent experiments each performed in triplicate. Data were analyzed by a Mann–Whitney U test. * p < 0.05, ** p < 0.005, and *** p < 0.001 vs. non-treated cells; ° p < 0.05 and °° p < 0.005 vs. Vx-809–treated cells; # p < 0.05 vs. TG-treated cells.*

### *3.2.2. Vx-809 has a protective role against Thapsigargin-Induced cell death*

Under ER stress conditions, the primary goal of the cell and the associated adaptive mechanisms is to restore homeostasis. However, when the stress persists and recovery attempts fail, the cell activates the programmed cell death pathway: apoptosis. Considering the modulation of CHOP, a well-known pro-apoptotic factor mediating this process, the effect of Vx-809 on apoptosis was further assessed by analysing the percentage of hypodiploid nuclei and the levels of caspase 4, an ER membrane-localized protease cleaved under ER stress conditions (Hitomi et al., 2004). As shown in Figure 15, Vx-809 significantly reduced ($p < 0.05$) the percentage of hypodiploid nuclei in TG-pretreated A549 (Figure 15A) and A375 (Figure 15B) cells. Moreover, flow cytometry analysis revealed a marked decrease ($p < 0.001$) in caspase 4 levels in Vx-809-treated A549 (Figure 15C) and A375 (Figure 15D) cells under ER stress, suggesting that Vx-809 contributes to the restoration of ER homeostasis.

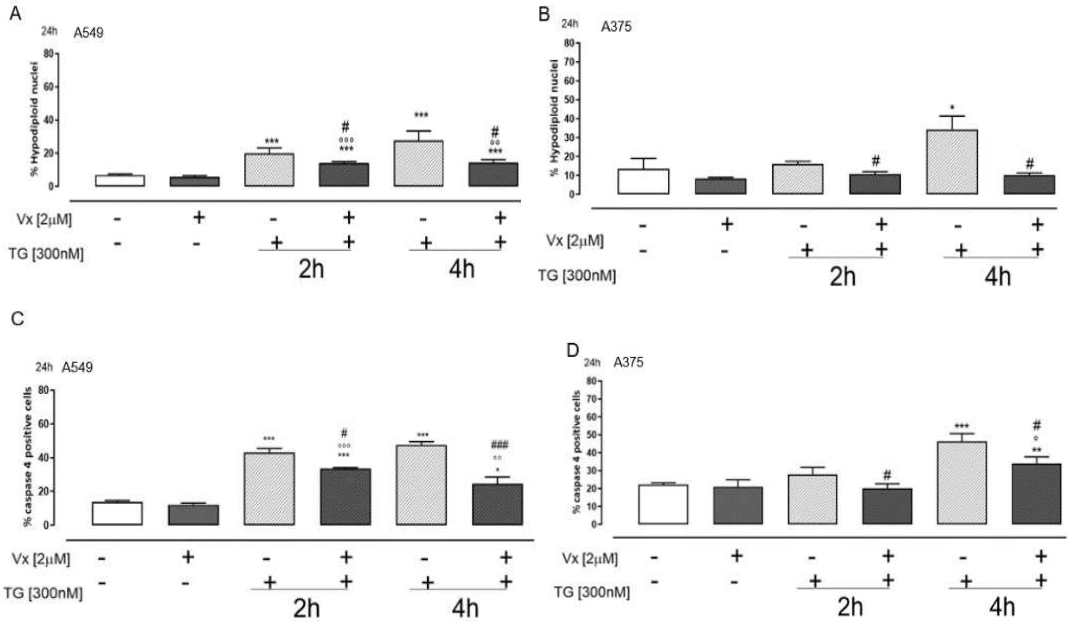


**Figure 15:** *Vx-809 shows protective anti-apoptotic role. Cells were pre-treated with 300 nM TG for 2 or 4 h to induce ER stress. Subsequently, 2 μM of the corrector Vx-809 were administered for 24 h. Then, A549 (A) and A375 (B) were stained by*

*propidium iodide and the fluorescence of individual nuclei was measured by flow cytometry. Panels (C, D) show caspase 4 content detected by flow cytometry analysis, respectively, in A549 and A375 cells. Data were expressed as mean ± S.E.M. of the percentage of caspase 4 positive cells from at least three independent experiments each performed in duplicate. Data were analyzed by a Mann–Whitney U test. * p < 0.05, ** p < 0.05, and *** p < 0.001 vs. non-treated cells; ° p < 0.05, °° p < 0.005, and °°° p < 0.001 vs. Vx-809–treated cells; # p < 0.05 and ### p < 0.001 vs. TG-treated cells.*

### *3.2.3 Modulation of intracellular and mitochondrial ROS by Vx-809.*

ER and oxidative stress are closely interconnected in both physiological and pathological contexts. During the accumulation of misfolded proteins within the ER lumen, activation of the UPR leads to increased ROS generation in the ER. Flow cytometric analysis using the fluorescent probe DCHF-DA revealed that Vx-809 treatment significantly reduced cytosolic ROS production ($p < 0.001$) in both TG-treated cell lines (Figure 16A and 16B). Given the established connection between ER stress and mitochondrial, and considering that they are a major source of ROS, mitochondrial ROS generation was also assessed (Fan *et al.,*2019). Results obtained using MitoSOX red showed that mitochondrial ROS production was significantly lower ($p < 0.001$) in A549 (Figure 16C) and A375 (Figure 16D) cells treated with Vx-809 after pre-treatment with TG, in particular after 4 hours from treatment.

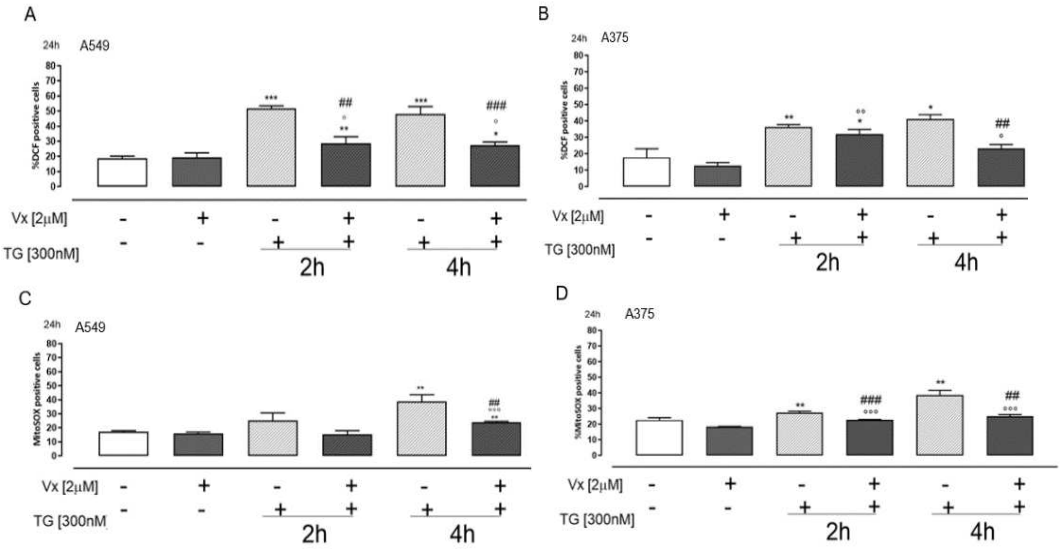


**Figure 16:** *Vx-809 interferes in the ROS production. Cells were pretreated with 300 nM TG for 2 or 4 h to induce ER stress. Subsequently, 2 μM of the corrector Vx-809 were administered for 24h. ROS generation was evaluated by the probe*

*2',7'dichlorofluorescein diacetate (H2DCF-DA) in A549 (A) and in A375 (B) cells. ROS production was expressed as mean ± SEM of the percentage of DCF-positive cells of at least three independent experiments each performed in duplicate. Superoxide production by mitochondria was evaluated by means of the probe MitoSOX Red in A549 (C) and A375 (D) cells by flow cytometry analysis. Mitochondrial superoxide production was expressed as mean ± S.E.M. of the percentage of MitoSOX-positive cells of at least three independent experiments each performed in duplicate. Data were analyzed by a Mann–Whitney U test. * p < 0.05, ** p < 0.005, and *** p < 0.001 vs. untreated cells; ° p < 0.05, °° p < 0.005, and °°° p < 0.001 vs. Vx-809–treated cells; ## p < 0.005 and ### p < 0.001 vs. TG-treated cells*

### *3.2.4 Restoration of $Ca^{2+}$ Homeostasis by VX-809 Post TG-ER Stress*

The essential role of calcium in proper protein folding within the ER has been widely described in the literature. Many ER-resident chaperones, such as BiP, calnexin, and calreticulin, are calcium-dependent. Moreover, the alteration of $Ca^{2+}$ homeostasis not only represents one of the main triggers of the UPR but also underlies several human pathologies.

To evaluate the effects of Vx-809 treatment on intracellular $Ca^{2+}$ levels in this experimental model, A549 cells, treated as previously described, were loaded with the fluorescent dye FURA2-AM in $Ca^{2+}$-free incubation medium (containing 0.5 mM EGTA). As shown in Figure 17A, the delta increase in $[Ca^{2+}]i$ achieved by Thapsigargin (1 nM), in Vx-809-treated cells previously pre-treated with TG for 4 hours, was greater than in TG-treated cells, highlighting the restoration of calcium accumulation in the ER. Therefore, this result supports the hypothesis that the corrector Vx-809 enhances calcium homeostasis following ER stress. Similarly, the findings show that Vx-809 treatment, after ER stress, induces a significant increase in the ionomycin (1 μM)-stimulated delta rise in $[Ca^{2+}]i$ ($p < 0.05$)(Figure 17B) compared to TG-treated cells, suggesting that the corrector exerts a beneficial effect on calcium balance. Furthermore, the enhancement of ER $Ca^{2+}$ storage is largely regulated by the SERCA II pump. Among the various regulatory mechanisms, the sarco/endoplasmic reticulum $Ca^{2+}$-ATPase (SERCA II) plays a pivotal role in maintaining intracellular $Ca^{2+}$ homeostasis (Zhang *et al.,* 2020). This pump actively transports $Ca^{2+}$ back into the ER lumen and represents the most ubiquitous calcium transporter in the cell.

Data on SERCA II expression in A549 cells revealed a significant decrease ($p < 0.005$) in its levels following Vx-809 treatment, particularly after 4 hours of TG pre-treatment. It is hypothesized that SERCA II expression increases upon ER stress induction as a protective response, promoting calcium reuptake into the ER to counteract cytosolic calcium overload, which can be detrimental to the cell.

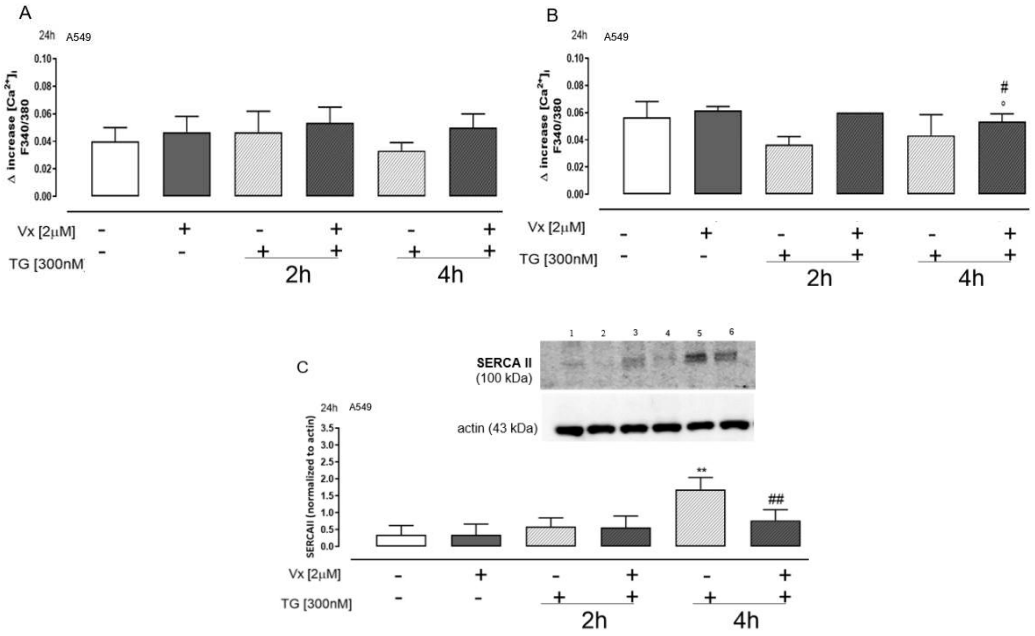


**Figure 17**: *Vx-809 interferes with calcium concentrations. Cells, to induce ER stress, were pretreated with 300 nM TG for 2 or 4 h. Subsequently, 2 μM of the corrector Vx-809 were administered for 24 h. The effect of Vx-809 after ER stress conditions on the reticular calcium pool was evaluated on cells in a calcium-free medium in the presence of TG (1 nM) (Panel (A)), while intracellular calcium content was evaluated by means of Ionomycin (1 μM) (Panel (B)). Results are expressed as mean ± S.E.M. of the delta (δ) increase of FURA 2 ratio fluorescence (340/380 nm) from at least three independent experiments each performed in duplicate. SERCAII expression was detected by Western blot analysis; 1 = ctrl, 2 = Vx-809, 3 = TG for 2 h, 4 = Vx-809 after pre-treatment with TG for 2 h, 5 = TG for 4 h, 6 = Vx-809 after pre-treatment with TG for 4 h. Actin protein expression was used as a loading control. Results are expressed as mean ± S.E.M from at least three independent experiments each performed in duplicate (Panel (C)). Data were analyzed by a Mann–Whitney U test. ** p < 0.005 vs. untreated cells; ° p < 0.05 vs. Vx-809–treated cells; # p < 0.05 and ## p < 0.005 vs. TG-treated cells.*

### *3.2.5 VX-890 modulates the Inflammatory Signaling*

Failure of the ER's adaptive capacity results in activation of UPR, which intersects with many different inflammatory and oxidative stress signaling

pathways. Several enzymes participate in free radical neutralization processes: glutathione peroxidase, superoxide dismutase (SOD) and catalase (Pecoraro *et al.,* 2020). The SODIII expression, which is widely expressed in the lungs and its concentration is increased by proinflammatory cytokines, was analysed. Western blotting analysis in Figure 18 shows a significant ($p < 0.05$) reduction of SOD III expression in Vx-809-treated cells after reticular stress induction versus TG-treated cells.

It is well established that the transcription factor NF-κB plays a central role in the inflammatory process. To assess the potential involvement of the corrector in this pathway, the expression levels of NF-κB and IKKα were analyzed in A549 cells treated as described above. Results showed that TG-treated A549 cells exhibited markedly increased levels of both proteins after 4 hours, confirming the establishment of a stress condition in our experimental model. Following stress induction and subsequent treatment with Vx-809 for 24 hours, a significant reduction ($p < 0.05$) in the expression of NF-κB (Figure 18B) suggesting a lack of nuclear translocation and IKKα (Figure 18C) was observed compared to TG-treated cells.

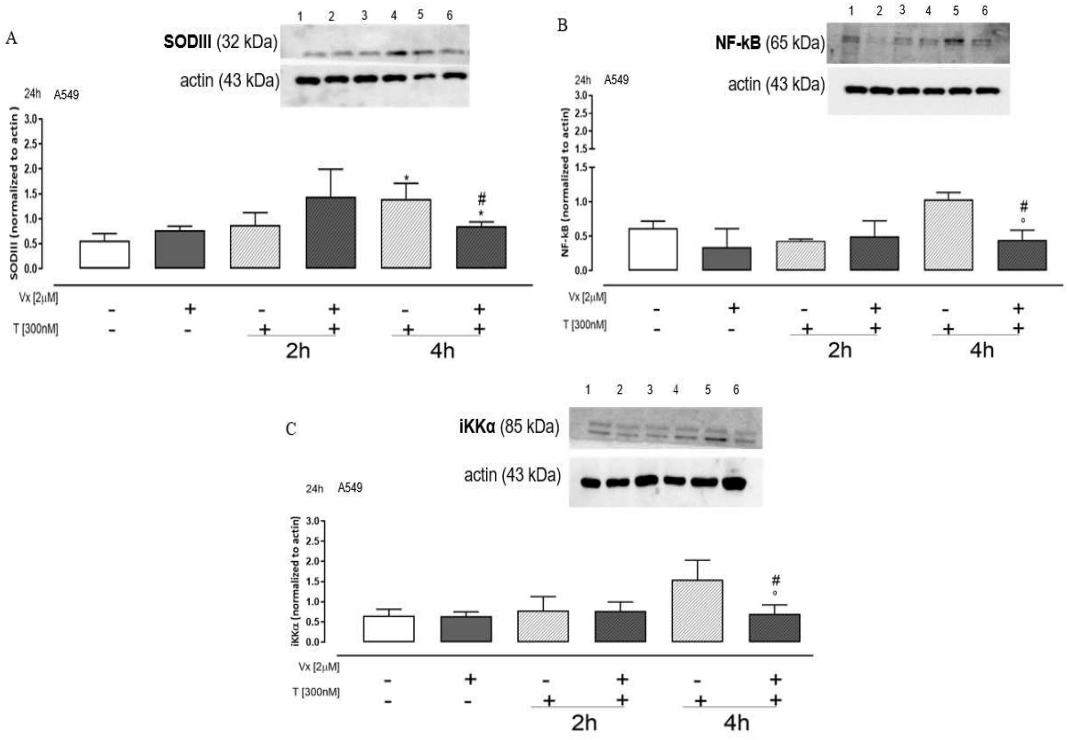


**Figure 18:** *The effect of Vx-809 on the inflammatory pathway. Western blot analysis: 1 = ctrl, 2 = Vx809, 3 = TG for 2 h, 4 = Vx-809 after pre-treatment with TG for 2 h, 5 =*

*TG for 4 h, 6 = Vx-809 after pre-treatment with TG for 4 h. Cells were pretreated with 300 nM TG for 2 or 4 h to induce ER stress. Subsequently, 2 μM of the corrector Vx-809 were administered for 24 h. SODIII (A), NF-kB (B), and iKKα (C) expressions were detected by Western blot analysis. Actin protein expression was used as a loading control. Results are expressed as mean ± S.E.M. from at least three independent experiments each performed in triplicate. Data were analyzed by a Mann–Whitney U test. * $p < 0.05$ vs. non-treated cells; ◦ $p < 0.05$ vs. Vx-809–treated cells; # $p < 0.05$ vs. TG-treated cells.*

### 3.3 Discussion

The ER is a pivotal organelle involved in protein processing as well as in the maintenance of cellular homeostasis. The accumulation of misfolded proteins triggers ER stress, followed by an adaptive response mediated by the activation of the UPR through its three main signaling branches: PERK, IRE1α, and ATF6. It is well established that the ER stress response regulates the onset, progression, and severity of several diseases, including cancer, diabetes, atherosclerosis, obesity, and neurodegenerative disorders. Lumacaftor (Vx-809) is a small-molecule corrector used in the treatment of CF. It targets the misfolded CFTR protein, promoting its proper folding and intracellular trafficking, thereby increasing the amount of functional protein at the cell surface (Berkers *et al.,* 2021).

The experimental model used in this thesis employs TG (300 nM), a well-known ER stress inducer (Wang *et al.,* 2014), to mimic the condition of ER stress caused by the accumulation of misfolded or unfolded proteins. TG acts by releasing calcium into the cytoplasm, thus reducing its availability for essential protein-folding processes.

Considering that the exact mechanism of action of these correctors remains incompletely understood and that no studies have clearly demonstrated a direct link between Vx-809 and CFTR in living cells, the first chapter of this work presents preliminary experiments designed to assess the potential involvement of Vx-809 in the complex protein processing machinery within the ER, where CFTR folding also takes place.

The involvement of Vx-809 in the UPR pathway was observed. The UPR represents the specific cellular response to alterations caused by misfolded

proteins; therefore, the ability of Vx-809 to modulate the protein expression levels of the main UPR sensors, analyzed by Western blot, provides strong indirect evidence of its role in supporting protein folding.

The induction of ER stress in the experimental model was confirmed by the increased expression of the ER-resident chaperone BiP following TG pretreatment. BiP is one of the most abundant proteins within the ER (Bakunts et al., 2017). It operates through a typical Hsp70 chaperone-substrate mechanism, in which misfolded proteins are recruited to the substrate-binding domain (SBD) of BiP by J-domain cochaperones (Kopp et al., 2019). After 24 hours of Vx-809 treatment, BiP expression significantly decreased, showing the same trend in both cell lines analyzed. A similar pattern was also observed for other key proteins involved in UPR regulation. Specifically, Vx-809 significantly reduced the expression of ATF4, ATF6, phosphorylated-PERK (pPERK), and CHOP. Overall, these findings demonstrated that Vx-809 was able to restore ER homeostasis that had been disrupted by cellular stress.

The fate of the cell depends also on the activity of the proteins involved in the UPR pathway. When the stress stimulus cannot be resolved and becomes chronic, cells initiate the apoptotic process. Indeed, CHOP is a pro-apoptotic transcription factor whose expression is directly promoted by ATF4 (Chipurupalli *et al.,* 2021). Furthermore, it has been reported that in cultured human cells, the activation of caspase-4 is induced and modulated by ER stress (Hitomi *et al.,* 2004). To investigate whether Vx-809 might also be involved in ER stress-induced apoptosis, both the percentage of hypodiploid nuclei and the activation of caspase-4 were evaluated by FACS analysis. According to the experimental model, treatment with TG led to a significant increase in both parameters; however, Vx-809 administration, in both cell lines and across all experimental time points, resulted in a marked reduction of caspase-4 activation and hypodiploid nuclei. These findings strongly suggest that the corrector Vx-809 also plays a protective role against apoptosis associated with the accumulation of misfolded proteins.

Under conditions of ER stress, several cellular equilibria undergo significant alterations. In fact, both ER stress and oxidative stress play crucial roles not

only in pathological but also in physiological contexts. The major defense networks that enable cells to adapt and survive under adverse conditions are activated in response to ER stress, oxidative stress, and inflammatory processes. Conversely, when these stressors become chronic, the resulting persistent ER stress, oxidative stress, and inflammation contribute to the onset and progression of numerous human diseases. To investigate these mechanisms, flow cytometry analyses were performed using the fluorescent probes DCHF-DA and MitoSOX to assess intracellular and mitochondrial ROS levels, respectively, in the presence and absence of the drug. As expected, ER stress induced by TG also triggered oxidative stress, as indicated by elevated ROS levels. Conversely, treatment with Vx-809 significantly reduced ROS production in both compartments, suggesting not only its ability to attenuate oxidative stress but also a potential modulatory effect at the mitochondrial level.

It has been extensively reported that calcium ions are essential for the proper functioning of the ER and for the activity of several calcium-dependent chaperones residing within this organelle. Moreover, calcium dysregulation underlies a wide range of human diseases. To assess the potential involvement of Vx-809 in calcium homeostasis, spectrofluorimetric experiments were performed using the fluorescent probe FURA-2AM in a calcium-free buffer. The results showed that in A549 cells subjected to ER stress, treatment with the corrector improved protein-folding conditions, favoring the recovery of both reticular and cytosolic $Ca^{2+}$ accumulation and reducing the levels of free calcium that are detrimental to cell viability. The ER serves as one of the major intracellular calcium reservoirs, the maintenance of luminal ER $Ca^{2+}$ steady-state levels is thus crucial for homeostasis and is regulated by the sarco-endoplasmic reticulum Ca2+ ATPase (SERCA) pumps, which couple ATP hydrolysis with active transport of Ca2+ from the cytosol back into the ER lumen.

Western blot analysis revealed that, following Vx-809 treatment, SERCA II expression was reduced, suggesting an improvement in calcium handling. This finding indicates that, during ER stress, the upregulation of SERCAII

represents a compensatory mechanism aimed at lowering cytoplasmic calcium levels by enhancing its reuptake into the ER. Treatment with the corrector appears to alleviate ER stress, thereby reducing the need for calcium sequestration from the cytosol and leading to decreased SERCAII expression.

As previously discussed, both ER stress and oxidative stress can trigger inflammatory processes. The primary goal of the cell under these conditions is to restore its original homeostatic state. The expression of the SOD3 protein is induced by pro-inflammatory cytokines (Choi *et al.,* 2023) and represents one of the main enzymatic defenses responsible for neutralizing reactive oxygen species (ROS). Accordingly, the data showed that, following ER stress induction with TG for 4 hours, cells activated protective mechanisms by increasing the expression of antioxidant proteins such as SOD3, in an attempt to counteract ROS-mediated damage. Treatment with the corrector markedly reduced SOD3 expression, further demonstrating the ability of this small molecule to assist cells in re-establishing their physiological homeostatic balance. It is well established that inflammation and ER stress are interconnected processes. Both represent short-term adaptive mechanisms essential for cellular function and organismal survival, yet both become detrimental when chronically activated. The contribution of Vx-809 to mitigating the inflammatory process associated with ER stress induced by the accumulation of misfolded proteins was further evaluated by examining its ability to modulate the expression of key regulatory factors within the proposed experimental model. Treatment with Vx-809 resulted in a significant reduction in IKKα levels, accompanied by a parallel decrease in NF-κB expression. These findings indicate that the corrector inhibited the NF-κB signaling pathway, a central regulator of inflammation, thereby limiting the propagation of the inflammatory response. Taken together, these preliminary findings provide highly promising evidence, suggesting that treatment with Vx-809 could potentially be extended to other disorders in which protein misfolding and the resulting ER stress play a key pathogenic role, such as neurodegenerative diseases including Parkinson’s and Alzheimer’s disease. The remarkable potential of this corrector lies in its ability not only to attenuate key markers of the UPR but also to mitigate major pathological processes

associated with ER dysfunction, including oxidative stress, inflammation, apoptosis, and calcium dysregulation.

In conclusion, these preliminary observations collectively suggest that Vx-809 holds significant therapeutic promise beyond its established role in CF. By alleviating ER stress and promoting proper protein folding, this corrector may represent a valuable tool in conditions where protein misfolding and ER dysfunction are central to disease progression, such as neurodegenerative disorders including Parkinson's and Alzheimer's disease. The broad potential of Vx-809 lies in its multifaceted action, capable not only of reducing the main markers of the UPR but also of mitigating interconnected pathological processes such as oxidative stress, inflammation, apoptosis, and calcium imbalance. These findings open new perspectives for future studies aimed at exploring the wider applicability of Vx-809 as a modulator of ER homeostasis and cellular stress responses.

# Chapter IV

# From VX-809 to VX-445: Exploring ER Stress Modulation and Mechanistic Pathways in SH-SY5Y Neuroblastoma Cells

## 4.1 Introduction

Neurodegenerative diseases feature a progressive, region-specific loss of neuronal function. Despite heterogeneity in symptoms and prevalence, they share a chronic, age-linked course, selective neuronal degeneration, and a common hallmark: aggregation of intrinsically disordered proteins (IDPs). IDPs can fold upon binding to protein or nucleic-acid partners, or undergo only local ordering; although the aggregates differ across disorders, the core misfolding process and its key features are largely similar (Soto *&* Pritzkow, 2018). Neuronal cells are highly sensitive to protein misfolding, which, if not managed by the cell, leads to synaptic dysfunction, apoptosis, and selective neuronal death (Ghemrawi *et al.,* 2020). In cases of severe protein misfolding, harmful effects may arise from a “gain of function,” as in Alzheimer’s disease (AD), Parkinson’s disease (PD), and Huntington’s disease, or from a loss of function, as in cystic fibrosis (CF). Consequently, proteostasis, which prevents aberrant protein aggregation, is essential to maintain cellular health and function.

The accumulation of misfolded proteins induces ER stress, which triggers the UPR and downstream pathways to restore the initial homeostatic state. The buildup of toxic protein species can kill neurons, and a growing body of studies identifies ER stress as a key mechanism underlying this neurotoxicity. Given the strong evidence for UPR activation in patients, such findings have increased interest in pharmacological modulation of the UPR as a potential disease-modifying approach in various neurodegenerative disorders. Closely linked to ER stress and neurodegenerative diseases is the dysregulation of

calcium homeostasis. In AD, for example, dysregulated cytosolic Ca2+ leads to ER-stress-mediated apoptosis and ER dysfunction; in PD, enhanced Ca2+ influx results in cell death (Magrinelli *et al.,* 2022). In this pathological framework, the ER redox balance, connected to both protein folding and cellular calcium homeostasis, is also compromised. Indeed, neurodegeneration associated with chronic ER stress may result from a synergistic combination of protein misfolding and accumulation of ROS (Goldsteins *et al.,* 2022).

Natural, synthetic, or pharmacological chaperones have shown promising results in the management of numerous protein conformational diseases and misfolding-induced neurotoxicity can be mitigated by increasing chaperone expression. Considering the hypotheses that have positioned VX-809 as a potential candidate for treating PMDs, and based on prior results in adenocarcinomic human alveolar basal epithelial cells (A549) and malignant melanoma cells (A375), where VX-809 was shown to modulate key effects associated with misfolded-protein-induced ER stress, this second chapter evaluates whether the potential off-label mechanism of VX-809 also extends to a neuroblastoma cell model, used *in vitro* to study neuronal function and differentiation, thereby allowing us to hypothesize the use of VX-890 for the treatment of NDs.

Furthermore, the literature extensively describes how these correctors interact with isolated CFTR domains *in vitro* or under non-physiological conditions, and it indicates that direct binding of correctors to CFTR in the complex cellular environment has yet to be demonstrated (Amico *et al.,* 2019; Fiedorczuk & Chen, 2022). These studies were undertaken to elucidate the drugs' mechanism of action, which remains incompletely defined. This knowledge gap, together with growing evidence that VX-809 may act through a broader mechanism involving interactions with additional protein partners and reducing ER stress induced by protein misfolding, highlights the need for further investigation.

In light of the replacement of VX-809 by VX-445 (Elexacaftor) in triple-combination therapy with potentiators, and their different chemical frameworks

and classifications (type 1 for VX-809, type 3 for VX-445), the present study expression proteomics was performed on SH-SY5Y neuroblastoma cells to examine changes in protein expression in the presence or absence of VX-445 under ER-stress conditions. Moreover, to probe the putative mechanism of action of VX-445 and identify potential protein interaction partners, an *in vitro* DARTS functional proteomics approach was applied. This analysis enabled the identification of protein partners primarily involved in oxidative stress and calcium regulation.

## 4.2 Results

### *4.2.1 Role of Vx-809 in UPR Pathway*

In neuronal cells, we applied the same experimental paradigm: ER stress due to misfolded-protein accumulation was induced with 300 nM TG for the indicated times. By blocking the SERCA pump, TG disrupts $Ca^{2+}$ homeostasis and mimics ER-stress conditions (Sehgal *et al.,* 2017), thereby activating key UPR proteins. Selected UPR-related proteins were assessed by Western blotting of cell lysates. As GRP78/BiP is a principal ER-stress sensor [26], western blot analysis of SH-SY5Y extracts showed that TG significantly increased GRP78/BiP levels at all pretreatment times ($p < 0.001$), confirming ER stress. Addition of VX-809 significantly reduced TG-induced GRP78/BiP overexpression, particularly at 30 min ($p < 0.05$) and 4 h ($p < 0.005$), as shown in Figure 19A.

Other UPR proteins were then examined. Given the importance of PERK signaling in neurodegeneration, the activated (phosphorylated) form, p-PERK, was evaluated by Western blotting. PERK activation is identified by the characteristic band shift of p-PERK, which results from autophosphorylation-dependent increases in apparent molecular weight [9]. The band shift was observed only in cells exposed to the stressor TG. Compared with TG alone, VX-809 reduced the p-PERK band shift as early as 1 h of TG pretreatment. We also assessed ATF4, a transcription factor induced downstream of PERK. As expected, ATF4 protein levels were significantly increased at all time points following TG treatment ($p < 0.001$). VX-809 significantly decreased TG-

induced ATF4 expression ($p < 0.005$), confirming its capacity to modulate ATF4 activation in neuroblastoma cells (Figure 19C).

The other essential UPR arm, ATF6, was analyzed next. Although the literature reports divergent roles, recent studies indicate that activation of ATF6 signaling in the brain can improve neuronal function (Wang *et al,* 2022). In our neuroblastoma cells, total ATF6 expression increased after 1 h and 4 h of TG pretreatment versus controls, consistent with ER-stress induction and UPR onset. VX-809 significantly reduced TG-induced ATF6 expression, particularly at 4 h ($p < 0.05$), restoring a physiological profile (Figure 19D). Finally, the third UPR branch, IRE1, was indirectly evaluated by RT-PCR. These experiments showed that VX-809 exertrd a corrective effect on XBP1 splicing (Figure 19B), a crucial transcription factor whose mRNA is spliced by the RNAse domain of IRE1 upon ER-stress activation.

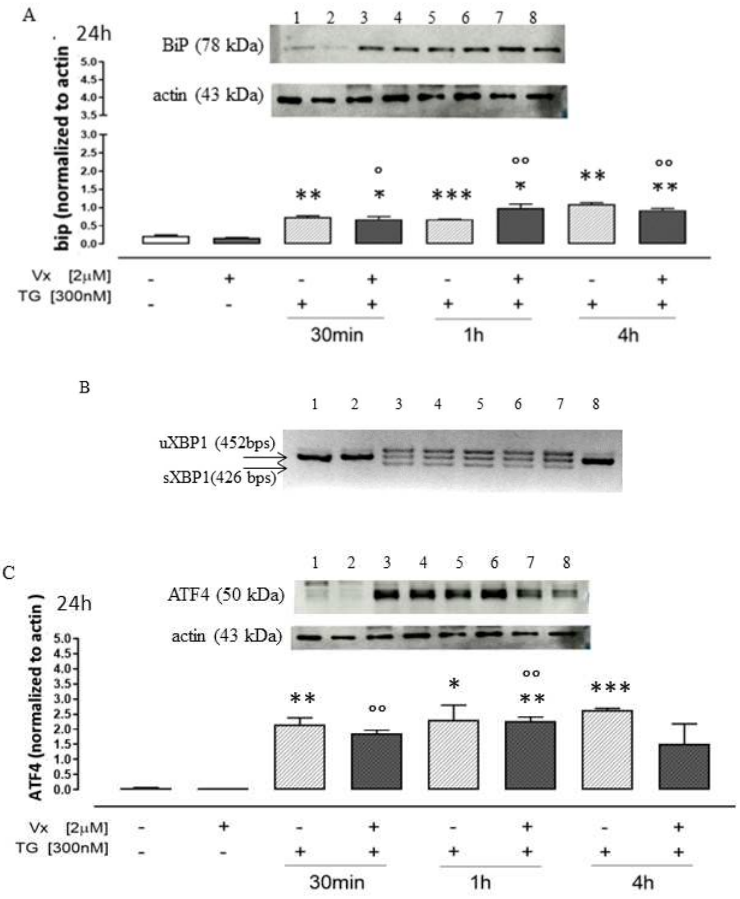

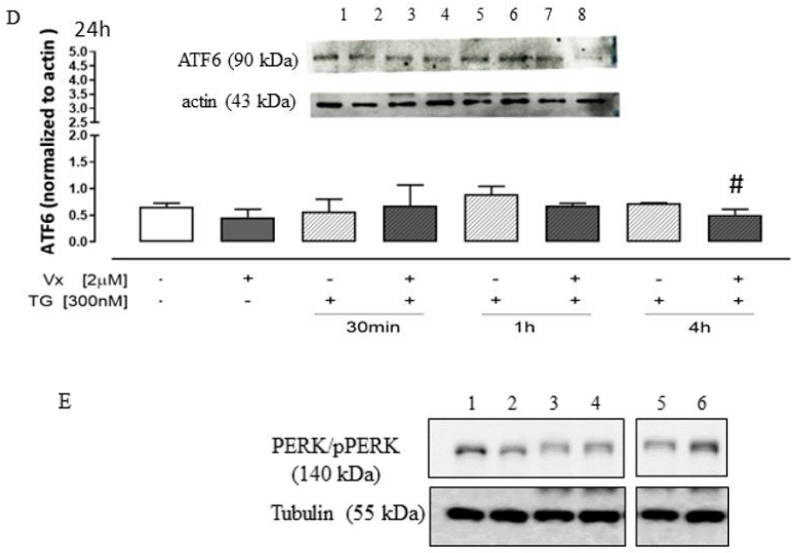


**Figure 19:** *Vx-809 acts on the UPR activation. The cells have been treated by the mentioned experimental protocol. BiP (Panel A), ATF4 (Panel C), ATF6 (Panel D), and PERK/pPERK (Panel E) expressions in Neuroblastoma cells were revealed by Western blot analysis and expression of actin or tubulin was employed as a loading control. 1: Ctrl, 2: Vx-809, 3: TG (30 min), 4: Vx-809 after TG (30 min) pre-treatment, 5: TG (1h), 6: Vx-809 treatment after TG (1h) pre-treatment, 7: TG (4h), 8: Vx-809 after TG (4h) pre-treatment. Panel B illustrates the gel migration of the 452 bps unsplit fragment of XBP1 mRNA (XBP1 u) and the 426 bp split fragment (XBP1 s), achieved by PCR. These results are presented as the average ± standard error of at least three separate, triplicate-performed studies. Data were processed according to the Mann-Whitney U-test. *P < 0.05, **P < 0.005 and ***P < 0.001 vs untreated cells; °P < 0.05 and °°P < 0.005 vs Vx-809 treated cells; #P < 0.05 vs TG treated cells.*

### *4.2.2 Vx-809 modulates Calcium signaling*

Since $Ca^{2+}$ dysregulation is one of the pathological factors underlying neurodegenerative diseases, we evaluated whether the corrector VX-809 could modulate intracellular calcium concentrations using FURA 2-AM in a calcium-free incubation medium. TG (1 nM) was used to assess ER calcium content. As shown in Figure 20, the delta (Δ) increase in ER calcium levels in VX-809-treated cells pretreated with TG for 30 min and 1 h was significantly higher ($p < 0.05$) than in TG-treated cells, indicating higher calcium retention in the ER, with improved calcium homeostasis. To study cytosolic calcium concentration, a potent and selective $Ca^{2+}$ ionophore, Ionomycin (1 μM), was used. Results showed that administration of the corrector during the 24 h following TG-induced stress produce a Δ increase in intracellular calcium

levels higher than that observed in TG-treated cells, suggesting improved intracellular calcium storage (Figure 20B) compared with cells not treated with the corrector.

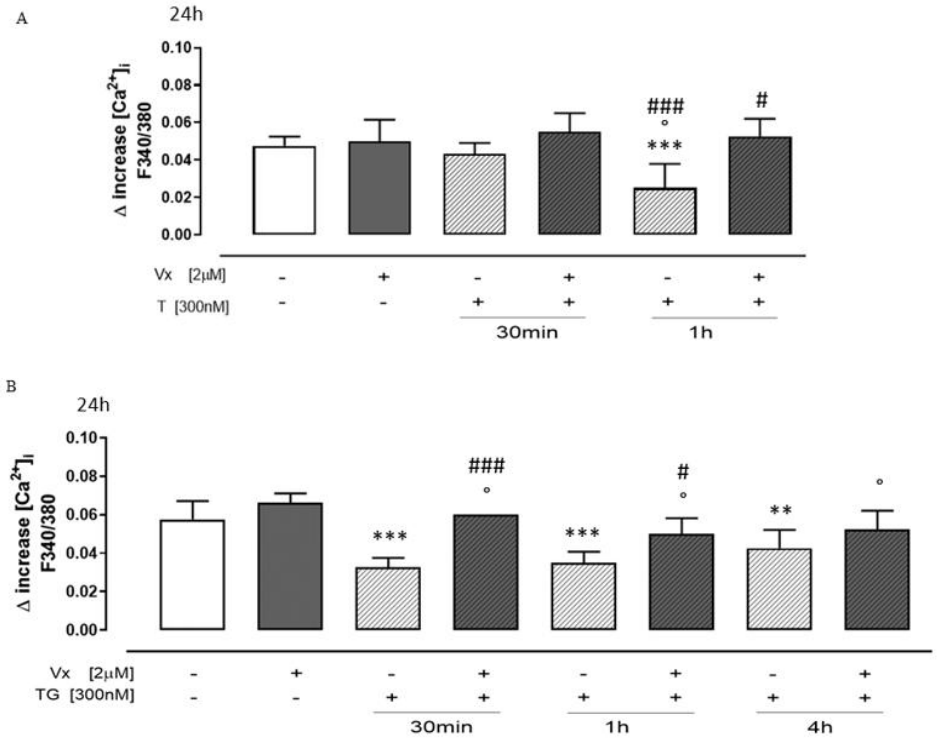


**Figure 20***: After TG-ER stress, the Vx-809 effect was determined on the reticular calcium pool in cells in calcium-free media in the presence of 1nM TG (Panel A), and intracellular calcium concentration was quantified using 1 μM of ionomycin (Panel B). Results show the mean ± S.E.M. of the delta (δ) increase in the fluorescence of the FURA 2 ratio (340/380 nm) from a minimum of three separate experiments, each carried out in duplicate. The findings are presented as the average ± standard error of duplicate data from a minimum of three separate and identical tests. Mann-Whitney U test analysis was done on the data. **P < 0.005 and ***P < 0.001 vs untreated cells; °P < 0.05 vs Vx-809 treated cells; #P < 0.05 and ###P < 0.001 vs TG treated cells*

### *4.2.3 The corrector Vx-809 is able to decrease both cytosolic and mitochondrial ROS levels*

ER stress activates interconnected pathways; notably, oxidative stress increases due to higher levels of ROS, affecting both the ER and mitochondria, which are tightly linked. Mitochondria are essential for neuronal survival and function and neuronal membranes contain high levels of polyunsaturated fatty acids, making them particularly susceptible to ROS damage. To investigate the effects of VX-809 on TG-induced cytosolic and mitochondrial ROS

production, flow-cytometric analyses were performed using the fluorescent probes DCHF-DA and MitoSOX Red, respectively. Our experiments showed that VX-809 treatment significantly reduced ($p < 0.001$) cytosolic (Figure 21A) and mitochondrial (Figure 21B) ROS levels in TG-treated cells at all experimental time points. SOD III, the major antioxidant enzyme that removes superoxide anions in cells and protecting against brain injury (Sun *et al.,* 2019) were also examined. Western blot analysis showed a significant increase ($p < 0.05$) in SOD III expression at 1 h and 4 h in VX-809-treated cells after induction of ER stress compared with TG-treated cells (Figure 21C), likely counteracting the ROS-related stress.

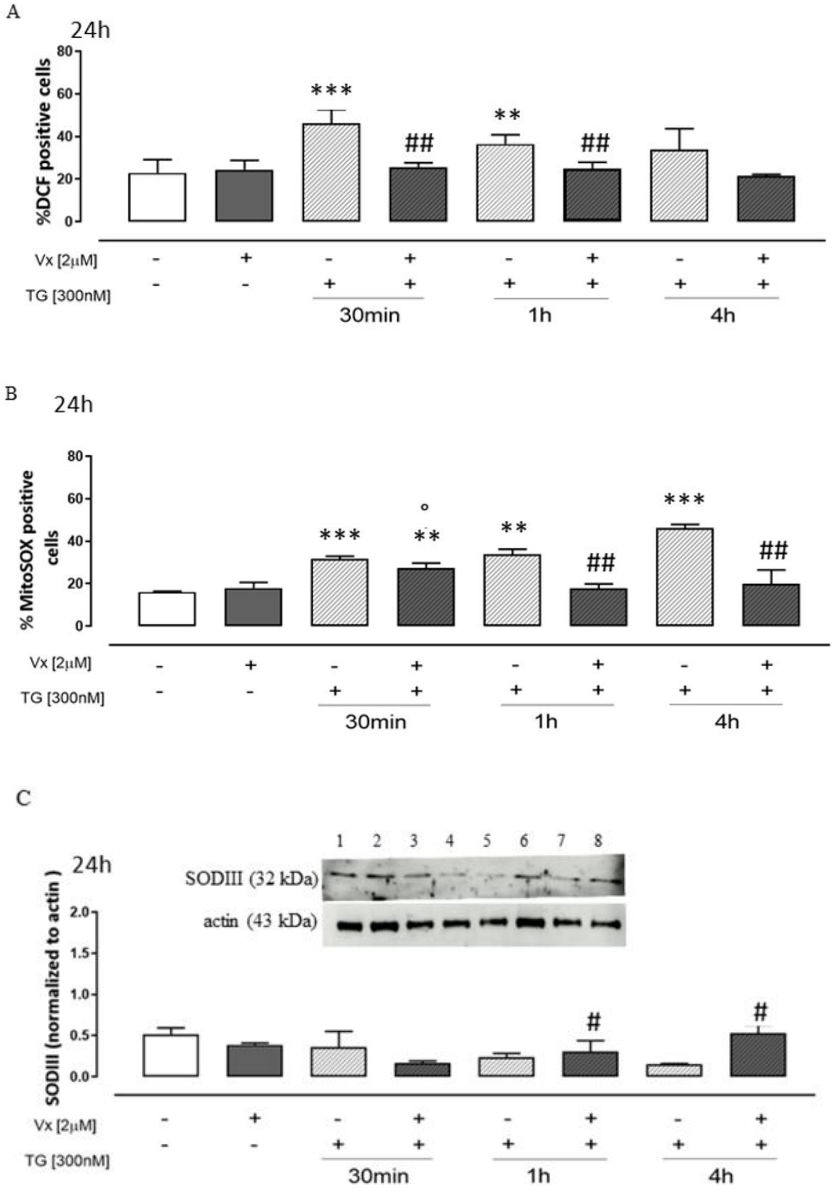

**Figure 21:** *Vx-809 mitigates the TG-induced oxidative damage. SHSY-5Y cells line was treated in according to the experimental plan. The probe 2',7'-dichlorofluorescein diacetate (H2DCF-DA) was used to measure the amount of ROS produced (Panel A). The percentage of DCF-positive cells in at least three independent experiments, each conducted in duplicate, was used to express the mean ± SEM of ROS generation. Using the MitoSOX Red probe, flow cytometry analysis was used to measure the amount of superoxide produced by the mitochondria in cells (Panel B). The expression of mitochondrial superoxide generation was calculated as the mean ± standard error of the proportion of cells positive for MitoSOX in three separate tests, each carried out in duplicate. SODIII expressions (Panel* ***C****) on Neuroblastoma cells were detected by Western blot assay. 1: Ctrl, 2: Vx-809, 3: TG (30 min), 4: Vx-809 after TG (30 min) pre-treatment, 5: TG (1h), 6: Vx-809 treatment after TG (1h) pre-treatment, 7: TG (4h), 8: Vx-809 after TG (4h) pre-treatment. Actin protein expression was used as loading control. Mann-Whitney U test was used to evaluate the data. **P < 0.005 and ***P < 0.001 vs untreated cells; °P < 0.05 vs Vx-809 treated cells; #P < 0.05 and ##P < 0.005 vs TG treated cells*

### *4.2.4 Vx-809 modulates Apoptotic process to Enhance Cellular Survival*

The first cellular response to ER-stress is UPR-activation to try to restore cellular homeostasis; however, if this mechanism fail, programmed cell death pathways are activated. Apoptosis is well-known to be the main form of neuronal death.

To assess the progression of the apoptotic process, flow cytometry was performed, to quantify both the percentage of hypodiploid nuclei with propidium iodide and the activation of caspase-4, an ER-resident protease specifically activated as a result of apoptosis induction mediated by ER stress. Caspase-4 is cleaved by calpain under ER stress conditions, and suppression of its activity partially inhibits cell death in humans, underscoring its critical role in ER stress- mediated apoptosis (Chukai *et al.,* 2022). Flow cytometry data (Figures 22A and 22B) from SH-SY5Y cells pre-treated with TG show increased levels of both apoptotic parameters. In contrast, Vx-809 administration significantly reduced ($p < 0.001$) both the percentage of hypodiploid nuclei and the caspase-4 expression at 30 min and at 4h of TG-pre-treatment. These results highlight the protective effect of the drug against apoptosis in neuronal cells.

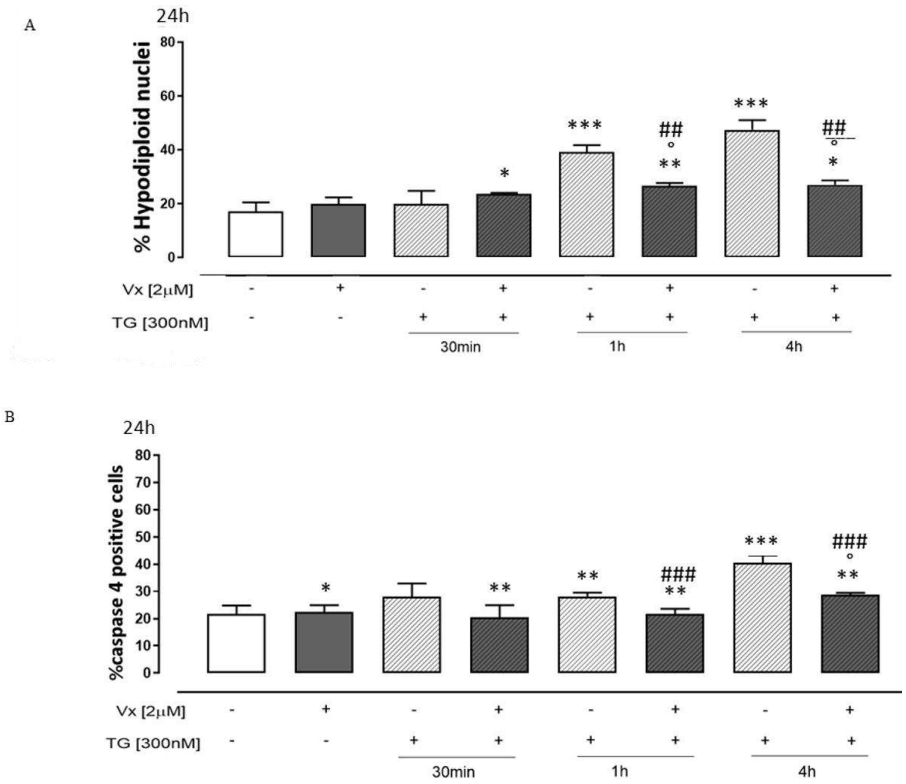


**Figure 22***: Vx-809 alters the process of apoptosis. SHSY-5Y cell line was treated following the experimental protocol. After, cells were stained by propidium iodide and fluorescence of individual nuclei was evaluated by flow cytometry (Panel A). The data are presented as the mean ± standard error of the percentage of hypodiploid nuclei from a minimum of three independent tests, each carried out in duplicate. The percentage of caspase 4 positive cells (Panel B) from at least three separate experiments, each carried out in duplicate, was given as mean ± S.E.M. The Mann-Whitney U test was utilized for data analysis. *P < 0.05, **P < 0.05 and ***P < 0.001vs non-treated cells; °P < 0.05 vs Vx-809 treated cells; ##P < 0.005 and ###P < 0.001 vs TG treated cells*

### *4.2.5 Vx-445 Fights Oxidative Stress triggered by ER-Stress condition*

Oxidative and endoplasmic reticulum stress are closely related and alterations in the cellular environment can exacerbate both, contributing to the development of various human pathologies. To evaluate whether the Vx-445 corrector also modulates the oxidative stress in the SH-SY5Y cell line, total ROS production induced by TG with or without Vx-445 were measured, using cytofluorimetric analysis with the fluorescent probe $H_2$DCF-DA. The result demonstrates that treatment with Vx-445 significantly reduced cytosolic ROS levels (Figure 23) in TG-treated cells at all evaluated time points.

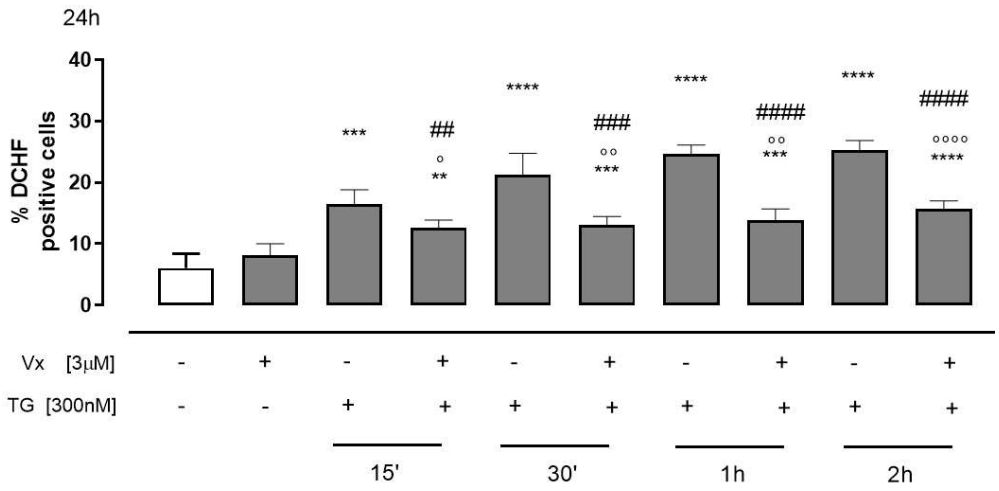


**Figure 23**: *Vx-445 acts on Thapsigargin induced-oxidative stress. To mimic the ER stress condition, cells were pretreated with 300 nM TG for different experimental times (15 min, 30 min, 1 h, and 2 h). The corrector Vx-445 (3 μM) was then administered for 24h. The probe 2',7'-dichlorofluorescein diacetate ($H_2$DCF-DA) was used to measure the amount of ROS produced in SH-SY5Y cells. The percentage of DCF-positive cells in at least three independent experiments, each conducted in triplicate, was used to express the mean ± SEM of ROS generation. The Mann–Whitney U test was used to evaluate the data. ** p < 0.005 and *** p < 0.001, **** p < 0.0001 vs. untreated cells; ° p < 0.05, °° p < 0.005, °°°° p < 0.0001 vs. Vx-445 -treated cells; ## p < 0.005, ### p < 0.001, #### p < 0.0001 vs. TG-treated cells.*

### *4.2.6 Vx-445 acts on Calcium Homeostasis after TG-ER-stress Induction*

The ER serves as the main intracellular calcium reserve, furthermore calcium plays a crucial role not only in the folding of proteins within the ER, supported by various calcium-dependent chaperones, but also as a key mediator of intracellular signaling in response to stimuli such as second messengers, kinases and other modulators (Liu *et al.,* 2024).

Given the fundamental importance of calcium homeostasis and its wide-ranging effects on physiology, whether the Vx-445 corrector could modulate this pathway like the previous corrector was investigated. The impact of Vx-445 on intracellular calcium concentrations was assessed using FURA-2 AM in a calcium-free incubation medium. To evaluate total cytosolic calcium levels Ionomycin (1 μM), was employed. The results (Figure 24) show that cells pretreated with TG and subsequently exposed to Vx-445 exhibited a significant increase ($p < 0.001$) in intracellular calcium levels compared with cells treated

with TG alone. These findings suggest that Vx-445 may restore intracellular calcium levels during the 24-hour treatment period, bringing them to their initial physiological state.

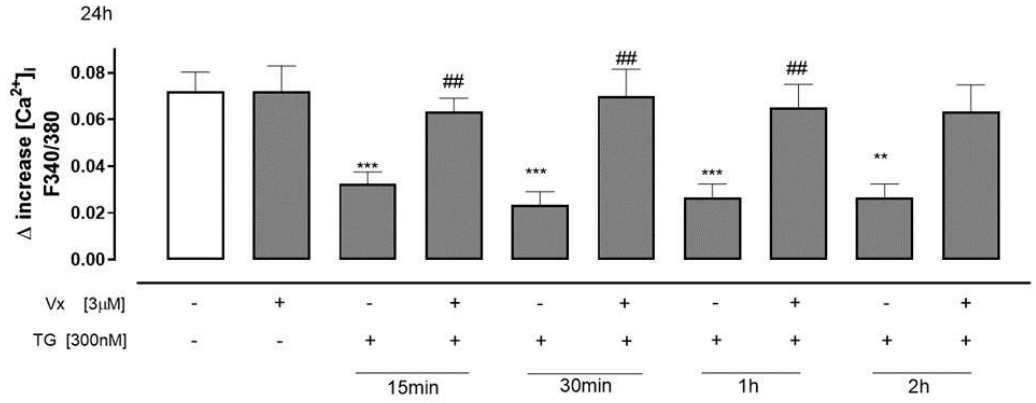


**Figure 24***: Vx-445 restores calcium homeostasis. To induce the ER-stress conditions, SHSY-5Y cells were pretreated with 300 nM TG in different experimental times: 15 min, 30 min, 1h and 2h. After that, Vx-445 (3 μM) was added for 24 h. The activity of Vx-445 on total calcium levels, after induced ER stress condition, was determined and quantified in cells in calcium-free media in the presence of 1 μM of Ionomycin (panel X). The results show the mean ± S.E.M. of the delta (Δ) increase in the fluorescence of the FURA 2 ratio (340/380 nm) from a minimum of three separate experiments, each carried out in triplicate. The findings are presented as the average ± standard error of triplicate data from a minimum of three separate and identical tests. The Mann–Whitney U test analysis was performed on the data. ** p < 0.005 and *** p < 0.001 vs. untreated cells; # p < 0.05 and ## p < 0.005 vs. TG-treated cells.*

### *4.2.7 Vx-445 shows mitochondrial action by modulating the release of cytochrome c*

The ER maintains extensive interactions with nearby organelles, including mitochondria, phagosomes, endosomes, lysosomes, and the plasma membrane (Lin *et al.,* 2021). Notably, the accumulation of misfolded proteins during ER stress has been shown to impair mitochondrial activity (Cortés Sanchón *et al.,* 2021). To investigate whether Vx-445 influences this process, cytochrome c (CytC) release was evaluated by Western blot analysis. According to the experimental protocol, TG was administered at the designated time points to induce ER stress in the SHSY-5Y cell line. Protein expression analysis shows an increase in CytC release after 1h of TG pretreatment, confirming the onset of stress condition. Conversely, exposure to Vx-445 for 24 hours reduced CytC levels (p<0,05), suggesting that Vx-445

may alleviate ER stress and indirectly contribute to restoring normal mitochondrial function (Figure 25).

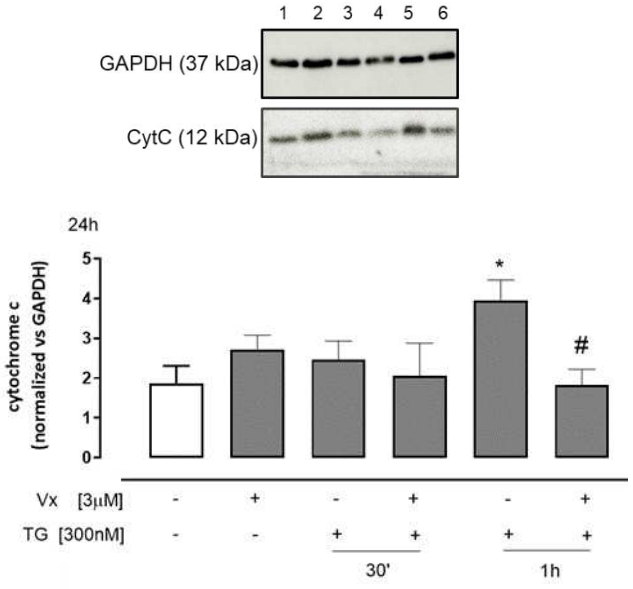


**Figure 25**: *Vx-445 reduces the release of mitochondrial CytC into the cytoplasm. Following the experimental plan, SHSY-5Y cells were pretreated with 300 nM TG in different experimental times: 30 min and 1h to induce thee ER-stress conditions: After that, Vx-445 (3 μM) was administrated for 24 h. The expression of CytC in neuroblastoma cell line was evaluated by Western Blot assay. 1= ctrl; 2 = Vx-445 ;3 = TG for 30 min; 4 = Vx-445 after TG pre-treatment for 30 min; 5 =TG for 1 h; 6 = Vx-445 after TG pre-treatment for 1 h. GAPDH protein expression was used as loading control. Results are expressed as mean ± S.E.M. from at least three independents. The Mann–Whitney U test analysis was performed on the data. * p < 0.05 vs. untreated cells; # p < 0.05 vs. TG-treated cells.*

### *4.2.8 Vx-445 reduces the expression of proteins with oxidoreductase activity, induced under cellular stress conditions.*

Proteomic expression analysis based on mass spectrometry with unlabeled quantification (LFQ) was performed to obtain a deeper understanding of the molecular mechanisms of Vx-445 action on SHSY-5Y cells. Three sets of samples were analyzed: proteins obtained from SHSY-5Y cell lysates under basal condition (control sample, CTRL), proteins obtained after 2 hours TG treatment (stress sample, TG) and proteins extracted after 24 hours treatment with TG and Vx-445 (corrector sample, TG_Vx-445). These samples were subjected to trypsin digestion and analyzed in parallel via nano-UHPLC-MS/MS.

A comprehensive bioinformatic analysis was then carried out to compare changes in proteins abundance across treatments. Approximately 7500 proteins groups were identified and quantified, and the differentially expressed proteins (DEPs) are detailed in the heat map reported in Figure 26.

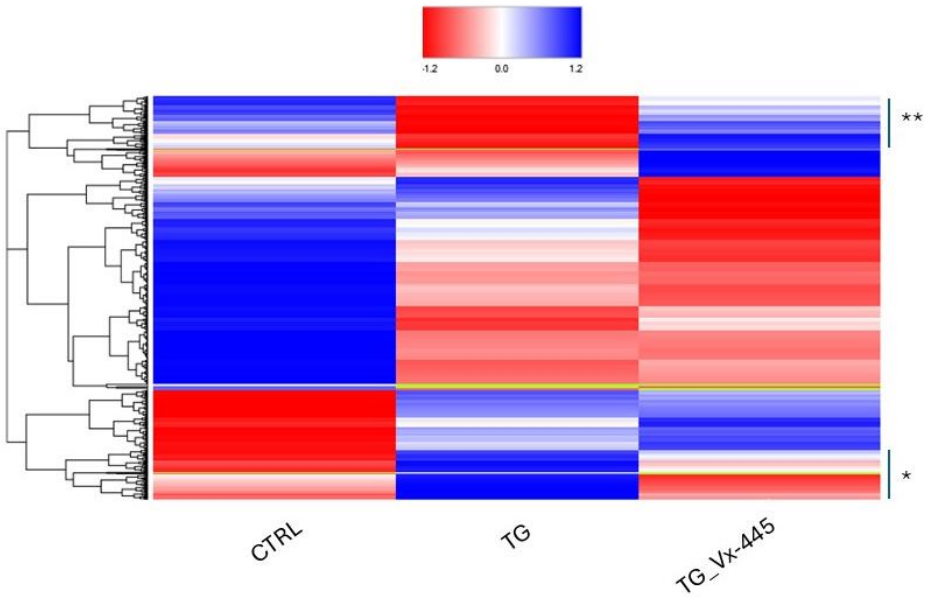


**Figure 26**: *Hierarchical clustering of SHSY-5Y proteome alterations upon TG and TG-Vx-445 treatment compared to CTRL. The red and the blue colors in the heat map are referred to the low and high abundance proteins, respectively. The * and ** segments are referred to proteins clusters whose abundance is altered by TG vs CTRL and restored by Vx-445.*

The proteomic profile revealed substantial variations in protein expression among the different populations. As highlighted in Figure 26, two segments of the heat map, marked by asterisks, are of particular interest: the one-asterisk segment (*) includes proteins that are upregulated by TG relative to the control and subsequently down regulated after Vx-445 treatment; on the other hand, the two-asterisks segment (**) contains proteins that are down regulated by TG relative to control cells and restored by Vx-445. The proteins belonging to the * (175 hits) and ** (20 hits) segments were independently subjected to STRING- based clustering analysis, as shown in Figure 27.

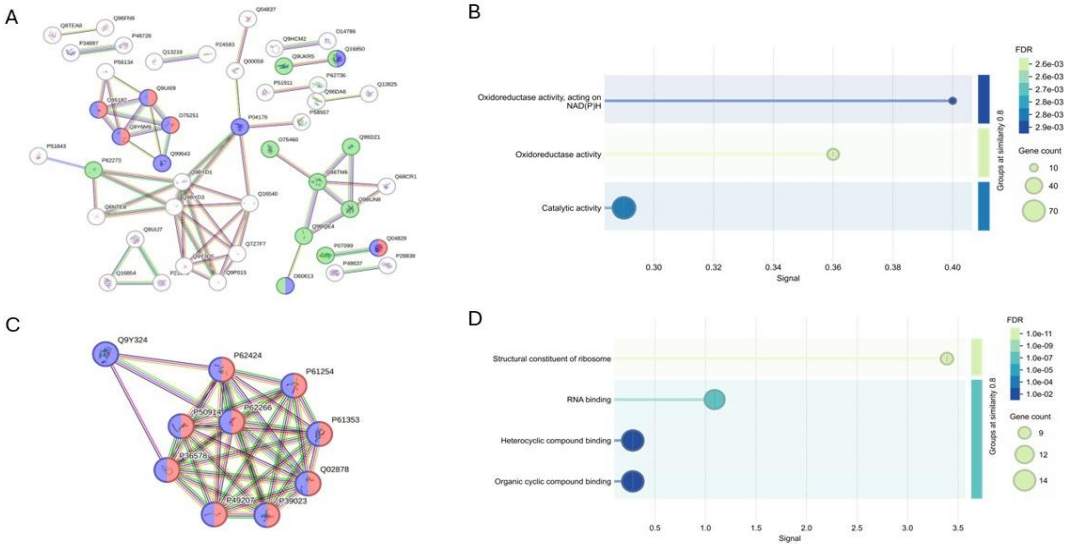


**Figure 27***: Cluster analysis of the proteins belonging to the * (A) and ** (C) segments, obtained by STRING software with a 0.7 confidence level. The disconnected nodes are hidden. Each protein is reported using its Uniprot code. Gene ontology (GO) enrichment analysis by molecular function of the proteins belonging to the * (B) and ** (D) segments, obtained by STRING software. The order of appearance in the bar graph is related to enrichment of proteins in each biological pathway. The FDR value is also reported*

The cluster and gene ontology analysis of the proteins in the * segment (Figure 27A and 27B) revealed that many of these proteins are localized to the ER (Figure 27A in green), as several possess oxidoreductase activity, either NAD[P]H dependent or independent (Fig. 5A in blue and red, respectively and Fig. 5B). This is in full agreement with the evidence that VX-445 counteracts oxidative stress: cells up regulate the expression of oxidoreductase enzymes after TG treatment and this upregulation is reversed when the corrector is added. Within * segment proteins, two hits are involved in calcium regulation, namely A-kinase anchor protein 5 (Uniprot code P24588) and the ADP-ribosyl cyclase/cyclic ADP-ribose hydrolase 2 (Uniport code Q10588). Additionally, Cytochrome C (Uniport code P9999) was found to be over expressed after TG treatment and slightly reduced by Vx-445.

Analysis of the ** segment (Figure 27C and 27D) revealed many hits belonging to the ribosome machinery (Figure 27C in blue and Figure 27D) as well as several hits elated to RNA binding (Figure 27C in red and Figure 27D). This observation is consistent with the known TG effect, which slows down or halts protein synthesis to prevent accumulation of misfolded proteins. Importantly, Vx-445 treatment reversed this effect restoring protein synthesis to physiologicl levels, as expected (Doutheil *et al.,* 1999).

### 4.2.9 Vx-445 protein partners identification in SHSY-5Y cell lysates by DARTS

DARTS (Drugs Affinity Responsive Target Stability) is a functional proteomics strategy aimed at the identification of small molecules' binding targets (and off-targets) in complex protein mixtures, such as cells proteomes, without the need to modify the compounds to be studied. It is a quick and straightforward method that relies on the target protein's stability against an unspecific protease (e.g., subtilisin) limited proteolysis, upon the small molecule interaction. In our experimental design, SHSY-5Y cells complete proteome was extracted using mild lysis conditions to preserve the macromolecular complexes. Proteins aliquots were then treated with increasing Vx-445 concentrations (1,10, and 100 µM) or the vehicle (negative control). Subsequently, the non-specific protease subtilisin was used to achieve limited proteolysis, except for the one untreated control sample (positive control). Following the enzyme's quench, SDS-PAGE was carried out, and its results were revealed by Coomassie blue staining (Fig. 28A). The gel lanes were then cut into bands, which underwent in situ trypsin digestion, obtaining peptides' mixtures for the nano-UHPLC-MS/MS analysis.

**Table 2**: *Filtered list of Vx-445 expected targets, reported with their accession number, description and molecular weight. √ is reported if the protein has been protected in the relative DARTS experiment*

| Accession | Description | MW [kDa] | DARTS 1 | DARTS 2 | DARTS 3 |
|---|---|---|---|---|---|
| **Q06323** | Proteasome activator complex subunit 1 | 28,7 | √ | √ | √ |
| **P36776** | Lon protease homolog, mitochondrial | 106,4 | √ | X | √ |
| **Q9Y6Y8** | SEC23-interacting protein | 111 | √ | X | √ |
| **Q9NX05** | Coactivator of PPAR-γ-like protein 2 | 120,5 | √ | X | √ |
| **Q15018** | BRISC complex subunit Abraxas 2 | 46,9 | √ | X | √ |
| **Q96FZ2** | Abasic site processing protein HMCES | 40,5 | √ | X | √ |
| **Q9Y295** | Development-regulated GTP binding protein 1 | 40,5 | √ | X | √ |
| **Q13011** | Δ(3,5)-Δ(2,4)-dienoyl-CoA isomerase | 35,8 | √ | X | √ |
| **P05141** | ADP/ATP translocase 2 | 32,8 | √ | X | √ |
| **P46926** | Glucamine-6-phphate isomerase 1 | 32,6 | √ | X | √ |
| **Q96CN7** | Isochorismatase domain-containing protein 1 | 32,2 | √ | X | √ |
| **O75828** | Carbonyl reductase [NADPH] 3 | 30,8 | √ | X | √ |
| **P15559** | NAD(P)H dehydrogenase [quinone] 1 | 30,8 | √ | X | √ |

| | | | | | |
|---|---|---|---|---|---|
| **O95865** | DimethylArg dimethylaminohydrolase 2 | 29,6 | √ | X | √ |
| **P61289** | Proteasome activator complex subunit 3 | 29,5 | √ | X | √ |
| **Q92688** | Acidic leucine-rich nuclear phospho 32B | 28,8 | √ | X | √ |
| **P12004** | Proliferating cell nuclear antigen | 28,8 | √ | X | √ |
| **P39687** | Acidic leucine-rich nuclear phospho 32 A | 28,6 | √ | X | √ |
| **P42345** | Serine/threonine-protein kinase mTOR | 288,7 | X | √ | √ |
| **Q659C4** | La-related protein 1B | 105,3 | X | √ | √ |
| **Q9H7Z7** | Prtaglandin E synthase 2 | 41,9 | X | √ | √ |
| **Q8IVD9** | NudC domain-containing protein 3 | 40,8 | X | √ | √ |
| **P48556** | 26S proteasome non-ATPase regul. subunit 8 | 39,6 | X | √ | √ |
| **Q86X76** | Deaminated glutathione amidase | 35,9 | X | √ | √ |
| **P42574** | Caspase-3 | 31,6 | X | √ | √ |
| **P62424** | Large ribomal subunit protein eL8 | 30 | X | √ | √ |
| **Q01081** | Splicing factor U2AF 35 kDa subunit | 27,9 | X | √ | √ |

Proteome Discoverer software was then used to identify and quantify the proteins. The abundance ratio of the proteins in the treated and untreated samples was compared to assess the degree of protection against proteolysis caused by Vx-445, then only proteins with a sample/control ratio ≥ 1.5 were considered as Vx-445 putative interactors. The final list of possible protein partners comprises around 30 hits (Table 1) observed in at least two out of three experiments; proteins involved in oxidoreductase process and proteostasis were reported in Figure 28B together with their protection percentage at 10 μM. In particular, it is noteworthy that the corrector is able to interact with several enzymes involved in redox processes, such as carbonyl reductase [NADPH] 3, NAD(P)H dehydrogenase [quinone] 1 and Lon protease homolog, mitochondrial. It is also interesting that Vx-445 directly binds to several proteins belonging to proteasome (such as Proteasome activator complex subunit 1 and 3 and 26S proteasome non-ATPase regulatory subunit 8) and with Large ribosomal subunit protein eL8, all involved in proteins biosynthesis and degradation. These gathered results provide insights into the putative direct targets of Vx-445 through which the corrector may exert its effect, at both the global proteome level and on important biological pathways.

A

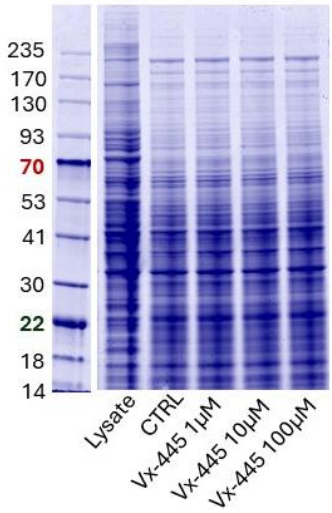


B

| | | % of Protection at 10 µM | | |
|---|---|---|---|---|
| Accession | Description | DARTS 1 | DARTS 2 | DARTS 3 |
| Q06323 | Proteasome activator complex subunit 1 | 49.6 | 104.9 | 55.6 |
| P36776 | Lon protease homolog, mitochondrial | 97.5 | X | 69.7 |
| O75828 | Carbonyl reductase [NADPH] 3 | 109.1 | X | 104.3 |
| P15559 | NAD(P)H dehydrogenase [quinone] 1 | 73.0 | X | 132.8 |
| P61289 | Proteasome activator complex subunit 3 | 4.71 | X | 15.48 |
| P48556 | 26S proteasome non-ATPase regul. subunit 8 | X | 22.2 | 41.3 |
| P62424 | Large ribomal subunit protein eL8 | X | 11.6 | 30.1 |

**Figure 28**:*(A)Coomassie stained SDS-PAGE of a representative DARTS experiment. (B) Filtered list of Vx-445 expected targets, reported with their accession number, description and protection from limited proteolysis, expressed as a %.*

### 4.3 Discussion

Among the primary challenges in today's field of medicine is the search for new therapeutic approaches to neurodegenerative disease. Central to these disorders is the aberrant folding, aggregation, and accumulation of proteins, which leads to the formation of toxic species that contribute to neuronal degeneration, examples are AD, PD, Huntington's disease (HD), and amyotrophic lateral sclerosis (ALS) (Koszła & Sołek, 2024).

Neurons are highly sensitive to alterations caused by protein misfolding; as terminal, highly differentiated cells, they cannot manage toxic molecules through mitotic division and therefore become increasingly susceptible to misfolded proteins with aging (Candelise *et al.,* 2021). The ER carries out numerous functions essential for cell viability; therefore, perturbation of its complex homeostasis, triggered by physiological, pathological, or environmental factors that interfere with ER protein folding (Coleman *et al.*, 2019) induced ER stress leading to intraluminal accumulation of misfolded proteins. For example, in AD, the most widely accepted model of pathogenesis centers on a sequence of events initiated by the accumulation of β-amyloid (Aβ) and tau proteins, ultimately resulting in neurodegeneration and clinical

manifestation of the disease (Frisoni *et al.,* 2022). Incorrect folding of these proteins leads to the formation of toxic aggregates in specific brain regions, which allow them to spread to connected areas (d'Errico *&* Meyer-Luehmann, 2022). Numerous studies indicate that fibrillary Aβ deposits form senile plaques while the concomitant appearance of neurofibrillary tangles, contritutes to neurofibrillary degeneration.

The buildup of such proteins in the ER lumen activates the UPR signaling. UPR activation results in the reduction of protein synthesis rates, upregulation of chaperone and other protein expression, and the degradation of improperly folded proteins located in the ER. These three pathways contribute to the reduction of protein aggregates, concurrently reinforcing the entire ER machinery for proper folding and degradation (Chen *et al.,* 2023). The UPR can restore proteostasis or, if stress is irreversible, initiate cell death. Overall, protein-misfolding-related neurodegenerative disorders are linked to the pathogenicity of chronic ER stress (Torres *et al.,* 2010).

Considering chapter one results, Lumacaftor (VX-809), the first corrector developed for the mutated CFTR protein in the treatment of CF (Regard *et al.,* 2022), was tested in an experimental model in which SH-SY5Y neuroblastoma cells were exposed to TG, an experimental tool commonly used as an ER-stress inducer that, by disrupting intracellular calcium homeostasis, causes accumulation of unfolded or misfolded proteins within the ER (Peng *et al.,* 2023). By mimicking this condition, we evaluated the potential *off-label* effect of VX-809, hypothesizing that the molecule, through an as-yet unknown mechanism, might indirectly act on misfolded proteins, thereby preventing activation of pathways involved in ER stress.

The first analysis aimed at assessing the involvement of VX-809 in modulating the UPR pathway in our experimental model was performed by Western blotting. Upon treatment with the ER stressor TG, the expression of the selected markers GRP78/BiP, ATF4, ATF6, and p-PERK, increased significantly. Administration of VX-809 over the subsequent 24 h significantly reduced the protein levels of these markers. The other UPR branch, IRE1, was likewise examined by evaluating its RNase activity on XBP1 mRNA splicing;

here, the drug also prevented the maturation of this transcription factor, restoring the cell to its initial homeostatic state. Notably, UPR markers have been identified in postmortem brain and spinal cord tissues from various NDs. For example, in PD, markers of PERK activation have been founded in post-mortem tissues, where dopaminergic neurons of the substantia nigra containing αSyn inclusions were also positive for phosphorylated PERK (Mercado *et al.,*2016). Moreover, in prion-infected mice, oral treatment with a highly selective PERK inhibitor that successfully crosses the blood–brain barrier markedly reduced neurodegeneration and clinical symptoms (Moreno *et al.,* 2013). Given the strong evidence of UPR activation in human patients, such studies highlight the possibility that pharmacological modulation of the UPR may confer disease-modifying benefits across multiple neurodegenerative disorders.

It’s well established that ER functions as a central hub for protein biosynthesis, as well as cholesterol and lipid production, and is the main $Ca^{2+}$ store within the cell. The ER's capacity to store and bind $Ca^{2+}$ is determined by the activity of the SERCA pump and the presence of $Ca^{2+}$-binding resident proteins, such as calreticulin (CRT), calnexin (CNX), and BiP/Grp78, which bind $Ca^{2+}$ with low affinity. The activity of molecular chaperones, including CRT, CNX, BiP/Grp78, and PDI, is dependent on their ability to bind to $Ca^{2+}$; thus, physiological levels of $Ca^{2+}$ within the ER are essential for proper protein folding (Lim *et al.,* 2023). Perturbations in calcium homeostasis are directly associated with ER stress and increased susceptibility to protein folding defects. Even under unstimulated conditions, the ER membrane is permeable to $Ca^{2+}$. The $Ca^{2+}$ gradient between the ER lumen and the cytosol drives $Ca^{2+}$ efflux through pore- or channel-like proteins, a phenomenon known as the "ER $Ca^{2+}$ leak" (Lemos *et al.,* 2021). The rate of this leak is relatively high: following SERCA inhibition, the ER can lose its releasable $Ca^{2+}$ within minutes. Given these factors, calcium dysregulation has been strongly implicated in neurodegenerative diseases (Sammels *et al.,* 2010). Alteration of cellular $Ca^{2+}$ homeostasis is considered one of the earliest and most widespread indicators of cellular malfunction in brain disorders, including Alzheimer's disease (AD)

(Arnst *et al.,* 2022). The current paradigm, which focuses on neurons, postulates that generalized $Ca^{2+}$ overload triggers the activation of mechanisms that ultimately lead to neuronal death (Calvo-Rodriguez *&* Bacskai, 2021).

Considering the critical role of calcium in the development of neurodegenerative disorders, spectrofluorometric analysis using the fluorescent probe FURA-2AM was performed to evaluate the corrector's ability to regulate calcium homeostasis. The results showed that, in the experimental model, the corrector enhanced protein processing, which in turn improved calcium homeostasis by restoring the balance between reticular and cytosolic calcium levels. This reduction in free $Ca^{2+}$ levels in neuronal cells consequently decreased the activation of mechanisms leading to cell death and neurodegeneration.

The human brain contains over 86 billion neurons and approximately 250-300 billion glial cells, together consuming more than 20% of total basal oxygen. In addition, cerebral mitochondria use inhaled oxygen to reduce $O_2$ to $H_2O$ and support adenosine triphosphate (ATP) synthesis. When the mitochondrial electron transport chain in neuronal cells operates inefficiently, expecially in the presence of excess oxygen, mitochondrial ROS can leak.

Physiological ROS levels, often referred to as "beneficial stress", are essential because they support key biochemical processes underpinning synaptic plasticity, cell-cell communication, memory formation, cell proliferation, and apoptosis; however, when produced in excess, ROS become harmful. The brain is particularly vulnerable to oxidative stress. Although redox signaling can act as an intrinsic sensor of oxidative burden, these signals become disregulated in pathological conditions such as neurodegenerative disorders characterized by misfolded proteins and aggregates formation (Koszła & Sołek, 2024). Under these conditions, ER stress and oxidative stress reinforce one another in a self-sustaining pathological loop (Esmaeili et al., 2022).

The cellular antioxidant network that safeguards tissues comprises both endogenous and exogenous factors. Endogenous antioxidants are further classified into enzymatic and non-enzymatic components, including inhibitors of pro-oxidant enzymes, cofactors required by antioxidant enzymes, ROS/RNS scavengers, and chelators of transition metals. Together, these are essential for maintaining redox balance in the brain and limiting oxidative stress. Among enzymatic antioxidant, SOD is a key enzyme that catalyzes the dismutation of the superoxide anion ($O_2\bullet^-$) into $H_2O_2$ (and $O_2$), and it also protects dehydratase enzymes from inactivation by superoxide. Humans express three SOD isoforms. Notably SODIII, also known as extracellular SOD (EC-SOD), is a Cu/Zn-containing enzyme synthesized within cells and secreted into the extracellular matrix. Unlike many stress-response proteins, SOD3 is not directly induced by its substrate or by general oxidants; rather, its expression is coordinated at the tissue level through cytokine-driven regulation (Lee et al., 2020).

For these reasons, neuronal SH-SY5Y cells, treated according to our experimental model, allowed us to highlight the antioxidant power of VX-809. In particular, the results demonstrated that administration of Vx-809, in a reticular stress model, led to a decrease in intracellular and mitochondrial ROS levels and an increase in the antioxidant enzyme SODIII, mainly at 1 and 4 hours after treatment, improving the cellular redox state.

Apoptosis, often referred to as “programmed cell death”, is a physiological form of cellular self-destruction that occurs across a range of biological contexts. In the developing brain and spinal cord, apoptosis shapes both the number and the types of cells, and is essential for building a functional neural network. Morphologically, apoptotic death is characterized by a well-defined sequence that includes shrinkage of nuclear and cytoplasmic compartments, chromatin condensation, DNA cleavage into oligonucleosomal fragments, and packaging of nuclear material into membrane-bound apoptotic bodies (Ekshyyan & Aw, 2004). Neuronal loss underlies NDs and the presence and accumulation of misfolded proteins place ER stress at the center of the pathological progression. From this arise collateral mechanisms, including

oxidative stress, DNA damage and disruption of intracellular $Ca^{2+}$ homeostasis that further exacerbate neuronal apoptosis, (Goyal *et al.,* 2024). The apoptotic machinery is also regulated by caspases; notably caspase-4, a member of the caspase-1 subfamily, is primarily localized at the ER membrane and is specifically activated under ER-stress conditions, with little response to other apoptotic stimuli (Hitomi *et al.,* 2004). Flow cytometrc analysis in our ER-stress model revealed a robust anti-apoptotic effect of VX-809 in neuronal cells. Quantification of hypodiploid nuclei using propidium iodide, and measurement of caspase-4–positive cells, showed that TG pretreatment significantly increased apoptosis, which was markedly reduced after 24 hours of VX-809 (Lumacaftor) exposure across all the examined experimental time points This highlights a relevant *off-label* potential for Lumacaftor, given that apoptosis is a principal mode of neuronal death in NDs (Koszła & Sołek, 2024).

To date, in the treatment of CF, the corrector VX-445 has replaced the previous corrector, VX-809 (Kapouni *et al.,* 2023). Considering the evidence showing that the Vx-809 corrector exerts broader effect by reducing cellular stress in the A549 and A375 cell lines and displaying neuroprotective properties in SH-SY5Y cells, a widely used in vitro model for neurodegenerative diseases, preliminary experiments were also conducted for VX-445 to assess whether VX-445 reproduces the behavior of the previous corrector. To better elucidate the mechanism of action of VX-445, an *in vitro* functional proteomics approach based on DARTS was applied to identify potential protein interaction partners within the complex cellular environment.

As described above, oxidative stress is closely linked to ER stress and, when chronic, can become harmful to neuronal cells. Vx-445 was found to significantly reduce ROS production following TG-induced ER stress at multiple time points, with effects detectable by flow cytometry after only 15 minutes. This highlight both the dynamic nature of redox balance and the sensitivity of neuronal cells to oxidative stress. Proteomic analyses further confirmed the redox-modulating role of Vx-44: clustering and gene ontology analyses revealed that TG upregulates oxidoreductase enzymes, an effect reversed by Vx-445. DARTS experiments also validated its interaction with

several redox-related enzymes, including [NADPH] 3 carbonyl reductase, NAD(P)H quinone dehydrogenase 1, and the mitochondrial protease Lon.

Throughout the cell life cycle, fluctuations in intracellular Ca2+ concentrations mediate essential biological functions. Our results showed that, like VX-809, VX-445 significantly reduced cytoplasmic calcium levels following TG-induced ER stress, suggesting a potential role in restoring Ca2+ homeostasis under conditions of cellular stress. In particular, proteomic analyses further support this role, revealing changes in proteins involved in calcium regulation, including A-kinase anchoring protein 5 (AKAP5). In the context of ER calcium modulation, protein kinase A (PKA) critically regulates the inositol 1,4,5-trisphosphate receptor 1 (IP3R) by sensitizing its channels to IP3 via phosphorylation of cytosolic serine residues (Makio *et al.,* 2024). AKAP5, a member of the AKAP family, is essential for managing calcium signaling because it is responsible for targeting PKA to specific subcellular sites bringing the holoenzyme closer to its substrates, thus amplifying cAMP-driven signaling (Feliciello *et al.,* 2001). Proteomic analysis also identified ADP-ribose cyclase/cyclic hydrolase 2 as another calcium-regulating protein. Its expression was reduced after TG treatment, but restored by Vx-445. Beyond calcium homeostasis, this enzyme regulates the second messenger cyclic ADP-ribose (cADPR), which acts through ryanodine receptors. It catalyzes both the synthesis of cADPR from $NAD^+$ and its hydrolysis to ADPR (Hirata *et al.,* 1994), linking ER calcium signaling to broader cellular regulatory mechanisms.

Growing evidence indicates that ER stress resulting from aberrant protein accumulation compromises mitochondrial function and that mitochondria are crucial for ROS generation, signaling, and regulation of apoptosis and neuronal survival (Oliveira, 2011). In this context, further similarities between the two correctors emerge as both act at the mitochondrial level; in particular VX-445 significantly reduces cytosolic levels of cytochrome c following ER stress suggesting its ability to indirectly modulate apoptosis induced by the accumulation of misfolded proteins and potentially limit neuronal loss. Under physiological conditions, cytochrome c resides in the mitochondrial

intermembrane and intercristae spaces, where it functions as an electron carrier in the respiratory chain. However, in response to proapoptotic stimuli, including ER stress, cytochrome c is released into the cytosol, where it activates apoptotic proteases (Garrido *et al.,* 2006).

Given the central role of cytochrome c in neuronal survival and the contribution of apoptosis to neuronal death, targeting this pathway represents a promising strategy for treating neurodegenerative diseases (Moujalled *et al.,* 2021). Proteomic analyses of VX-445 further revealed broad effects on the ribosomal machinery and other RNA-associated proteins. Consistently, Figure X (heat map) shows that the corrector counteracts TG- induced suppression of protein-synthesis, restoring cells toward their initial homeostatic state.

Taken together, these findings, supported by expression proteomics and DARTS, provide a strong rationale for exploring *off-label* applications also for VX-445. The corrector modulates ROS levels, calcium signaling, and apoptosis, thereby re-establishing cellular homeostasis disrupted by TG-induced ER stress.

# Chapter V

# *Investigation of VX-445 in ER Stress-Driven Inflammation and Preliminary Analyses of the Corrector's Potential Role in Mitochondrial Responses to ER Perturbation*

## 5.1 Introduction

The ER performs essential cellular functions. It is well established that conditions disrupting normal protein processing in the ER trigger ER stress, which initially activates the UPR to restore homeostasis; if recovery fails, apoptosis ensues (Zimmermann *et al.,* 2022). The UPR "gatekeeper" in mammalian cells is the chaperone BiP/GRP78, which under basal conditions keeps the principal ER stress sensors (IRE1, PERK, ATF6) inactive. When misfolded proteins accumulate, BiP engages them as a chaperone, permitting sensor activation. Like other ER-resident chaperones, BiP also functions as a $Ca^{2+}$-binding protein. Calcium regulation is vital: the ER is a major reservoir and, as a pivotal second messenger, $Ca^{2+}$ participates in numerous homeostatic pathways; and Its dysregulation underlies many human diseases, including neurodegeneration (Lim *et al.,* 2023).

When ER stress becomes irreparable, apoptosis can be driven by caspase-4 (Zou *et al.,* 2021), which resides in the ER and closely associates with key ER-stress indicators, including BiP. Thus, caspase-4 plays a fundamental role and may represent a therapeutic target in ER-stress–associated pathologies (Hitomi *et al.,* 2004). Numerous studies describe the tight connection between ER stress and inflammation: beyond being classified as an "inflammatory" caspase, ER stress can both drive and result from chronic inflammation, which accompanies disorders such as diabetes, obesity, neurodegenerative and neuromuscular diseases, arthritis and spondyloarthropathies, respiratory

inflammatory conditions, and inflammatory bowel diseases; these are often linked to protein misfolding and ER dysfunction, and UPR activation is common in many chronic inflammatory and autoimmune conditions (Sonninen *et al.,* 2020). In particular, the three arms of the canonical UPR intersect with inflammation and stress pathways, including the NF-κB–IκB kinase (IKK) and JNK–AP1 axes. Moreover, ER-stress–induced activation of JAK1/STAT3 promotes expression of IL-6 and several chemokines that drive inflammation (Meares *et al.,* 2014). Consequently, inflammation and ER stress are tightly interconnected. While their acute activation is protective, chronic engagement becomes detrimental (Hasnain et al., 2012).

At present, CF treatment widely employs triple-combination regimens that pair correctors with potentiators. Among these, the corrector VX-445 (Elexacaftor) has replaced its predecessor, VX-809, in clinical practice. Previous studies on VX-890 have shown that it not only improves CFTR proteostasis but also exerts broader protective effects in non-CF models, reducing ER-stress markers, restoring intracellular $Ca^{2+}$ homeostasis, and mitigating inflammation (Pecoraro *et al.,* 2023; Pecoraro *et al.,* 2024). For VX-445, potential off-target effects on other misfolded proteins or ER-stress pathways remain unexplored. In this thesis, the hypothesis that VX-445 can likewise act as a broader modulator of proteostasis was analyzed, in particular, attenuating ER stress and its downstream consequences, including inflammation, in non-CF cellular contexts. ER stress is induced using the well-known inducer thapsigargin (TG), which inhibits SERCA, with the focus primarily on the associated inflammatory response.

The correct functioning of the ER also depends on the functional balance established with mitochondria, with which it is physically in contact at the level of the MAMs, mitochondria-associated membranes, (Watanabe & Yamanaka, 2025). Preliminary experiments were therefore performed to assess the effects of VX-445 on mitochondrial function under ER-stress conditions. Because neurons are highly dependent on mitochondria (Oliveira, 2011), these pilot experiments were conducted on two different nervous cell lines: SH-SY5Y neuroblastoma cells and the MO3.13 immortal human–human hybrid cell line,

which expresses phenotypic characteristics of primary oligodendrocytes. The results showed that VX-445 beneficially modulated and restored $Ca^{2+}$ homeostasis, mitochondrial oxidative stress, mitochondrial membrane potential and apoptosis strongly supporting its potential off-label application to neurodegenerative diseases (NDs).

## 5.2 Results

### *5.2.1 Protective Role of Vx-445 in Preserving ER Calcium Balance During Stress*

Calcium dysregulation is one of the main consequences that occur when the cell experiences a condition of ER-stress and is associated with many pathologies and can also lead to cell death (Zhang *et al.,* 2023). Thus, the effects of Vx-445 administration on intracellular calcium concentrations in a calcium-free incubation medium were evaluated with Fura 2-AM. ER calcium levels were assessed using TG (1 nM). As shown in Figure X, Vx-445-treated cells that had been pretreated with TG showed a significant increase in calcium ER levels than TG-treated cells. Particularly, this effect was observed at 15-30 min and at 1-2h in SH-SY5Y cells (Figure 29A) and at 2-4 h for A549 cells (Figure 29B) ($p < 0.0001$). This observation suggests that in the presence of Vx-445, the ER stores more calcium, thereby improving calcium homeostasis.

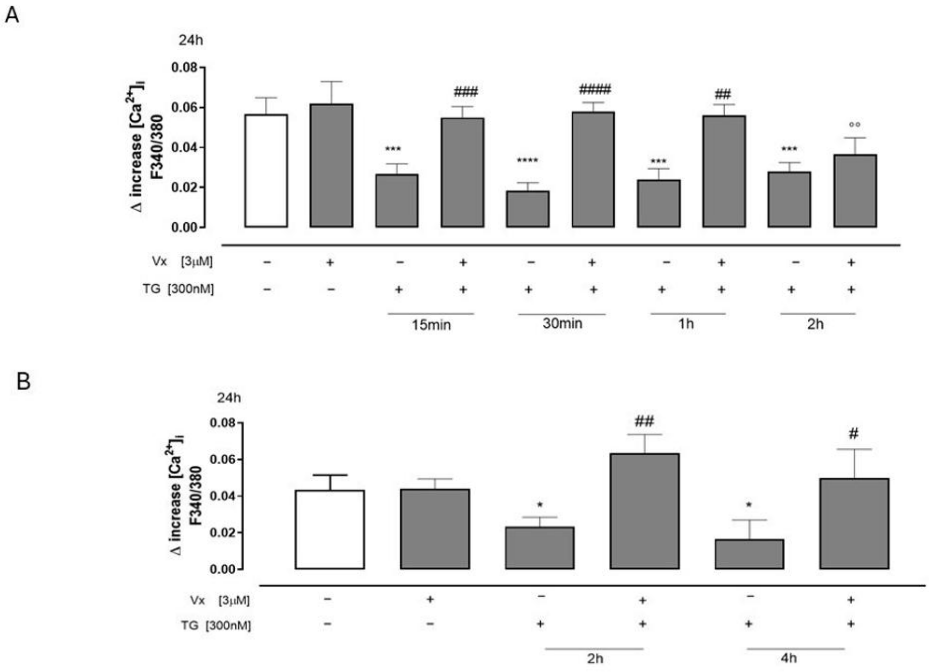

**Figure 29***: Effect of Vx-445 on ER calcium content. SH-SY5Y (A) cells were pretreated with 300 nM TG for 15 min, 30 min, 1h and 2h and A549 (B) for 2h and 4h to induce ER stress, followed by 24 h treatment with 3 μM Vx-445. Reticular calcium levels were measured in calcium-free medium containing 1 nM TG. Data represent mean ± SEM of ΔFura-2 (340/380 nm) fluorescence ratio from at least three independent experiments performed in duplicate. Statistical analysis was performed using the Mann–Whitney U test: *p < 0.05, ***p < 0.001, ****p < 0.0001 vs. untreated; °°p < 0.005 vs. Vx-445-treated cells; #p < 0.05, ##p < 0.005, ###p < 0.001, ####p < 0.0001 vs. TG-treated cells*

### *5.2.2 The Corrector modulates the activation of Procaspase-4*

Accumulation of unfolded and misfolded proteins and impairment of calcium homeostasis lead to ER stress, initiating the UPR that results in inhibition of protein synthesis, increased expression of ER protein folding chaperones and/or apoptosis. Caspase 4 is involved in UPR-dependent apoptosis by initiating a series of caspase activations (Moorwood & Barton, 2014). Consequently, caspase 4 activation in both cell lines treated with Vx-445 under ER stress conditions was analyzed. Flow cytometric assay showed a significant decrease in levels of caspase 4 ($p < 0.05$), particularly 4 h post treatment (Figure 30). This suggests that the corrector enhances reticular integrity, potentially mitigating ER stress-induced apoptotic signaling, and contributing to its overall cytoprotective effect

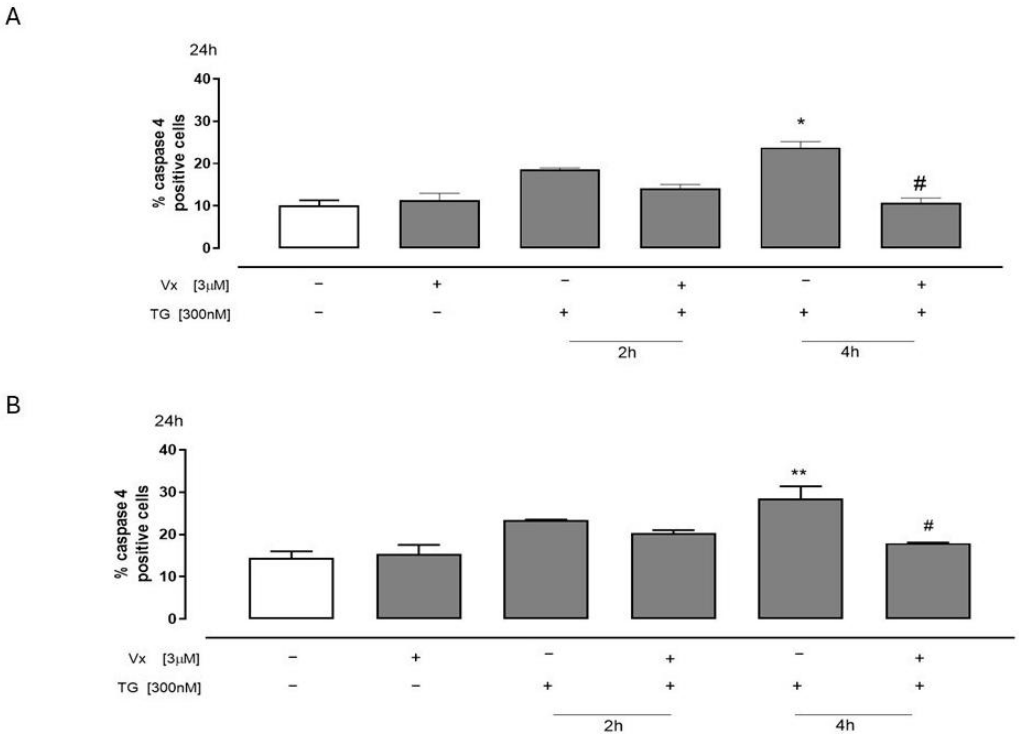


**Figure 30:** *Vx-445 interferes with the cleavage of procaspase 4 induced by ER stress. To mimic ER stress, 300 nM TG was administered prior to treatment for 2 or 4 h in both SH-SY5Y (A) and A549 (B) cells. After that, Vx-445 (3 μM) was given for 24 h. The mean ± S.E.M. was used to determine the proportion of caspase 4-positive cells from at least three different experiments, each conducted in triplicate. Data were analyzed using the Mann–Whitney U test. # p < 0.05 vs TG-treated cells; ** p < 0.005 and * p < 0.05 vs untreated cells. The first white bar represents untreated cells.*

### *5.2.3 Vx-445 Attenuates ER Stress-Mediated GRP78/BiP Upregulation*

Under physiological conditions, the 78 kDa glucose regulatory protein chaperone (GRP78/BiP) keeps the three UPR sensors inactive by binding to their luminal domains. However, under ER stress conditions, BiP demonstrates high affinity for misfolded proteins, resulting in dissociation from UPR sensors. Detachment facilitates their activation and subsequent downstream signaling pathway (Zhu *et al.,* 2022). Western blotting analysis of SH-SY5Y and A549 cell lysates showed that TG treatment significantly ($p < 0.001$) increases expression of BiP in all pretreatment time points, thereby confirming the establishment of ER stress. As illustrated in Figure 31 Vx-445 administration reduced TG-induced Grp78/BiP overexpression, suggesting that this corrector may mitigate UPR activation by restoring ER homeostasis.

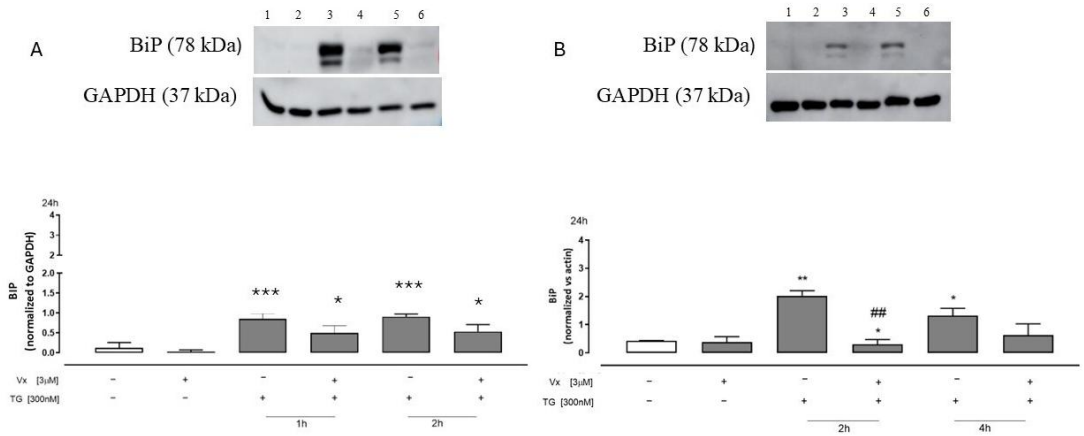


**Figure 31:** *Vx-445 disrupts BiP signaling. Western blot analysis of BiP expression in Neuroblastoma (A) and Adenocarcinomic (B) cells. ER stress was induced with 300 nM TG for 1, 2, or 4 h, followed by 3 μM Vx-445 for 24 h. Panel A: (1) untreated, (2) Vx-445, (3) TG 1h, (4) TG 1h + Vx-445, (5) TG 2h, (6) TG 2h + Vx-445. Panel B: (1) untreated, (2) Vx-445, (3) TG +2h, (4) TG 2h + Vx-445, (5) TG 4h, (6) TG 4h + Vx-445. GAPDH served as loading control. Data represent mean ± S.E.M. of ≥3 independent experiments. The statistical analysis was performed by Mann–Whitney U test: *p < 0.05, **p < 0.005, ***p < 0.001 vs untreated; ##p < 0.005 vs TG-treated cells*

### *5.2.4 ER-Stress Modulation by VX-445 Blunts NF-κB/STAT3 Pathways*

Cytoplasmic localization of NF-kB is controlled by a family of inhibitory proteins, IkBs, which bind NF-kB, masking its nuclear localization signal and thus preventing nuclear translocation. Following exposure to various extracellular stimuli, IkB triggers rapid phosphorylation, ubiquitination, and ultimately proteolytic degradation, leading to NF-kB release, nuclear translocation, and activation of gene transcription. IkBα expression has been evaluated since the protein is a master regulator of NF-kB signaling (Solt *et al.,* 2008) and is involved in chronic inflammatory processes (Perez *et al.,* 2015). As shown in Figure 32, a significant increase in IkBα levels ($p < 0.0001$) was observed by flow cytometry in both Vx-445 treated cell lines under ER stress conditions. These data suggest that Vx-445 treatment shifts the balance towards the non-phosphorylated form of IkBα, potentially leading to NF-kB inhibition.

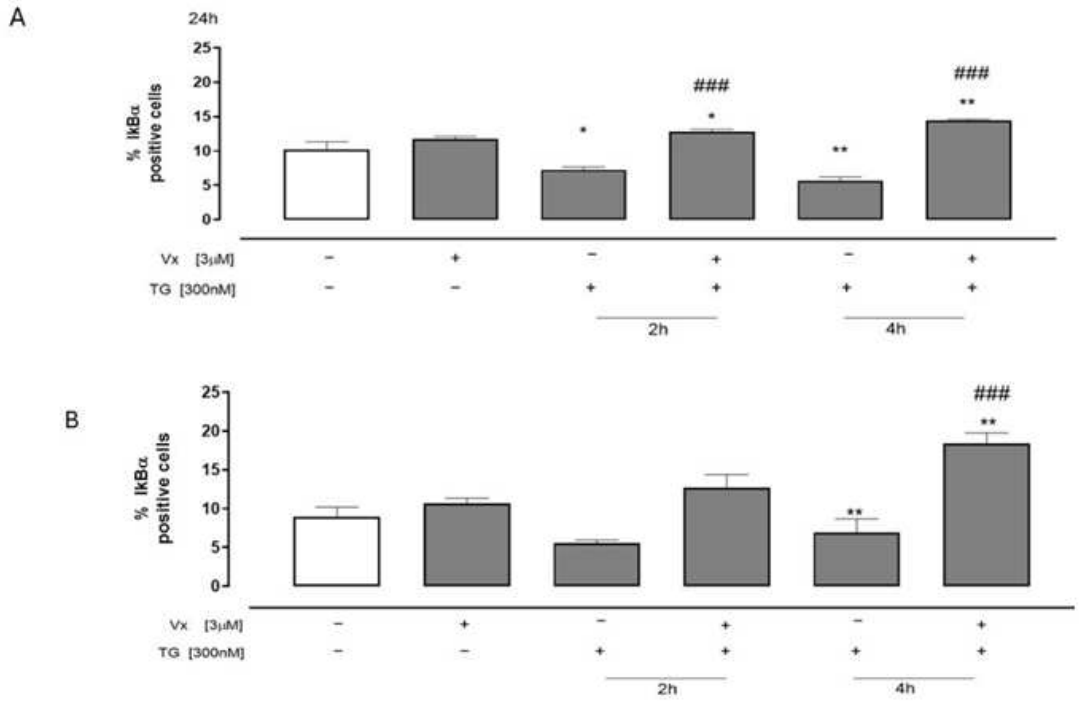


**Figure 32:** *The Vx-445 impact on IkBα pathway. To induce ER stress, 300 nM TG had been pretreated for 2h or 4h in Neuroblastoma (A) and Adenocarcinomic (B) cells. Subsequently, 3 μM of the Vx-445 was administered for 24h. IkBα levels were assessed by flow cytometry. Data are expressed as mean ± S.E.M. of percentage of IkBα positive cells from at least three independent experiments each performed in triplicate. Data was subjected to a Mann- Whitney U test analysis. * p < 0.05 and ** p < 0.005 vs untreated cells; ### p < 0.001 vs TG-treated cells*

STAT3 is the most extensively studied anti-inflammatory response signaling pathway responsible for regulating the intensity and duration of inflammation. Its impairment can lead to uncontrolled and increasing inflammation. Membrane receptor signaling mediated by diverse ligands induce JAK kinase activation, subsequently leading to tyrosine phosphorylation of different STAT transcription factor (Shen *et al.* 2020). In A549 and SH-SY5Y cell lines, using flow cytometry, the phosphorylated form of STAT3 (p-STAT3) was analyzed to test the activation. The results observed showed a significant increase ($p< 0.001$) in p-STAT3 levels in cells pretreated with TG for 2 and 4 h towards untreated cells, confirming the onset of ER stress. Vx-445 treatment significantly ($p<0.001$) decreased levels of TG-induced p-STAT3, further substantiating its role in modulating the stress response (Figure 33).

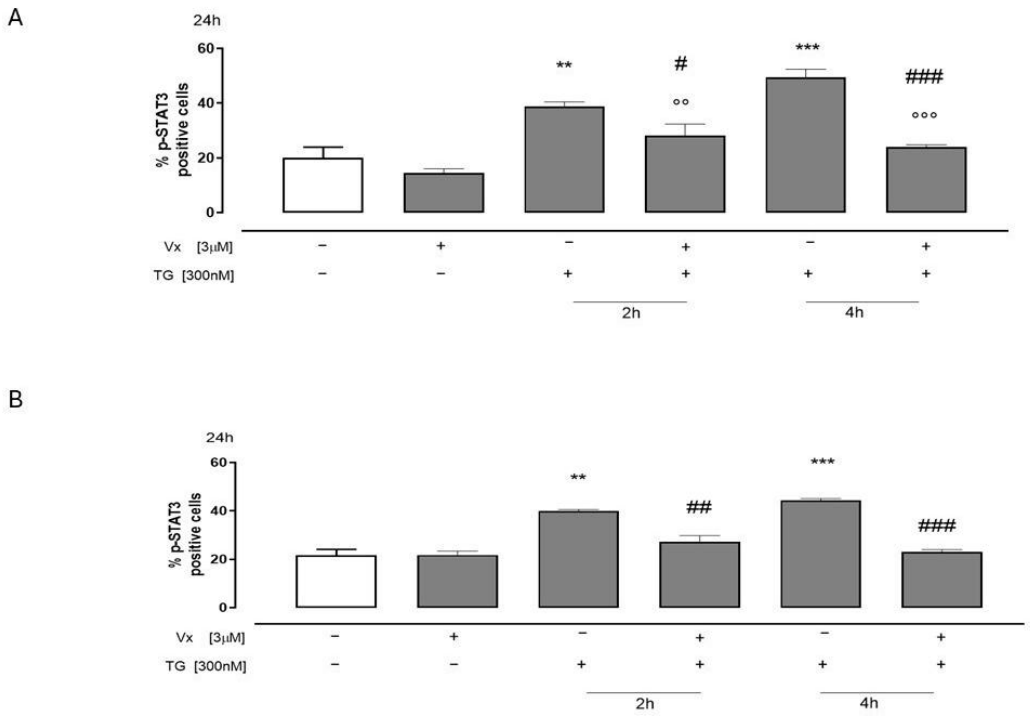


**Figure 33**: *Vx-445 role in regulating p-STAT3. SH-SY5Y (A) and A549 (B), were treated beforehand with 300 nM TG for 2h or 4h, to cause ER stress. Then, 3 μM Vx-445 was added for 24h and by flow cytometry analysis, p-STAT3 levels were assessed. Data are expressed as the mean ± S.E.M. of percentage of p-STAT3 positive cells from at least three independent experiments each performed in triplicate. Analysis of Mann–Whitney U test was used on data. ** p < 0.005 and *** p < 0.001 vs nontreated cells; °° p < 0.005 and °°° p < 0.001 vs Vx-445-treated cells; # p < 0.05, ## p < 0.005 and ### p < 0.001 vs TG- treated cells*

### *5.2.5 Vx-445 can reduce the IL-6 release*

Some evidence supports that NF-κB is involved in gene regulation related to neuronal survival, inflammatory responses and cancer. Furthermore, NF-κB is a key transcription factor that promotes the induction of proinflammatory factors, such as IL-6 (Jill *et al.,* 2023) and the COXII (Kaltschmidt *et al.,* 2002) protein, which, together with STAT3 phosphorylation contributes to a proinflammatory state. For these reasons, the expression of both of IL-6 and COXII were studied in the experimental model proposed.

As shown in Figure 34, ELISA assay demonstrated a significant reduction ($p < 0.05$) in IL-6 release in Vx-445–treated SH-SY5Y (Figure 34A) and A549 (Figure 34B) cells following TG pretreatment, particularly at 4 h.

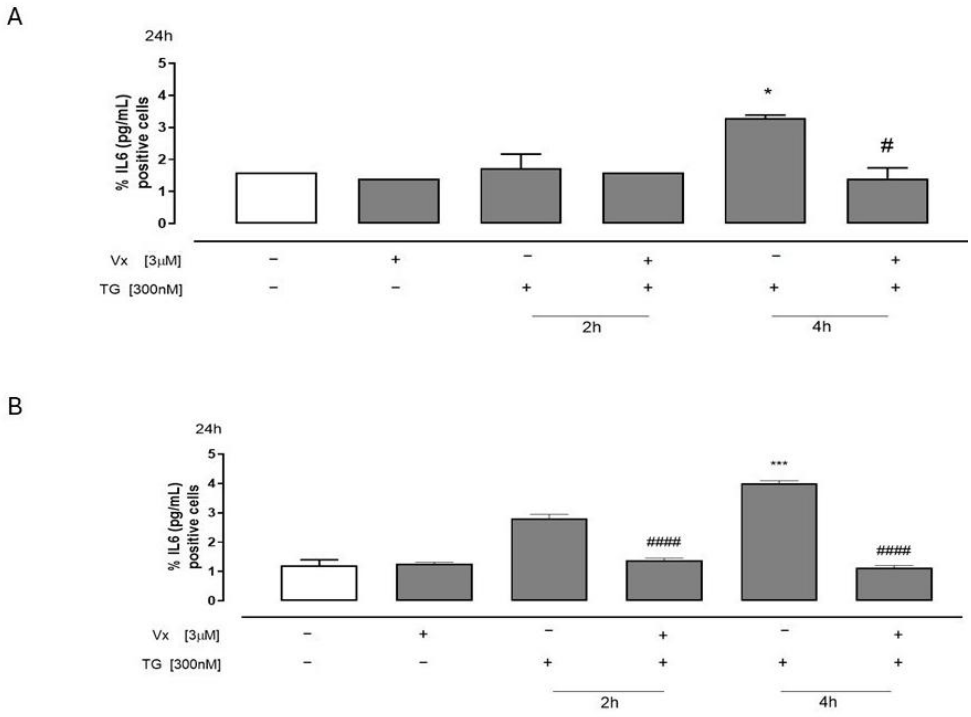


**Figure 34:** *Vx-445 interferes with cytokines expression. The levels of IL-6 in cell supernatant were measured using commercially available ELISA. SH-SY5Y (A) and A549 (B) were treated beforehand with 300 nM TG until 2 h or 4 h, to cause ER stress. After, 3 μM Vx-445 was added until 24h. The findings are shown as the mean ± standard error of at least three separate, duplicate-run trials. The Mann-Whitney U test was used to evaluate the data. * $p < 0.05$ and *** $p < 0.001$ vs untreated cells; # $p < 0.05$ and #### $p < 0.0001$ vs TG-treated cells.*

Furthermore, Vx-445 demonstrated the ability to decrease COXII protein expression (Figure 35), as assessed by flow cytofluorimetry, in both cell lines pre-treated with TG at both selected experimental time intervals. Together, these results indicate that VX-445 exerts a broad, multi-target anti-inflammatory action by modulating upstream signaling mediators (IκBα, p-STAT3) as well as downstream effectors (IL-6, COXII), thereby supporting its potential as a therapeutic candidate in ER stress–associated disorders.

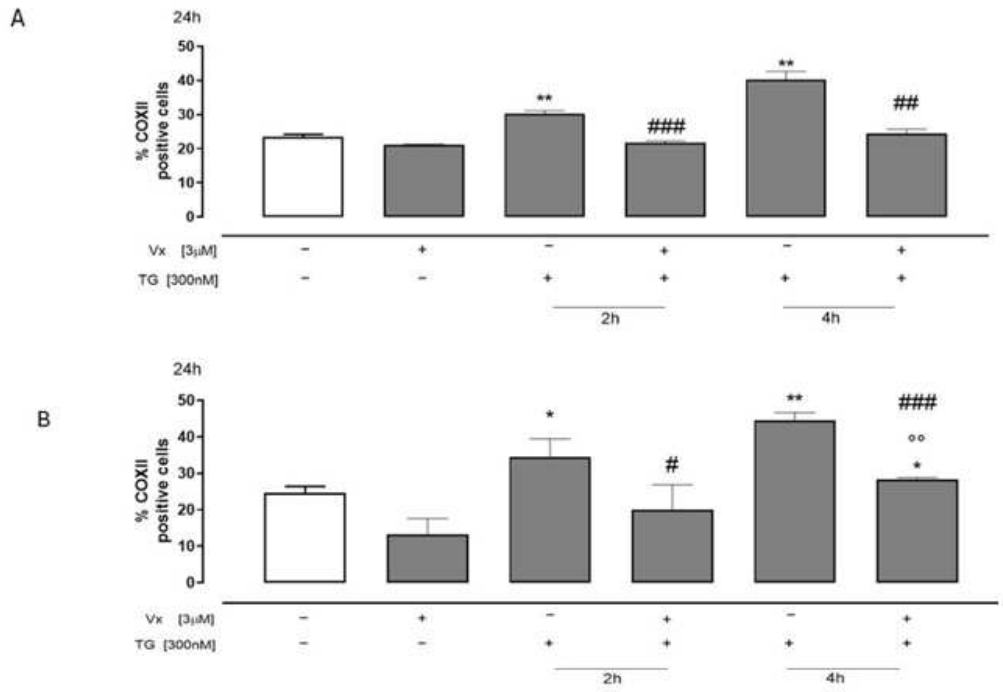


**Figure 35**: *Vx-445 effect on COXII levels. To cause ER stress, SH-SY5Y (A) and A549 (B) cells were following the protocol with 300 nM TG for 2 or 4 h. Then, over 24h, 3 μM of Vx-445 was administrated. Flow cytometry analysis was used to check the COXII level. The percentage of COXII-positive cells from at least three separate experiments, each conducted in triplicate, was expressed as mean ± S.E.M. The data was subjected to a Mann-Whitney U test analysis. * p < 0.05 and ** p < 0.005 in vs nontreated cells; # p < 0.05, ## p < 0.005 and ### p < 0.001 vs TG-treated cells*

### *5.2.6 Vx-445 Interferes in NO Release Under ER Stress*

Nitric oxide (NO) is a key signalling molecule in the inflammatory response. Under physiological conditions, it generally exerts anti-inflammatory functions, whereas in pathological settings its excessive production turns it into a pro-inflammatory mediator that sustains and amplifies inflammation (Sharma *et al.,* 2007). To investigate the effects of Vx-445 on TG-induced NO production, flow cytometric analyses were performed using the fluorescent probe DAF-2DA. Results demonstrated that treatment with Vx-445 significantly ($p<0.0001$) reduced NO production (Figure 36) in TG-treated cells at all time points. These findings suggest that Vx-445 may reduce ER stress-induced inflammation not only by modulating protein-folding sensors and inflammatory cytokines, but also by limiting excessive NO production.

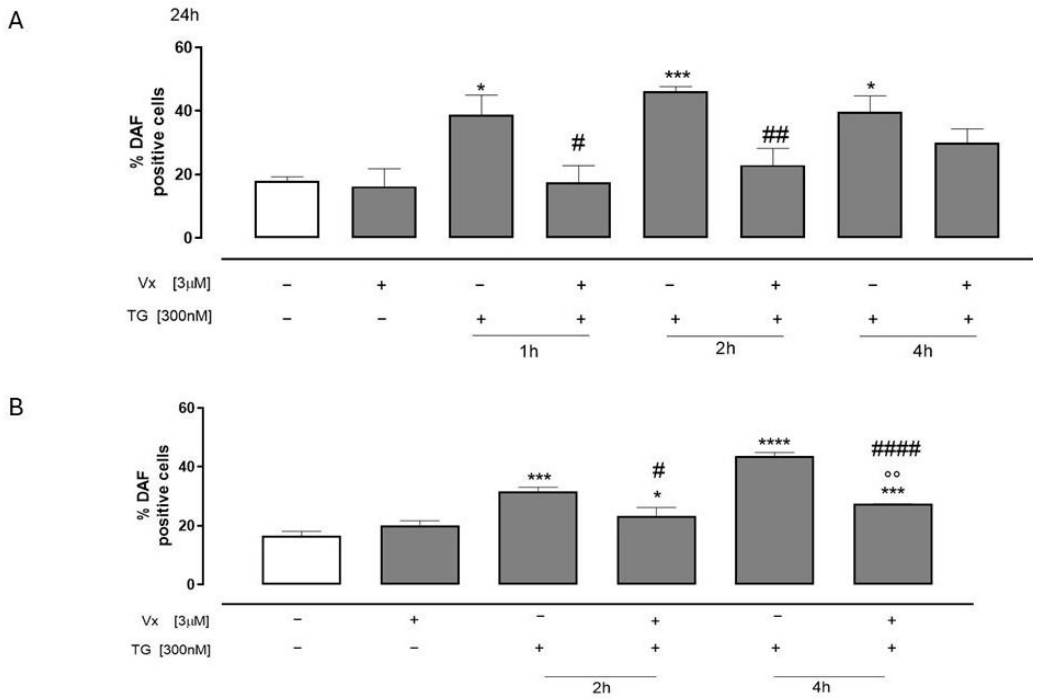


**Figure 36**: *Vx-445 counteracts NO production. ER stress was induced, treating with 300 nM TG until 1h, 2h or 4 SH-SY5Y cells (A) and for 2h or 4h A549 (B) cells. Subsequently, 3 μM of Vx-445 was then added for the entire day. Probe 4,5-Diaminofluorescein Diacetate, DAF- 2 DA, has been employed to quantify NO levels. Mean ± SEM of NO generation was expressed as the proportion of DAF-positive cells derived from a minimum of three separate experiments, each carried out in duplicate. The data was assessed using the Mann–Whitney U test. * p < 0.05, *** p < 0.001 and **** p < 0.001 vs nontreated cells; °° p < 0.005 vs Vx-445-treated cells; # p < 0.05 ## p < 0.005 and #### p < 0.0001 vs TG-treated cells*

### *5.2.7 Starting Point for Exploring ER-Mitochondrial Interplay: UPR modulation by VX-445*

The ER plays a crucial role in maintaining cellular proteostasis; when this delicate equilibrium is perturbed, ER stress arises and underlies many neurodegenerative diseases (Shi *et al.,* 2022). To restore the initial homeostasis, the cell activates the UPR, with the dissociation of GRP78/BiP from the luminal domains of the principal ER-stress proteins. BiP is one of the chaperon ER-resident and the main ER-stress sensor (Brenner *et al.,* 2025). To validate the ER-stress induction model based on TG-induced disruption of protein processing, we assessed in the MO3.13 cell line whether the corrector VX-445 modulates BiP expression as showed above for the SH-SY5Y cells (Figure 37). Western blotting confirmed that, following TG-induced ER stress, BiP expression increased significantly at all experimental time points ($p<0.001$), consistent with a stress condition; meanwhile, drug treatment

reduced BiP expression ($p<0.05$), supporting its ability to attenuate this principal ER-stress sensor and restore the initial homeostatic condition in MO3.13 as well.

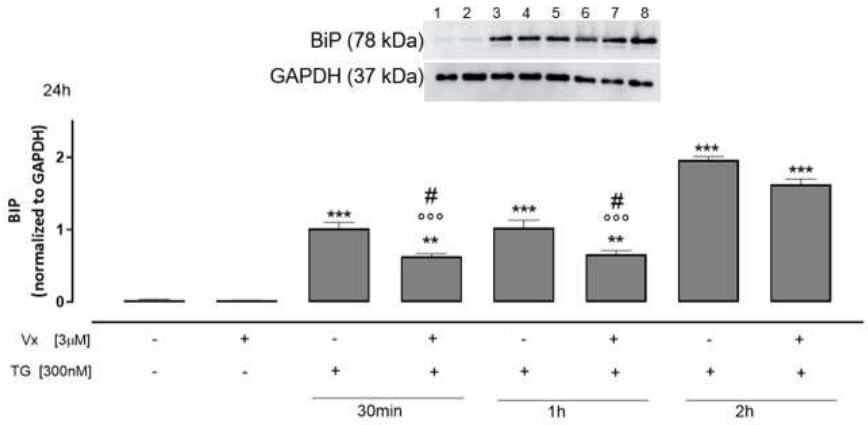


**Figure 37***: Vx-445 modulates BiP expression. Western blot analysis: 1: ctrl, 2: Vx-445, 3:TG for 30 min, 4: Vx-445 after 30 min of TG pretreatment; 5:TG for 1h, 6: Vx-445 after 1h of TG pretreatment, 7:TG for 2h, 8: Vx-445 after 2h of TG pretreatment. Cells were pretreated with 300 nM TG for 2 or 4 h to induce ER stress. Subsequently, 3 μM of Vx-445 were administered for 24 h. BiP expressions on MO3.13 was detected by Western blot analysis. GAPDH protein expression was used as a loading control. Results are expressed as mean ± S.E.M. from at least three independent experiments each performed in triplicate. Data were analyzed by a Mann–Whitney U test. *** $p < 0.001$ vs. non-treated cells; °°° $p < 0.001$ vs. Vx-445-treated cells; # $p < 0.05$ vs. TG-treated cells.*

ER-mitochondria interface at mitochondria-associated membranes (MAMs) is one of the most studied interaction, moreover, MAMs are hotspots for transferring stress signals from the ER to mitochondria, particularly when ER homeostasis fails (Kumar & Maity, 2021). Key ER-stress sensors, including BiP, reside at MAMs (Martucciello *et al.,* 2020), and western blot analysis in both neuronal cell lines were used to test whether the corrector modulates the expression of IRE1 and ATF4, a downstream effector of the PERK pathway that localizes at ER–mitochondria contact sites. Accordingly, after exposure to TG at the specified time points, cells were treated with the corrector for the subsequent 24h. Protein-expression data confirmed the stress condition under TG, evidenced by increased ATF4 levels. treatment with the corrector reduced this stress signature, significantly lowering ATF4 expression after 1h pre-treatment in both lines ($p<0.05$) (Figure 38A and 38B).

IRE1 followed a similar pattern; oligodendrocytes (MO3.13) were more sensitive, showing a significant reduction in IRE1 expression with as little as 30 min of TG pre-treatment plus corrector ($p<0.05$)(Figure 38C and 38D) These preliminary results indicate that the corrector can modulate this ER-stress sensor that are localized at MAMs levels, suggesting that the corrector can have a repercussion in mitochondrial function.

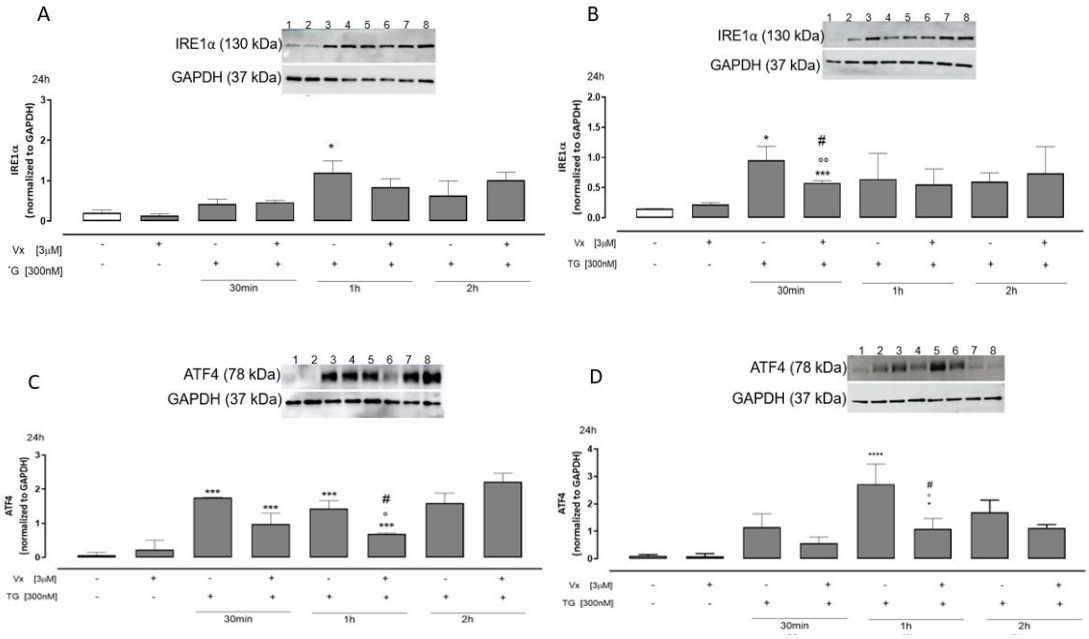


**Figure 38**: *Vx-445 acts on UPR component resident in MAMs. Western blot analysis: 1: ctrl, 2: Vx-445, 3:TG for 30 min, 4: Vx-445 after 30 min of TG pretreatment; 5:TG for 1h, 6: Vx-445 after 1h of TG pretreatment, 7:TG for 2h, 8: Vx-445 after 2h of TG pretreatment. Cells were pretreated with 300 nM TG for 2 or 4 h to induce ER stress. Subsequently, 3 μM of Vx-445 were administered for 24. IRE1α for SH-SY5Y (A) and MO3.13(B) and ATF4 for SH-SY5Y(C) and for MO3.13(D) expressions were revealed by Western blotting analysis. GAPDH expression was employed as a loading control. These results are presented as the average ± standard error of at least three separate, triplicate-performed studies. Data were processed according to the Mann–Whitney U-test. * $p < 0.05$, **** $p < 0.001$ vs. untreated cells; ° $p < 0.05$ and °° $p < 0.005$ vs. Vx-445-treated cells; # $p < 0.05$ vs. TG-treated cells.*

### *5.2.8 The corrector modulates mitochondrial calcium signaling, a key pathway in neuronal cells*

In neuronal cells, mitochondrial $Ca^{2+}$ levels are tightly regulated, and their imbalance compromises key mitochondrial functions, leading to increased production of ROS and activation of apoptosis, hallmark processes in several

neurodegenerative disorders, including Alzheimer's disease (Calvo-Rodriguez & Bacskai, 2021). Given the crucial role of mitochondria in neuronal health, the ability of VX-445 to modulate mitochondrial calcium levels was investigated. Treatment with CCCP (5 μM), which disrupts oxidative phosphorylation, induces mitochondrial depolarization and the subsequent release of calcium into the cytosol, detectable by spectrofluorimetric analysis. As shown in Figure 39, in both cell lines, TG-pretreated samples displayed a significantly reduced Δ increase in calcium at all experimental time points ($p < 0.001$), reflecting calcium depletion from mitochondrial stores caused by ER stress. Conversely, 24-hour VX-445 treatment restored cells to homeostatic conditions, with Δ increase values comparable to control levels. This demonstrates the corrector's ability to re-establish mitochondrial calcium storage and restore cellular homeostasis across all experimental time points.

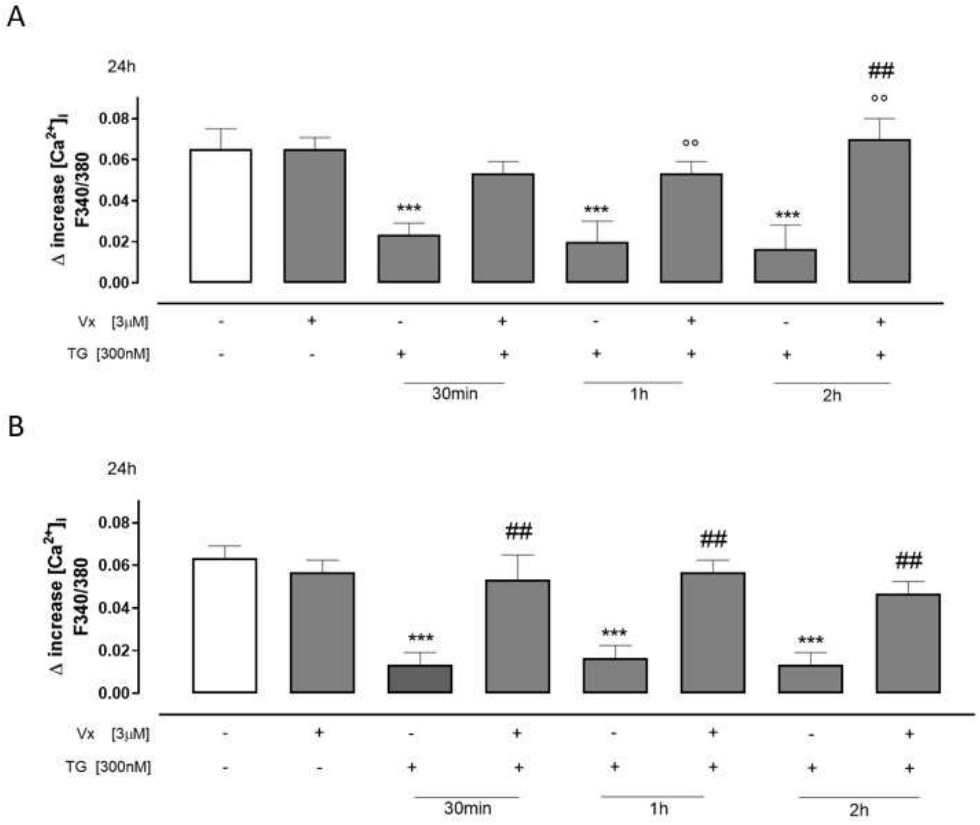


**Figure 39:** *Vx-445 acts on calcium signaling. Cells were pretreated with 300 nM TG for 30 min or 1 or 2h, to induce ER stress. Following this, Vx-445 (3 μM) was added for 24h. After ER stress, the effect on mitochondrial calcium levels of SH-SY5Y (A) and MO3.13 (B) cells were quantified using 5 μM of carbonyl cyanide m-chlorophenylhydrazone (CCCP) in calcium-free media. The results show the mean ± S.E.M. of the delta (δ) increase in the fluorescence of the FURA 2 ratio (340/380 nm)*

*from a minimum of three separate experiments, each carried out in duplicate. The findings are presented as the average ± standard error of duplicate data from a minimum of three separate and identical tests. The Mann–Whitney U test analysis was performed on the data. *** p < 0.001 vs. untreated cells; °° p < 0.005 vs. Vx-809-treated cells; ## p < 0.005 vs. TG-treated cells.*

### *5.2.9 Involvement of the VX-445 in the reduction of mitochondrial ROS levels*

Mitochondria are the primary source of ROS within the cell, with enzymes of the electron transport chain being the main contributors to this process (Hernansanz-Agustín & Enríquez, 2021). When ROS production and clearance become unbalanced, a condition known as oxidative stress develops. Together with neuroinflammation, it represents a hallmark of neurodegeneration, contributing to disease progression (Simpson & Oliver, 2020). Using the fluorescent probe MitoSOX, highly selective dye for superoxide ions produced principally in the mitochondrion, flow cytometric analysis revealed the dynamics of ROS production in both neuronal cell lines treated according to the experimental protocol. Treatment with TG induced pronounced oxidative stress at all time points. In contrast, 24h-VX-445 administration markedly reduced mitochondrial ROS levels, an effect evident as early as 15 minutes in SH-SY5Y cells, demonstrating a strong antioxidant activity that persisted after 2 hours of TG pretreatment ($p < 0.005$) in MO3.13 cells.

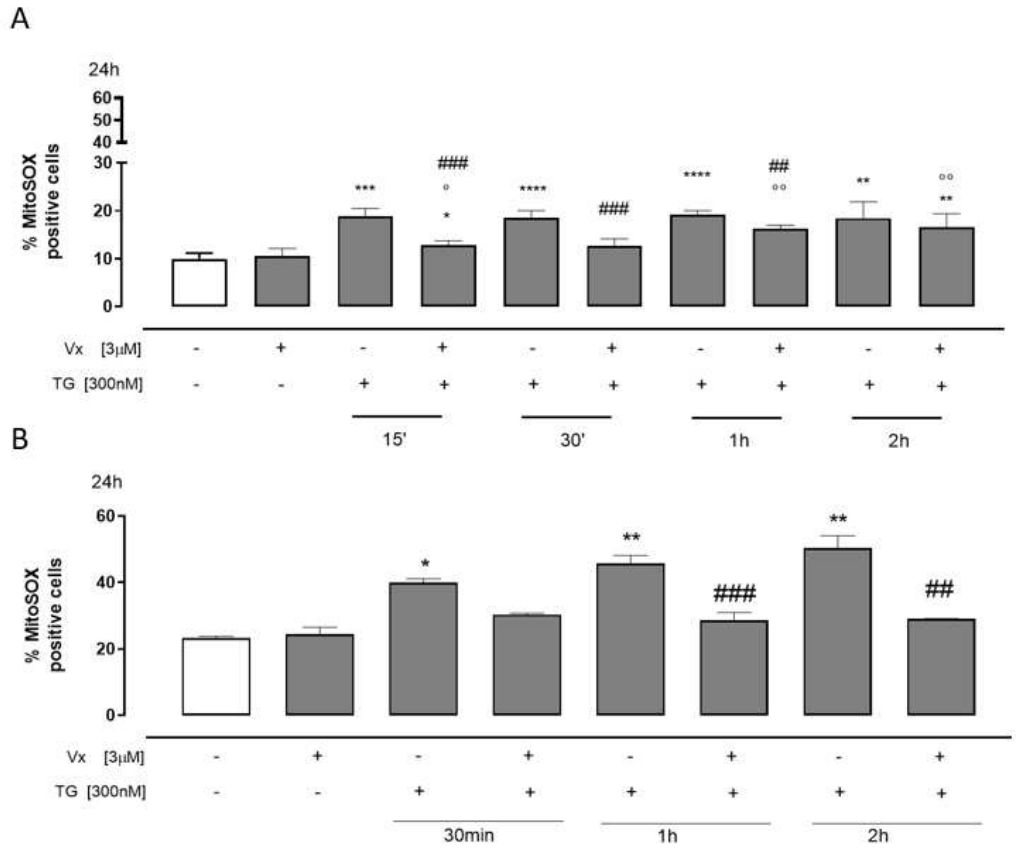


**Figure 40:** *Vx-445 Involvement with Mitochondrial ROS levels. SH-SY5Y (A) and MO3.13 (B) cells were treated with TG (300 nM) for 15min, 30min, 1h and 2h. Subsequently, they were treated with Vx-445 (3 µM) for 24 hours. MitoSOX Red probe with flow cytometry analysis was used to measure the amount of superoxide produced by the mitochondria in cells. The expression of mitochondrial superoxide generation was calculated as the mean ± standard error of the proportion of cells positive for MitoSOX in three separate tests, each carried out in duplicate. The Mann–Whitney U test was used to evaluate the data. * p < 0.05, ** p < 0.005, *** p < 0.001,**** p < 0.0001 vs. untreated cells; ° p < 0.05; °° p < 0.005 vs. Vx-445-treated cells; ## p < 0.005, ### p < 0.001 vs TG-treated cells.*

### *5.2.10 VX-445 supports the recovery of mitochondrial membrane potential after ER stress induction*

The mitochondrial membrane potential (ΔΨm) is a key component in energy accumulation during oxidative phosphorylation. Together with the proton gradient (ΔpH), ΔΨm constitutes the hydrogen ion electrochemical potential used to synthesize ATP. However, persistent alterations in either parameter can be deleterious; long-term changes in ΔΨm may trigger cell death and contribute to several pathologies including NDs (Huang *et al.,* 2021). To evaluate ΔΨm modulation, the cationic fluorescent dye TMRE

(Tetramethylrhodamine Ethyl Ester) was employed. Due to its lipophilic nature, TMRE accumulates within mitochondria proportionally to ΔΨm. Flow cytometric analysis confirmed that TG-pretreated samples exhibited a significant reduction in fluorescence intensity, reflecting ER stress-induced mitochondrial depolarization. The effect was more pronounced in SH-SY5Y neuroblastoma cells across all experimental time points ($p<0.005$), while MO3.13 cells showed a significant decrease only after 2h of TG pretreatment. On the other hand, treatment with the VX-445 corrector restored the cells to their initial homeostatic state, re-establishing baseline ΔΨm values. A particularly significant recovery was observed after 2h of pretreatment in both cell lines, $p < 0.05$ in SH-SY5Y cells and $p < 0.001$ in MO3.13 cells, highlighting the compound's ability to recover mitochondrial integrity after ER-stress conditions.

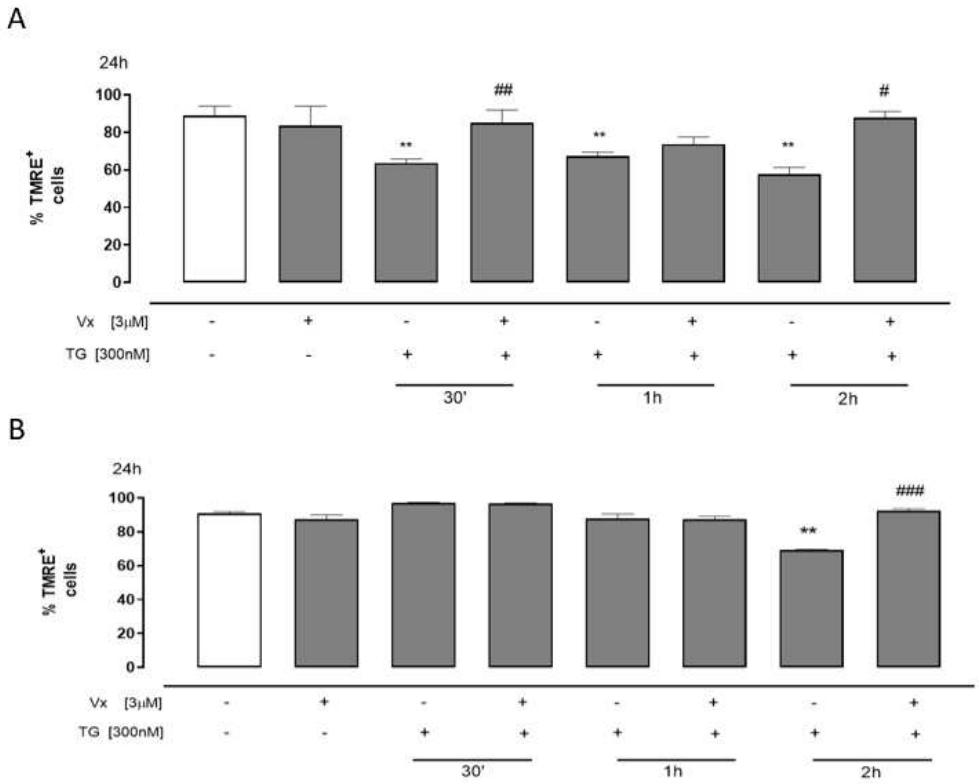


**Figure 41:** *Vx-445 restores TMRE levels. SH-SY5Y (A) and MO3.13 (B) s were treated with TG (300 nM) for 30 min, 1h and 2h. Subsequently, they were treated with Vx-445 (3 μM) for 24 hours. The fluorescent dye TMRE (150 nM) was used to evaluate mitochondrial membrane potential via flow cytometry. Data are expressed as the mean ± SEM of three different experiments, each conducted in triplicate. The results were analyzed by the nonparametric Mann-Whitney test. ** indicates $p < 0.005$ towards the control; # $p< 0.05$; ## $p < 0.005$ and ### $p < 0.001$ vs TG-treated cells.*

### *5.2.11 VX-445 shapes apoptotic responses induced by ER stress*

Neurodegenerative disorders are defined by the progressive loss of selective neuronal populations and the accumulation of disease-specific protein aggregates (Soto & Pritzkow, 2018). Despite their heterogeneity, they converge on shared pathogenic mechanisms, including oxidative stress, neuroinflammation, and programmed cell death, among which apoptosis represents a major modality (Cenini *et al.,* 2020). In our experimental model, apoptosis was quantized by flow cytometry using propidium iodide (PI), fluorescent DNA intercalant. As Showed in Figure 42, both neuroblastoma cells and oligodendrocytes showed an increased percentage of hypodiploid nuclei in samples treated with TG alone, with a robust effect at all time points in SH-SY5Y cells, whereas in MO3.13 cells a significant effect was detected only after 2 h of TG pre-treatment ($p < 0.001$). This also underscores that distinct neural cell populations differ in their susceptibility to apoptosis. In both cell lines, subsequent administration of VX-445 for 24 h reduced apoptotic responses, with an early decrease already evident in SH-SY5Y cells ($p < 0.05$ at 15 min; $p < 0.005$ at 30 min), while in MO3.13 cells a marked reduction emerged after 2 h of TG pre-treatment ($p < 0.001$). These prelaminar results show the VX-445 ability to modulate this pivotal process in neurodegenerative diseases.

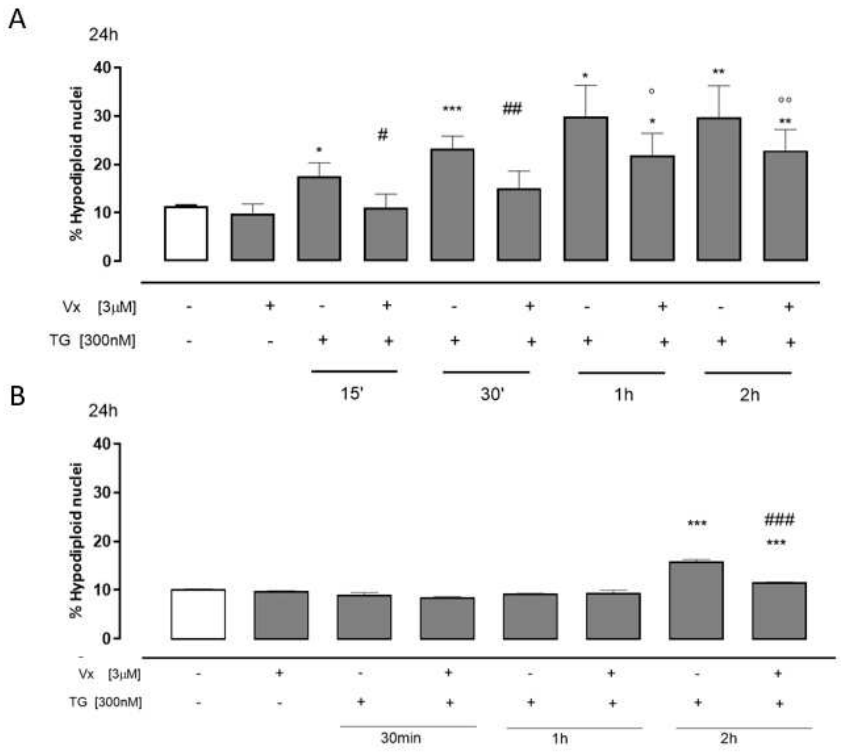


**Figure 42**: *Vx-445 modulates apoptotic process. SH-SY5Y (A) and MO3.13 (B) cells were treated with TG (300 nM) for 15min, 30min, 1h and 2h. Subsequently, they were treated with Vx-445 (3 µM) for 24 hours. After, the cells were stained by propidium iodide, and the fluorescence of individual nuclei was evaluated by flow cytometry. The data are presented as the mean ± standard error of the percentage of hypodiploid nuclei from a minimum of three independent tests, each carried out in in triplicate. The results were analyzed by the nonparametric Mann-Whitney test. * p < 0.05; ** p < 0.005; ***p < 0.001 vs the control; °p < 0.05; °° p< 0.05 vs Vx-445-teatred cells, # p< 0.05; ## p < 0.005 and ### p < 0.001 vs TG-treated cells*

### *5.2.12 Mitochondria-mediated apoptosis, VX-445 impacts cytochrome c release and Bcl-2 expression*

The role of mitochondria in cell death is unequivocally established in apoptosis, and they are crucial for initiating this process. Cytochrome c (Cyt c) plays a central role in the intrinsic apoptotic pathway, also known as the Bcl-2 or mitochondrial pathway: following mitochondrial outer membrane permeabilization (MOMP), Cyt c is released into the cytosol and, together with an adaptor protein, drives apoptosome formation, which in turn activates caspases (Bock *et al.,* 2020). During this phase, levels of the anti-apoptotic protein B-cell lymphoma-2 (Bcl-2) decrease, thereby favoring the onset of apoptosis (Li *et al.,* 2022). Both flow cytometry and Western blot analysis

showed that the corrector VX-445 modulates the expression of these two key factors. After administration of the stressor TG, we observed a concomitant increase in percentage of Cyt c release, and a reduction in Bcl-2 expression, parameters indicative of an advancing apoptotic process. In contrast, administration of the corrector reversed these changes, significantly lowering Cyt c release and increasing expression of the anti-apoptotic protein Bcl-2, that is particularly evident after 1 h of TG pre-treatment in the SH-SY5Y cell line ($p < 0.05$) (Figure 43A and 43C). MO3.13 cells displayed a different temporal profile, with significant effects of VX-445 at shifted time points, Cyt c expression was significantly reduced at 2 h, and the anti-apoptotic effect was already apparent at 30 min (Figure 43B and 43D). Taken together, these findings indicate that the corrector can modulate the mitochondrial apoptotic pathway, underscoring a protective effect in neural cells.

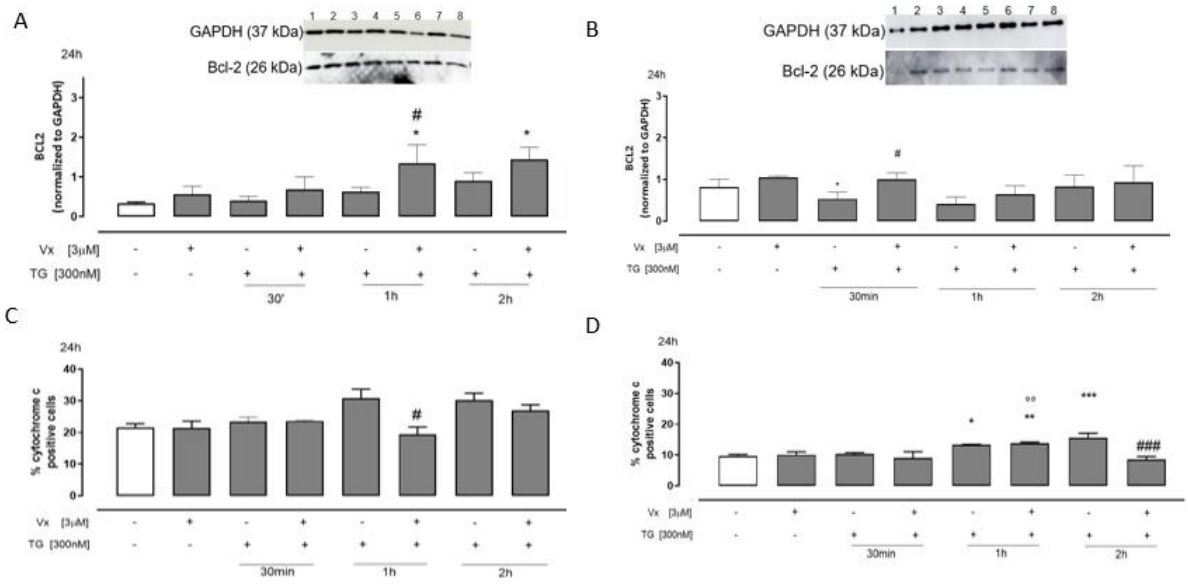


**Figure 43:** *Vx-445 acts on mitochondrial apoptosis. SH-SY5Y and MO3.13 cells were treated with TG (300 nM) for 30 min,1h,2h. Subsequently, Vx-445 (3 µM) for 24h was added. Bcl2 expression in SH-SY5Y(A) and MO3.13 (B) was observed with Western blotting analysis with respective normalization to GAPDH. Western blot analysis: 1: ctrl, 2: Vx-445, 3:TG for 30 min, 4: Vx-445 after 30 min of TG pretreatment; 5:TG for 1h, 6: Vx-445 after 1h of TG pretreatment, 7:TG for 2h, 8: Vx-445 after 2h of TG pretreatment. Cytochrome c released was evaluated with flow cytometry in SH-SY5Y(C) and MO3.13 (D). The data are expressed as mean ± SEM of three different experiments, each conducted in triplicate. The results were analyzed using the nonparametric Mann-Whitney test. * $p < 0.05$, ** $p < 0.005$, *** $p < 0.001$ vs. untreated cells; °° $p < 0.005$ vs. Vx-445-treated cells; # $p < 0.05$ vs TG-treated cells.*

## 5.3 Discussion

The inflammatory process represents the primary and most immediate defense mechanism (acute inflammation) activated to protect the organism from various insults. These may derive from pathogens, as in the case of pathogen-associated molecular patterns (PAMPs), which are recognized by pattern recognition receptors (PRRs). However, inflammation can also be triggered when the immune system detects molecules released by damaged cells, known as damage-associated molecular patterns (DAMPs), which are likewise recognized by PRRs. When the organism fails to return to its initial physiological state, persistent and chronic inflammation becomes detrimental and is associated with several human pathological conditions.

Moreover, growing epidemiological, clinical, and experimental evidence indicates that inflammation can also arise independently of PRR-mediated recognition and signaling, as a consequence of cellular stress, a condition in which intracellular biological processes are disrupted (Chipurupalli *et al.,* 2021), ultimately leading to increased inflammation associated with pathologies such as neurodegenerative disorders, metabolic syndromes, Cystic fibrosis, and ischemia (Hartl, 2017).

A key feature of the above conditions is protein misfolding, which causes their accumulation within the ER, resulting in ER stress and subsequent activation of the UPR, a key pathway aimed at restoring homeostasis. However, under chronic stress conditions, sustained UPR activation can trigger inflammation, primarily through the NF-κB pathway. This activation promotes the production and release of pro-inflammatory mediators. In this context, the close link between protein misfolding, ER stress, and the inflammatory process becomes evident (Chen *et al.,* 2023).

Vx-445 (Elexacaftor) is a pharmacological compound extensively used in CF therapy and was approved by the FDA in 2019 as part of a triple combination therapy with others modulator. Although it is known to assist in the folding and stability of the CFTR protein, its potential impact on reducing ER stress and modulating inflammation is not yet fully elucidated. In the previous chapter, hypothetical protein partners were evaluated using

functional proteomics and DARTS techniques, with which the corrector could interact beyond its canonical target, in order to support potential off-label uses. In this chapter, the ability of VX-445 to indirectly attenuate the protein misfolding-related inflammatory response by modulating ER-related stress and related principal pathways is explored in greater depth.

To mimic the stress of protein misfolding, cells were pretreated with TG, a non-competitive inhibitor of the SERCA pump (Sarco-dependent ATPase/Reticular Ca2+). This caused Ca2+ to leak out of the ER, which accumulated in the cytoplasm, preventing the ER from normal protein processing. This led to ER stress and UPR activation, thereby also disrupting the activation of the inflammatory response. The A549 (alveolar basal epithelial) and SH-SY5Y (neuroblastoma) cell lines were used to conduct the different experiments since the accumulation of misfolded proteins is characteristic of pathologies such as cystic fibrosis, Parkinson's and Alzheimer's diseases.

Calcium is an exceptionally versatile molecule, acting as a key second messenger and contributing to the regulation of numerous processes, including metabolism, secretion, muscle contraction, neuronal excitability, and cell death. Its signalling efficiency relies on a steep concentration gradient, up to $10^5$-fold, between the extracellular and intracellular compartments. This gradient is maintained not only across the plasma membrane but also among intracellular organelles and the cytosol, enabling rapid and tightly controlled calcium-dependent signalling events. The ER, the principal intracellular calcium reservoir, stores approximately 0.2–2 mM calcium (Zhang *et al.,* 2015), with free luminal concentrations ranging from ~100 to 800 µM. Preserving this gradient requires continuous energetic investment, as ATP-dependent pumps and transporters work against electrochemical forces. When cytosolic calcium levels rise uncontrollably, pathological cascades can be triggered, ultimately activating the canonical mitochondrial apoptotic pathway (Berridge *et al.,* 2000).

Importantly, disruptions in calcium gradients, particularly within the ER lumen, have been associated with various diseases, including diabetes,

neurological and vascular disorders, viral infections, and cancer (Lin et al., 2013). These pathological conditions share the accumulation of misfolded proteins within the ER, which disrupts calcium homeostasis and consequently triggers ER stress and activation of the UPR. ER stress is closely interconnected with pathological processes that arise concurrently with this condition; indeed, among the UPR targets the transcription factor NF-κB is the master regulator of inflammation. In the experimental system employed, induction of ER stress with TG, that perturbs the finely regulated calcium equilibrium, revealed that the corrector, by mitigating ER stress, facilitates the physiological restoration of ER calcium stores. According to this observation, proper protein folding alleviates ER stress, which in turn prevents calcium dysregulation, which is a trigger of apoptosis and inflammation.

Closely related to ER stress is apoptosis mediated by caspase-4, a protein localized in this compartment and closely associated with several key factors in ER stress-induced cell-death pathways, including GRP78/BiP. Moreover, caspase-4 is linked to inflammation both because its chromosomal colocalization classifies it among inflammatory caspases, suggesting that these enzymes evolved from a common ancestor through gene duplication and share functions in innate immunity and inflammatory processes, and because caspase-4 has been shown to participate in inflammation, underscoring its role in lipopolysaccharide (LPS)-induced inflammatory responses (Lakshmanan & Porter, 2007). Flow-cytometric analysis of caspase-4 release in the experimental model further indicates that the corrector, by reducing ER-stress, also decreases the release of this closely associated caspase in both cellular models examined.

GRP78/BiP protein acts as a master regulator of the UPR, playing a crucial role in stress adaptation, anti-inflammatory regulation, and immunomodulatory functions (Panayi, & Corrigall, 2006). Western blotting analysis shows a substantial decrease in GRP78/BIP expression suggesting a restoration of endoplasmic reticulum homeostasis, potentially mitigating stress-induced chronic inflammation, after VX-445 treatment

As previously mentioned, ER stress due to abnormal protein folding also triggers the inflammatory process by activating key factors such as NF-κB. Normally maintained in the cytoplasm in complex with IκBα, an inhibitor of NF-κB. Canonical NF-κB activation involves phosphorylation of IκBα by IκB kinase (IKK), followed by proteasome-mediated degradation of IκBα. Specifically, in canonical activation, IKKβ, a subunit of IKK, phosphorylates IκBα on serines 32 and 36, leading to its polyubiquitination and proteasomal degradation, releasing NF-κB for nuclear translocation and target gene activation. ER stress condition suppresses IκBα synthesis to drive NF-κB activation (Lahiri *et al.,* 2025) Indeed, in the proposed experimental model, drug administration, after inducing ER stress, produced a significant increase in Ik-Bα levels, with consequent inhibition of the transduction pathway mediated by it and therefore of the inflammatory process.

Other mediators involved in the inflammatory process exhibit the same trend. Numerous studies have demonstrated the link between ER stress and inflammation through the activation of proteins such as STAT3, which is induced upstream by alterations of the UPR that activate the JAK/STAT signalling pathway. STAT3 acts as a central regulator and is activated via tyrosine phosphorylation in response to cytoplasmic cytokine signalling. Once activated, it translocates to the nucleus, where it functions as a transcription factor. It is therefore crucial to modulate STAT3 expression, and consequently its activation, as its function is strictly dependent on the cellular environment (Grassmann et al., 2025). As shown by flow cytometry analysis, VX-445 reduced p-STAT3 activation, thereby limiting the amplification of the inflammatory process associated with ER stress.

UPR components are tightly integrated with key inflammatory signalling pathways including increased expression of pro-inflammatory cytokines, like IL-6 (da Silva et al., 2025). IL-6 is one of the cytokines induced by NF-κB and is further linked to STAT3, as it acts as an activator of STAT3 itself. In fact, the IL-6/JAK/STAT3 axis has been extensively implicated in both physiological and pathological conditions (Jill et al., 2023). NF-κB activation by endoplasmic reticulum stress leads to the induction of many genes with pro-inflammatory

effects; indeed, it is well known that COX-2 is upregulated under inflammatory condition. COX is a key rate-limiting enzyme that catalyzes the synthesis of prostaglandins and thromboxane A2 from arachidonic acid. COX-2, in particular, is an immediate early gene, whose expression is low or absent under physiological conditions in most tissues (Liang et al., 2025). According to the proposed experimental model, the corrector VX-445 further confirmed its ability to modulate the inflammatory process associated with ER stress by significantly reducing the levels of IL-6 detected in the culture medium by ELISA assay and the expression of COX-2 analysed by flow cytometry, respectively. Considering the effects that VX-445 exerted upstream (IκBα, p-STAT3) and downstream in the inflammatory process (IL-6, COXII), these results suggest a multi-target anti-inflammatory effect highlighting its potential as a therapeutic agent in ER stress-related pathologies.

VX-445 revealed an additional anti-inflammatory effect, through flow cytometric analysis, significantly reducing the production of NO in both cell lines demonstrating an influence on oxidative stress signaling linked to inflammation. Nitric oxide (NO) is a versatile bioactive molecule essential for numerous physiological processes, including vascular tone regulation, immune defense and neurotransmission. Due to its gaseous form, NO has a short half-life, and its physiological role is concentration-dependent, often limiting its function to a single target site. NO has protective effects at pico- and nanomolar concentration; however, it is cytotoxic at higher concentrations. It can react with ROS, particularly superoxide, to form peroxynitrate, causing the peroxidation of lipids, thiols, amines, fatty acids, tyrosine nitrate, and guanine hydroxylase at low pH, leading to oxidative/nitrosative stress (Andrabi et al., 2023).

The ER and mitochondria are not only organelles in physical contact at MAMs, but their proper function also depends on a tight functional cross-talk. A recent study on Wolfram syndrome (SW), a neurodegenerative disorder caused by mutations in the ER transmembrane protein genes (*WFS1* or *CISD2)* clearly illustrates this relationship: these mutations disrupt ER–mitochondria interactions, impair $Ca^{2+}$ transfer and mitochondrial function, and

ultimately lead to bioenergetic deficits and oxidative stress (Cartes-Saavedra *et al.,*2025).

It is widely documented that the UPR, triggered by ER stress, is governed by three principal sensors IRE1, PERK, and ATF6, whose signaling determines cell fate. Increasingly, inter-organelle crosstalk is being investigated to clarify its impact on human disease (Gordaliza-Alaguero et al., 2019). The main NDs are associated with ER-stress condition due to the accumulation of misfolded proteins with consequent activation of the UPR. Recent studies have shown that reducing the expression of key UPR sensors such as PERK and IRE1, which are located at ER–mitochondria contact sites, also improves mitochondrial function. In the proposed experimental model, VX-445 was found to reduce the expression of ATF4, the main downstream effector of PERK signaling, as well as the expression of IRE1 (Chu et al., 2021; Gundu et al., 2024). These results are encouraging, as they suggest potential involvement of VX-445 at the mitochondrial level as well.

Calcium signaling is essential for neuronal function, regulating gene transcription, energy production, proteostasis, and synaptic structure and function. Since many neurological disorders share calcium-mediated alterations, it has been proposed that neurodegenerative diseases may share an upstream etiopathogenic basis linked to calcium dysregulation (Alzheimer's, Parkinson's, and Huntington's disease). In neurons, calcium enters mainly through plasma membrane channels and is rapidly buffered by dedicated systems, calcium-binding proteins, and intracellular organelles such as the ER, mitochondria, and lysosomes. (Schrank *et al.,* 2020). Through spectrofluorimetric studies it was possible to demonstrate that VX-445 restore the initial homeostatic state of mitochondrial calcium following TG induced-ER stress. This finding is highly promising, as mitochondria are essential organelles for nervous cells.

Mitochondrial ROS are implicated in the onset and progression of numerous pathological conditions, including NDs. In this context, they are also tightly linked to calcium regulation: activation of L-type $Ca^{2+}$ channels in the plasma membrane during normal autonomous pacemaking activity of dopaminergic

neurons in the substantia nigra promotes transient mitochondrial ROS production and increases neuronal vulnerability to lesions during Parkinson's disease development. Moreover, mitochondrial ROS can impair neuronal glycolytic metabolism, rendering energy production insufficient to meet the high metabolic demands of neurons and thereby facilitating the initiation of apoptosis. Several additional examples corroborate these observations (Hernansanz-Agustín & Enríquez, 2021). It is therefore crucial to modulate their production. In this framework, VX-445 further demonstrated its involvement at the mitochondrial level by significantly reducing mitochondrial ROS levels compared with samples treated with TG alone.

For mitochondria to define "optimal" ΔΨm values is difficult because an excessively high ΔΨm promotes an exponentially increases production of ROS, with potential pathological effects. However, an excessively low ΔΨm is also dangerous; in addition to compromising ATP production, it may reduce ROS levels too drastically, leading to "reductive stress", a condition that is as harmful as oxidative stress. For these reasons to keep the value of ΔΨm in the right balance is essential. Under ER-stress conditions induced by the accumulation of misfolded or unfolded proteins, mitochondria undergo collapse of the membrane potential associated with calcium overload, leading to increased oxidative stress. Excess mitochondrial $Ca^{2+}$ induces the opening of the mitochondrial permeability transition pore, which can result in the blockade of ATP production and, ultimately, in apoptosis. Indeed, in early stages the loss of ΔΨm can be partial and transient; in advanced stages it becomes significant and irreversible (Bernardi *et al.,* 2023). Surprisingly, VX-445 was able to reverse the mitochondrial membrane depolarization induced by TG treatment, clearly restoring the mitochondrial membrane potential in drug-treated samples to values comparable to those of the control.

From a physiological perspective, apoptosis is an homeostatic process essential for maintaining cell populations balance within developing tissues and for the proper assembly of neuronal circuits during nervous system maturation (Kupcho et al., 2019; Wong & Marin, 2019). By contrast, under pathological conditions, apoptosis is triggered when cells are damaged by

disease, harmful insults like an unresolved ER-stress condition, or aging and is typically associated with increased cytosolic calcium levels and DNA fragmentation (Erekat, 2022). Mitochondria-mediated apoptosis plays a central role in the neuronal loss typical of NDs. In this thesis, apoptosis was assessed alongside PI-based detection of cell death, to provide an overview of the process. The expression of the anti-apoptotic protein Bcl-2 and the release of cytochrome c were evaluated as key markers of the mitochondrial pathway. The integration of these parameters highlighted the specific contribution of the mitochondrial pathway to ER-stress-associated apoptosis and clarified how treatment with VX-445, within the proposed experimental model, influences this process in a neurodegenerative context. The presence of the drug attenuated the apoptosis as demonstrated by the reduction of hypodiploid nuclei, the decreased release of cyt-c, and the increased expression of the anti-apoptotic protein Bcl-2 especially in the early phase of ER-stress induction with TG.

# General conclusion

Overall, this work supports the view that CFTR correctors, originally developed for cystic fibrosis, act as broader modulators of ER stress and proteostasis rather than exclusively as mutation-specific CFTR chaperones. Across different cell models exposed to thapsigargin-induced ER stress, VX-809 consistently influenced UPR signaling, $Ca^{2+}$homeostasis, oxidative imbalance, apoptosis and, in later stages, inflammatory pathways, delineating a cytoprotective profile that extends beyond the canonical CFTR context. The subsequent characterization of VX-445 (Elexacaftor), the corrector currently used in clinical practice, confirmed and strengthened this evidence, showing a comparable ability to restore ER homeostasis and revealing, through proteomic and DARTS-based analyses, drug-responsive protein networks that begin to clarify its pleiotropic mechanism of action. The produced data so far indicating an impact of VX-445 on mitochondrial function under ER-stress conditions further point to a role at the ER–mitochondria interface. Taken together, these findings provide a well-founded rationale for considering CFTR correctors as candidate modulators of chronic ER stress in misfolding-associated diseases beyond cystic fibrosis.

# Publications

## Publications

### *Published Articles*

Pecoraro, M., **Serra, A**., Pascale, M., & Franceschelli, S. (2023). Vx-809, a CFTR Corrector, Acts through a General Mechanism of Protein Folding and on the Inflammatory Process. International journal of molecular sciences, 24(4), 4252. https://doi.org/10.3390/ijms24044252

Pecoraro, M., **Serra, A**., Pascale, M., & Franceschelli, S. (2024). The ER Stress Induced in Human Neuroblastoma Cells Can Be Reverted by Lumacaftor, a CFTR Corrector. Current issues in molecular biology, 46(9), 9342–9358. https://doi.org/10.3390/cimb46090553

Pecoraro, M., **Serra, A**., Lamberti, M. J., Pascale, M., & Franceschelli, S. (2025). New Role of Protein Misfolding Corrector in the ER Stress-Inflammation Axis: Possible Therapeutic Indication in Neuronal and Epithelial Tumor Cells. International Journal of Molecular Sciences, 26(22), 10846. https://doi.org/10.3390/ijms262210846

### *Manuscript in preparation*

**Serra, A**., Morretta, E., Pecoraro, M., Lamberti, M. J., Monti, M.C., Pascale, M., Franceschelli, S., “Functional proteomics and biological screening of protein misfolding under ER stress condition in neuroblastoma cell model”

# Bibliography


Acosta-Alvear D, Harnoss JM, Walter P, Ashkenazi A. Homeostasis control in health and disease by the unfolded protein response. Nat Rev Mol Cell Biol. 2025 Mar;26(3):193-212. Epub 2024 Nov 5. PMID: 39501044.

Amanakis, G. & Murphy, E. Cyclophilin D: An Integrator of Mitochondrial Function. Front. Physiol. 11, (2020).

Amico, G., Brandas, C., Moran, O., & Baroni, D. (2019). Unravelling the Regions of Mutant F508del-CFTR More Susceptible to the Action of Four Cystic Fibrosis Correctors. International journal of molecular sciences, 20(21), 5463

Andrabi, S. M., Sharma, N. S., Karan, A., Shahriar, S. M. S., Cordon, B., Ma, B., & Xie, J. (2023). Nitric Oxide: Physiological Functions, Delivery, and Biomedical Applications. Advanced science (Weinheim, Baden-Wurttemberg, Germany), 10(30), e2303259.

Anwar, S., Peng, J. L., Zahid, K. R., Zhou, Y. M., Ali, Q., & Qiu, C. R. (2024). Cystic Fibrosis: Understanding Cystic Fibrosis Transmembrane Regulator Mutation Classification and Modulator Therapies. Advances in respiratory medicine, 92(4), 263–277.

Arnst, N., Redolfi, N., Lia, A., Bedetta, M., Greotti, E., & Pizzo, P. (2022). Mitochondrial Ca2+ Signaling and Bioenergetics in Alzheimer's Disease. Biomedicines, 10(12), 3025.

Baatallah, N., Elbahnsi, A., Mornon, J. P., Chevalier, B., Pranke, I., Servel, N., Zelli, R., Décout, J. L., Edelman, A., Sermet-Gaudelus, I., Callebaut, I., & Hinzpeter, A. (2021). Pharmacological chaperones improve intra-domain stability and inter-domain assembly via distinct binding sites to rescue misfolded CFTR. Cellular and molecular life sciences: CMLS, 78(23), 7813–7829.

Bakunts, A., Orsi, A., Vitale, M., Cattaneo, A., Lari, F., Tadè, L., Sitia, R., Raimondi, A., Bachi, A., & van Anken, E. (2017). Ratiometric sensing of BiP-client versus BiP levels by the unfolded protein response determines its signaling amplitude. eLife, 6, e27518.

Bardin, E., Pastor, A., Semeraro, M., Golec, A., Hayes, K., Chevalier, B., Berhal, F., Prestat, G., Hinzpeter, A., Gravier Pelletier, C., Pranke, I., & Sermet-Gaudelus, I. (2021). Modulators of CFTR. Updates on clinical development and future directions. European journal of medicinal chemistry, 213, 113195.

Baroni D. (2025). Unraveling the Mechanism of Action, Binding Sites, and Therapeutic Advances of CFTR Modulators: A Narrative Review. Current issues in molecular biology, 47(2), 119.

Basile, A., Pascale, M., Franceschelli, S., Nieddu, E., Mazzei, M. T., Fossa, P., Turco, M. C., & Mazzei, M. (2012). Matrine modulates HSC70 levels and rescues ΔF508-CFTR. Journal of cellular physiology, 227(9), 3317–3323.

Benedetti R, Romeo MA, Arena A, Gilardini Montani MS, Di Renzo L, D'Orazi G, et al. ATF6 prevents DNA damage and cell death in colon cancer cells undergoing ER stress. Cell Death Discov. 2022;8:295.

Berkers, G., van der Meer, R., Heijerman, H., Beekman, J. M., Boj, S. F., Vries, R. G. J., van Mourik, P., Doyle, J. R., Audhya, P., Yuan, Z. J., Kinnman, N., & van der Ent, C. K. (2021). Lumacaftor/ivacaftor in people with cystic fibrosis with an A455E-CFTR mutation. Journal of cystic fibrosis: official journal of the European Cystic Fibrosis Society, 20(5), 761–767.

Bernardi, P., Gerle, C., Halestrap, A. P., Jonas, E. A., Karch, J., Mnatsakanyan, N., Pavlov, E., Sheu, S. S., & Soukas, A. A. (2023). Identity, structure, and function of the mitochondrial permeability transition pore: controversies, consensus, recent advances, and future directions. Cell death and differentiation, 30(8), 1869–1885.

Berridge, M. J., Lipp, P., & Bootman, M. D. (2000). The versatility and universality of calcium signalling. Nature reviews. Molecular cell biology, 1(1), 11–21.

Blank, C. U., Haining, W. N., Held, W., Hogan, P. G., Kallies, A., Lugli, E., Lynn, R. C., Philip, M., Rao, A., Restifo, N. P., Schietinger, A., Schumacher, T. N., Schwartzberg, P. L., Sharpe, A. H., Speiser, D. E., Wherry, E. J., Youngblood, B. A., & Zehn, D. (2019). Defining 'T cell exhaustion'. Nature reviews. Immunology, 19(11), 665–674.

Bock, F. J. & Tait, S. W. G. Mitochondria as multifaceted regulators of cell death. Nat. Rev. Mol. Cell Biol. 21, 85–100 (2020).

Bock, F. J., & Tait, S. W. G. (2020). Mitochondria as multifaceted regulators of cell death. Nature reviews. Molecular cell biology, 21(2), 85–100.

Brenner, J. C., Zirden, L. C., Buzuk, L., Almeida-Hernandez, Y., Radzuweit, L., Diamantino, J., Kaschani, F., Kaiser, M., Sanchez-Garcia, E., Poepsel, S., & Hellerschmied, D. (2025). Conformational plasticity of a BiP-GRP94 chaperone complex. Nature structural & molecular biology, 32(10), 1947–1958.

Cabral-Miranda, F., Tamburini, G., Martinez, G., Ardiles, A. O., Medinas, D. B., Gerakis, Y., Hung, M. D., Vidal, R., Fuentealba, M., Miedema, T., Duran-Aniotz, C., Diaz, J., Ibaceta-Gonzalez, C., Sabusap, C. M., Bermedo-Garcia, F., Mujica, P., Adamson, S., Vitangcol, K., Huerta, H., Zhang, X., … Hetz, C. (2022). Unfolded protein response IRE1/XBP1 signaling is required for healthy mammalian brain aging. The EMBO journal, 41(22), e111952.

Calvo-Rodriguez, M., & Bacskai, B. J. (2021). Mitochondria and Calcium in Alzheimer's Disease: From Cell Signaling to Neuronal Cell Death. Trends in neurosciences, 44(2), 136–151.

Candelise N, Scaricamazza S, Salvatori I, et al. Protein Aggregation Landscape in Neurodegenerative Diseases: Clinical Relevance and Future Applications. Int J Mol Sci. 2021;22(11):6016. Published 2021 Jun 2.

Cao T, Peng B, Zhou X, Cai J, Tang Y, Luo J, Xie H, Zhang J, Liu S. Integrated signaling system under endoplasmic reticulum stress in eukaryotic microorganisms. Appl Microbiol Biotechnol. 2021 Jun;105(12):4805-4818. Epub 2021 Jun 9. PMID: 34106312.

Carreras-Sureda A., Jaña F., Urra H., Durand S., Mortenson D.E., Sagredo A., Bustos G., Hazari Y., Ramos-Fernández E., Sassano M.L., et al. Publisher Correction: Non-canonical function of IRE1α determines mitochondria-associated endoplasmic reticulum composition to control calcium transfer and bioenergetics. Nat. Cell Biol. 2019;21:913.

Cartes-Saavedra, B., Ghosh, A., & Hajnóczky, G. (2025). The roles of mitochondria in global and local intracellular calcium signalling. Nature reviews. Molecular cell biology, 26(6), 456–475.

Celik, C., Lee, S. Y. T., Yap, W. S., & Thibault, G. (2023). Endoplasmic reticulum stress and lipids in health and diseases. Progress in lipid research, 89, 101198.

Cenini, G., Lloret, A., & Cascella, R. (2020). Oxidative stress and mitochondrial damage in neurodegenerative diseases: From molecular mechanisms to targeted therapies. Oxidative Medicine and Cellular Longevity, 2020, 1270256.

Chen C, Zhang X. IRE1alpha-XBP1 pathway promotes melanoma progression by regulating IL-6/STAT3 signaling. J Transl Med. 2017;15:42.

Chen G, Wei T, Ju F, Li H. Protein quality control and aggregation in the endoplasmic reticulum: From basic to bedside. Front Cell Dev Biol. 2023;11:1156152. Published 2023 Apr 19.

Chen X, Shi C, He M, Xiong S, Xia X. Endoplasmic reticulum stress: molecular mechanism and therapeutic targets. Signal transduction and targeted therapy. 2023; 8(1): 352.

Chen, S., Novick, P., & Ferro-Novick, S. (2013). ER structure and function. Current opinion in cell biology, 25(4), 428–433.

Chen, X., Shi, C., He, M., Xiong, S., & Xia, X. (2023). Endoplasmic reticulum stress: molecular mechanism and therapeutic targets. Signal transduction and targeted therapy, 8(1), 352.

Cheung, E. C. & Vousden, K. H. The role of ROS in tumour development and progression. Nat. Rev. Cancer 22, 280–297 (2022).

Chipuk, J. E., Mohammed, J. N., Gelles, J. D. & Chen, Y. Y. Mechanistic connections between mitochondrial biology and regulated cell death. Developmental Cell 56, 1221–1233 (2021)

Chipurupalli, S., Samavedam, U., & Robinson, N. (2021). Crosstalk Between ER Stress, Autophagy and Inflammation. Frontiers in medicine, 8, 758311.

Choi, H., Miller, M. R., Nguyen, H. N., Surratt, V. E., Koch, S. R., Stark, R. J., & Lamb, F. S. (2023). Extracellular SOD modulates canonical TNFα signaling and α5β1 integrin transactivation in vascular smooth muscle cells. Free radical biology & medicine, 209(Pt 1), 152–164.

Chu, B., Li, M., Cao, X., Li, R., Jin, S., Yang, H., Xu, L., Wang, P., & Bi, J. (2021). IRE1α-XBP1 Affects the Mitochondrial Function of Aβ25-35-Treated SH-SY5Y Cells by Regulating Mitochondria-Associated Endoplasmic Reticulum Membranes. Frontiers in cellular neuroscience, 15, 614556.

Coleman OI, Haller D. ER Stress and the UPR in Shaping Intestinal Tissue Homeostasis and Immunity. Front Immunol. 2019;10:2825. Published 2019 Dec 4.

Colla, E., Coune, P., Liu, Y., Pletnikova, O., Troncoso, J. C., Iwatsubo, T., Schneider, B. L., & Lee, M. K. (2012). Endoplasmic reticulum stress is important for the manifestations of α-synucleinopathy in vivo. The Journal of neuroscience: the official journal of the Society for Neuroscience, 32(10), 3306–3320.

Costa, R. O., Lacor, P. N., Ferreira, I. L., Resende, R., Auberson, Y. P., Klein, W. L., Oliveira, C. R., Rego, A. C., & Pereira, C. M. (2012). Endoplasmic reticulum stress occurs downstream of GluN2B subunit of N-methyl-d-aspartate receptor in mature hippocampal cultures treated with amyloid-β oligomers. Aging cell, 11(5), 823–833.

D'Amico, D., Sorrentino, V. & Auwerx, J. Cytosolic Proteostasis Networks of the Mitochondrial Stress Response. Trends Biochem Sci. 42, 712–725 (2017).

Da Silva, A. S. R., da Luz, C. M., Marafon, B. B., Tavares, M. E. A., Neto, I. V. S., Gomes Carolino, R. O., da Silva Ferreira, D. C., Marinho, J. T., Teixeira, G. R., Cintra, D. E., Pauli, J. R., Ropelle, E. R., de Freitas, E. C., & Pinto, A. P. (2025). Interleukin-6 modulates endoplasmic reticulum stress signaling and mitochondrial protein complexes in the kidney following acute exhaustive exercise. Cell stress & chaperones, 30(5), 100111.

Di Conza G, Ho PC. ER Stress Responses: An Emerging Modulator for Innate Immunity. Cells. 2020;9(3):695. Published 2020 Mar 12.

Duran-Aniotz, C., Cornejo, V. H., Espinoza, S., Ardiles, Á. O., Medinas, D. B., Salazar, C., Foley, A., Gajardo, I., Thielen, P., Iwawaki, T., Scheper, W., Soto, C., Palacios, A. G., Hoozemans, J. J. M., & Hetz, C. (2017). IRE1 signaling exacerbates Alzheimer's disease pathogenesis. Acta neuropathologica, 134(3), 489–506.

Eckford, P. D., Ramjeesingh, M., Molinski, S., Pasyk, S., Dekkers, J. F., Li, C., Ahmadi, S., Ip, W., Chung, T. E., Du, K., Yeger, H., Beekman, J., Gonska, T., & Bear, C. E. (2014). VX-809 and related corrector compounds exhibit secondary activity stabilizing active F508del-CFTR after its partial rescue to the cell surface. Chemistry & biology, 21(5), 666–678.

Egawa, N., Yamamoto, K., Inoue, H., Hikawa, R., Nishi, K., Mori, K., & Takahashi, R. (2011). The endoplasmic reticulum stress sensor, ATF6α, protects against neurotoxin-induced dopaminergic neuronal death. The Journal of biological chemistry, 286(10), 7947–7957.

Ekshyyan, O., & Aw, T. Y. (2004). Apoptosis: a key in neurodegenerative disorders. Current neurovascular research, 1(4), 355–371.

Ellgaard, L., McCaul, N., Chatsisvili, A., & Bra20man, I. (2016). Co- and Post-Translational Protein Folding in the ER. Traffic (Copenhagen, Denmark), 17(6), 615–638.

Erekat N. S. (2022). Apoptosis and its therapeutic implications in neurodegenerative diseases. Clinical anatomy (New York, N.Y.), 35(1), 65–78.

Esmaeili, Y., Yarjanli, Z., Pakniya, F., Bidram, E., Łos, M. J., Eshraghi, M., Klionsky, D. J., Ghavami, S., & Zarrabi, A. (2022). Targeting autophagy, oxidative stress, and ER stress for neurodegenerative disease treatment. Journal of controlled release: official journal of the Controlled Release Society, 345, 147–175.

Fan Y, Simmen T. Mechanistic Connections between Endoplasmic Reticulum (ER) Redox Control and Mitochondrial Metabolism. Cells. 2019;8(9):1071. Published 2019 Sep 12.

Farrell, P., Férec, C., Macek, M., Frischer, T., Renner, S., Riss, K., Barton, D., Repetto, T., Tzetis, M., Giteau, K., Duno, M., Rogers, M., Levy, H., Sahbatou, M., Fichou, Y., Le Maréchal, C., & Génin, E. (2018). Estimating the age of p.(Phe508del) with family studies of geographically distinct European populations and the early spread of cystic fibrosis. European journal of human genetics: EJHG, 26(12), 1832–1839.

Fernandes T, Domingues MR, Moreira PI, Pereira CF. A Perspective on the Link between Mitochondria-Associated Membranes (MAMs) and Lipid Droplets Metabolism in Neurodegenerative Diseases. Biology (Basel). 2023;12(3):414. Published 2023 Mar 8.

Fiedorczuk, K., & Chen, J. (2022). Molecular structures reveal synergistic rescue of Δ508 CFTR by Trikafta modulators. Science (New York, N.Y.), 378(6617), 284–290.

Filadi R., Greotti E., Pizzo P. Highlighting the endoplasmic reticulum-mitochondria connection: Focus on Mitofusin 2. Pharmacol. Res. 2018;128:42–51.

Friedman JR, Voeltz GK. 2011. The ER in 3D: a multifunctional dynamic membrane network. Trends Cell Biol. 21:709–17

Frisoni GB, Altomare D, Thal DR, et al. The probabilistic model of Alzheimer disease: the amyloid hypothesis revised. Nat Rev Neurosci. 2022;23(1):53-66.

Fusakio ME, Willy JA, Wang Y, et al. Transcription factor ATF4 directs basal and stress-induced gene expression in the unfolded protein response and cholesterol metabolism in the liver. Mol Biol Cell. 2016; 27(9): 1536-1551

Gami-Patel, P., van Dijken, I., Meeter, L. H., Melhem, S., Morrema, T. H. J., Scheper, W., van Swieten, J. C., Rozemuller, A. J. M., Dijkstra, A. A., & Hoozemans, J. J. M. (2021). Unfolded protein response activation in C9orf72 frontotemporal dementia is associated with dipeptide pathology and granulovacuolar degeneration in granule cells. Brain pathology (Zurich, Switzerland), 31(1), 163–173.

Ghadge, G. D., Sonobe, Y., Camarena, A., Drigotas, C., Rigo, F., Ling, K. K., & Roos, R. P. (2020). Knockdown of GADD34 in neonatal mutant SOD1 mice ameliorates ALS. Neurobiology of disease, 136, 104702.

Ghemrawi, R., & Khair, M. (2020). Endoplasmic Reticulum Stress and Unfolded Protein Response in Neurodegenerative Diseases. International journal of molecular sciences, 21(17), 6127.

Ghemrawi, R., Kremesh, S., Mousa, W. K., & Khair, M. (2025). The Role of ER Stress and the Unfolded Protein Response in Cancer. Cancer genomics & proteomics, 22(3), 363–381.

Giacomello, M., Pyakurel, A., Glytsou, C. & Scorrano, L. The cell biology of mitochondrial membrane dynamics. Nat. Rev. Mol. Cell Biol. 21, 204–224 (2020).

Goldsteins G, Hakosalo V, Jaronen M, Keuters MH, Lehtonen Š, Koistinaho J. CNS Redox Homeostasis and Dysfunction in Neurodegenerative Diseases. Antioxidants (Basel). 2022;11(2):405. Published 2022 Feb 16.

Gordaliza-Alaguero, I., Cantó, C., & Zorzano, A. (2019). Metabolic implications of organelle-mitochondria communication. EMBO reports, 20(9), e47928.

Goyal R, Wilson K, Saharan A, Gautam RK, Chopra H, Gupta S, et al. Insights on aspects of apoptosis in neurodegenerative disorders: a comprehensive review. Explor Med. 2024;5:89–100.

Grassmann, S., Kim, H., Friedrich, C., Pujol, M., Fan, S., Zhang, J., Beroshvili, G., Buchholz, V. R., Gasteiger, G., & Sun, J. C. (2025). STAT3 operates as an inflammation-dependent transcriptional switch. bioRxiv: the preprint server for biology, 2025.09.26.678857.

Green, D. M., Lahiri, T., Raraigh, K. S., Ruiz, F., Spano, J., Antos, N., Bonitz, L., Christon, L., Gregoire-Bottex, M., Hale, J. E., Langfelder-Schwind, E., La Parra Perez, Á., Maguiness, K., Massie, J., McElroy-Barker, E., McGarry, M. E., Mercier, A., Munck, A., Oliver, K. E., Self, S.,Ren, C. L. (2024). Cystic Fibrosis Foundation Evidence-Based Guideline for the Management of CRMS/CFSPID. Pediatrics, 153(5), e2023064657.

Gundu, C., Arruri, V. K., Sherkhane, B., Khatri, D. K., & Singh, S. B. (2024). Indole-3-propionic acid attenuates high glucose induced ER stress response and augments mitochondrial function by modulating PERK-IRE1-ATF4-CHOP signalling in experimental diabetic neuropathy. Archives of physiology and biochemistry, 130(3), 243–256.

Hanahan D. (2022). Hallmarks of Cancer: New Dimensions. Cancer discovery, 12(1), 31–46.

Hartl F. U. (2017). Protein Misfolding Diseases. Annual review of biochemistry, 86, 21–26.

Hasan, S.-A.-M., James, A. W., Fazili, F. M., Tarabishi, S., Sheikh, N. M., & Shah, Z. A. (2024). Endoplasmic Reticulum Stress in Neurodegenerative Diseases. Journal of Dementia and Alzheimer's Disease, 1(2), 87-97.

Hasnain, S.Z.; Lourie, R.; Das, I.; Chen, A.C.; McGuckin, M.A. The interplay between endoplasmic reticulum stress and inflammation. Immunol. Cell Biol. 2012, 90, 260–270

He, L., Kota, P., Aleksandrov, A. A., Cui, L., Jensen, T., Dokholyan, N. V., & Riordan, J. R. (2013). Correctors of ΔF508 CFTR restore global conformational maturation without thermally stabilizing the mutant protein. FASEB journal: official publication of the Federation of American Societies for Experimental Biology, 27(2), 536–545.

Hernansanz-Agustín P, Enríquez JA. Generation of Reactive Oxygen Species by Mitochondria. Antioxidants (Basel). 2021;10(3):415. Published 2021 Mar 9.

Hetz, C., Zhang, K., & Kaufman, R. J. (2020). Mechanisms, regulation and functions of the unfolded protein response. Nature reviews. Molecular cell biology, 21(8), 421–438.

Hitomi J, Katayama T, Eguchi Y, et al. Involvement of caspase-4 in endoplasmic reticulum stress-induced apoptosis and Abeta-induced cell death. J Cell Biol. 2004;165(3):347-356.

Huang, C. F., Liu, S. H., Su, C. C., Fang, K. M., Yen, C. C., Yang, C. Y., Tang, F. C., Liu, J. M., Wu, C. C., Lee, K. I., & Chen, Y. W. (2021). Roles of ERK/Akt signals in mitochondria-dependent and endoplasmic reticulum stress-triggered neuronal cell apoptosis induced by 4-methyl-2,4-bis(4-hydroxyphenyl)pent-1-ene, a major active metabolite of bisphenol A. Toxicology, 455, 152764.

Huang, M., & Xin, W. (2018). Matrine inhibiting pancreatic cells epithelial-mesenchymal transition and invasion through ROS/NF-κB/MMPs pathway. Life sciences, 192, 55–61.

Hung V, Lam SS, Udeshi ND, et al. Proteomic mapping of cytosol-facing outer mitochondrial and ER membranes in living human cells by proximity biotinylation. Elife. 2017;6:e24463. Published 2017 Apr 25.

Hwang, T. C., Yeh, J. T., Zhang, J., Yu, Y. C., Yeh, H. I., & Destefano, S. (2018). Structural mechanisms of CFTR function and dysfunction. The Journal of general physiology, 150(4), 539–570.

Im, J., Hillenaar, T., Yeoh, H. Y., Sahasrabudhe, P., Mijnders, M., van Willigen, M., Hagos, A., de Mattos, E., van der Sluijs, P., & Braakman, I. (2023). ABC-transporter CFTR folds with high fidelity through a modular, stepwise pathway. Cellular and molecular life sciences: CMLS, 80(1), 33.

Jha, M. K., & Morrison, B. M. (2018). Glia-neuron energy metabolism in health and diseases: New insights into the role of nervous system metabolic transporters. Experimental neurology, 309, 23–31.

Jia Z, Li H, Xu K, et al. MAM-mediated mitophagy and endoplasmic reticulum stress: the hidden regulators of ischemic stroke. Front Cell Neurosci. 2024;18:1470144. Published 2024 Nov 21.

Jill, N., Bhootra, S., Kannanthodi, S., Shanmugam, G., Rakshit, S., Rajak, R., Thakkar, V., & Sarkar, K. (2023). Interplay between signal transducers and activators of transcription (STAT) proteins and cancer: involvement, therapeutic and prognostic perspective. Clinical and experimental medicine, 23(8), 4323–4339.

Kaltschmidt, B.; Linker, R.A.; Deng, J.; Kaltschmidt, C. Cyclooxygenase-2 is a neuronal target gene of NF-kappaB. BMC Mol. Biol. 2002, 3, 16

Kim Chiaw, P., Wellhauser, L., Huan, L. J., Ramjeesingh, M., & Bear, C. E. (2010). A chemical corrector modifies the channel function of F508del-CFTR. Molecular pharmacology, 78(3), 411–418.

Kim, S., Kim, D. K., Jeong, S., & Lee, J. (2022). The Common Cellular Events in the Neurodegenerative Diseases and the Associated Role of Endoplasmic Reticulum Stress. International journal of molecular sciences, 23(11), 5894.

Kopp MC, Larburu N, Durairaj V, Adams CJ, Ali MMU. UPR proteins IRE1 and PERK switch BiP from chaperone to ER stress sensor. Nat Struct Mol Biol. 2019 Nov;26(11):1053-1062. Epub 2019 Nov 6. PMID: 31695187; PMCID: PMC6858872.

Koszła, O., & Sołek, P. (2024). Misfolding and aggregation in neurodegenerative diseases: protein quality control machinery as potential therapeutic clearance pathways. Cell communication and signaling: CCS, 22(1), 421.

Kumar, V., & Maity, S. (2021). ER Stress-Sensor Proteins and ER-Mitochondrial Crosstalk-Signaling Beyond (ER) Stress Response. Biomolecules, 11(2), 173.

Kurekova, S.; Pavlikova, L.; Seres, M.; Bohacova, V.; Spaldova, J.; Breier, A.; Sulova, Z. Do wolframin, P-glycoprotein, and

Lahiri, A., Sims, S. G., Herstine, J. A., Meyer, A., Marshall, M. J., Jahan, I., Adhicary, S., Bradbury, A. M., & Meares, G. P. (2025). Endoplasmic Reticulum Stress Amplifies Cytokine Responses in Astrocytes via a PERK/eIF2α/JAK1 Signaling Axis. Glia, 73(11), 2273–2288.

Lakshmanan, U., & Porter, A. G. (2007). Caspase-4 interacts with TNF receptor-associated factor 6 and mediates lipopolysaccharide-induced NF-kappaB-dependent production of IL-8 and CC chemokine ligand 4 (macrophage-inflammatory protein-1 ). Journal of immunology (Baltimore, Md.: 1950), 179(12), 8480–8490.

Lee, K. H., Cha, M., & Lee, B. H. (2020). Neuroprotective Effect of Antioxidants in the Brain. International journal of molecular sciences, 21(19), 7152.

Li, R. L., Wang, L. Y., Duan, H. X., Zhang, Q., Guo, X., Wu, C., & Peng, W. (2022). Regulation of mitochondrial dysfunction induced cell apoptosis is a potential therapeutic strategy for herbal medicine to treat neurodegenerative diseases. Frontiers in pharmacology, 13, 937289.

Liang, C., Guo, L., Tian, X., Mu, Z., Chen, M., Hu, Y., & Su, J. (2025). The interaction between COX-2 and endoplasmic reticulum stress is involved in liver ischemia-reperfusion injury in mice. Molecular biology reports, 52(1), 710.

Lin JH, Walter P, Yen TS. Endoplasmic reticulum stress in disease pathogenesis. Annu Rev Pathol. 2008;3:399-425.

Lin, Y., Zhang, C., Xiang, P., Shen, J., Sun, W., & Yu, H. (2020). Exosomes derived from HeLa cells break down vascular integrity by triggering endoplasmic reticulum stress in endothelial cells. Journal of extracellular vesicles, 9(1), 1722385.

Liu F, Chang L, Hu J. Activating transcription factor 6 regulated cell growth, migration and inhibiteds cell apoptosis and autophagy via MAPK pathway in cervical cancer. J Reprod Immunol. 2020;139:103120.

Liu, Y., Xu, C., Gu, R., Han, R., Li, Z., & Xu, X. (2024). Endoplasmic reticulum stress in diseases. MedComm, 5(9), e701.

Longo, F., Mancini, M., Ibraheem, P. L., Aryal, S., Mesini, C., Patel, J. C., Penhos, E., Rahman, N., Mamcarz, M., Santini, E., Rice, M. E., & Klann, E. (2021). Cell-type-specific disruption of PERK-eIF2α signaling in dopaminergic neurons alters motor and cognitive function. Molecular psychiatry, 26(11), 6427–6450.

Loo, T. W., Bartlett, M. C., & Clarke, D. M. (2013). Corrector VX-809 stabilizes the first transmembrane domain of CFTR. Biochemical pharmacology, 86(5), 612–619.

Ma K, Chen G, Li W, Kepp O, Zhu Y, Chen Q. Mitophagy, Mitochondrial Homeostasis, and Cell Fate. Front Cell Dev Biol. 2020;8:467. Published 2020 Jun 24.

Magrinelli, F., Mehta, S., Di Lazzaro, G., Latorre, A., Edwards, M. J., Balint, B., Basu, P., Kobylecki, C., Groppa, S., Hegde, A., Mulroy, E., Estevez-Fraga, C., Arora, A., Kumar, H., Schneider, S. A., Lewis, P. A., Jaunmuktane, Z., Revesz, T., Gandhi, S., Wood, N. W., … Bhatia, K. P. (2022). Dissecting the Phenotype and Genotype of PLA2G6-Related Parkinsonism. Movement disorders: official journal of the Movement Disorder Society, 37(1), 148–161.

Mao, H., Chen, W., Chen, L., & Li, L. (2022). Potential role of mitochondria-associated endoplasmic reticulum membrane proteins in diseases. Biochemical pharmacology, 199, 115011.

Martucciello S, Masullo M, Cerulli A, Piacente S. Natural Products Targeting ER Stress, and the Functional Link to Mitochondria. Int J Mol Sci. 2020;21(6):1905. Published 2020 Mar 11.

McDonald, E. F., Meiler, J., & Plate, L. (2023). CFTR Folding: From Structure and Proteostasis to Cystic Fibrosis Personalized Medicine. ACS chemical biology, 18(10), 2128–2143.

Meares GP, Liu Y, Rajbhandari R, Qin H, Nozell SE, Mobley JA, et al. PERK-dependent activation of JAK1 and STAT3 contributes to endoplasmic reticulum stress-induced inflammation. Mol Cell Biol. 2014;34:3911–25

Mercado, G., Castillo, V., Soto, P., & Sidhu, A. (2016). ER stress and Parkinson's disease: Pathological inputs that converge into the secretory pathway. Brain research, 1648(Pt B), 626–632.

Modesti L, Danese A, Angela Maria Vitto V, et al. Mitochondrial Ca2+ Signaling in Health, Disease and Therapy. Cells. 2021;10(6):1317. Published 2021 May 25.

Molenaars, M. et al. A Conserved Mito-Cytosolic Translational Balance Links Two Longevity Pathways. Cell Metab. 31, 549–563.e547 (2020).

Moore, P. J., & Tarran, R. (2018). The epithelial sodium channel (ENaC) as a therapeutic target for cystic fibrosis lung disease. Expert opinion on therapeutic targets, 22(8), 687–701.

Moreno, J. A., Halliday, M., Molloy, C., Radford, H., Verity, N., Axten, J. M., Ortori, C. A., Willis, A. E., Fischer, P. M., Barrett, D. A., & Mallucci, G. R. (2013). Oral treatment targeting the unfolded protein response prevents neurodegeneration and clinical disease in prion-infected mice. Science translational medicine, 5(206), 206ra138.

Mori K. (2024). Elucidation of molecular mechanism of the unfolded protein response. The Keio journal of medicine, 73(1), 13.

Morretta, E., A. D'Agostino, E. Cassese, B. Maglione, A. Petrella, C. Schiraldi, M.C. Monti, 2022. Label-free quantitative proteomics to explore the action mechanism of the pharmaceutical-grade Triticum vulgare extract in speeding up keratinocyte healing. Molecules 27, 1108.

Moujalled, D., Strasser, A. Liddell, J.R. 2021. Molecular mechanisms of cell death in neurological diseases. Cell Death Differ. 28, 2029–2044.

Naranjo, J. R., Zhang, H., Villar, D., González, P., Dopazo, X. M., Morón-Oset, J., Higueras, E., Oliveros, J. C., Arrabal, M. D., Prieto, A., Cercós, P., González, T., De la Cruz, A., Casado-Vela, J., Rábano, A., Valenzuela, C., Gutierrez-Rodriguez, M., Li, J. Y., & Mellström, B. (2016). Activating transcription factor 6 derepression mediates neuroprotection in Huntington disease. The Journal of clinical investigation, 126(2), 627–638.

Nguyen, T. T., Wei, S., Nguyen, T. H., Jo, Y., Zhang, Y., Park, W., Gariani, K., Oh, C. M., Kim, H. H., Ha, K. T., Park, K. S., Park, R., Lee, I. K., Shong, M., Houtkooper, R. H., & Ryu, D. (2023). Mitochondria-associated programmed cell death as a therapeutic target for age-related disease. Experimental & molecular medicine, 55(8), 1595–1619.

Okiyoneda, T., Veit, G., Dekkers, J. F., Bagdany, M., Soya, N., Xu, H., Roldan, A., Verkman, A. S., Kurth, M., Simon, A., Hegedus, T., Beekman, J. M., & Lukacs, G. L. (2013). Mechanism-based corrector combination restores ΔF508-CFTR folding and function. Nature chemical biology, 9(7), 444–454.

Panayi, G. S., & Corrigall, V. M. (2006). BiP regulates autoimmune inflammation and tissue damage. Autoimmunity reviews, 5(2), 140–142.

Pecoraro M, Franceschelli S, Pascale M. Lumacaftor and Matrine: Possible Therapeutic Combination to Counteract the Inflammatory Process in Cystic Fibrosis. Biomolecules. 2021;11(3):422. Published 2021 Mar 13.

Peng SY, Tang JY, Lan TH, et al. Oxidative-Stress-Mediated ER Stress Is Involved in Regulating Manoalide-Induced Antiproliferation in Oral Cancer Cells. Int J Mol Sci. 2023;24(4):3987. Published 2023 Feb 16.

Perez, J.M.; Chirieleison, S.M.; Abbott, D.W. An IκB Kinase-Regulated Feedforward Circuit Prolongs Inflammation. Cell Rep. 2015, 12, 537–544.

Perkins HT, Allan V. Intertwined and Finely Balanced: Endoplasmic Reticulum Morphology, Dynamics, Function, and Diseases. Cells. 2021 Sep 7;10(9):2341. PMID: 34571990; PMCID: PMC8472773.

Phillips, B. P., Gomez-Navarro, N., & Miller, E. A. (2020). Protein quality control in the endoplasmic reticulum. Current opinion in cell biology, 65, 96–102.

Preissler, S., & Ron, D. (2019). Early Events in the Endoplasmic Reticulum Unfolded Protein Response. Cold Spring Harbor perspectives in biology, 11(4), a033894.

Regard L, Martin C, Burnet E, Da Silva J, Burgel PR. CFTR Modulators in People with Cystic Fibrosis: Real-World Evidence in France. Cells. 2022;11(11):1769. Published 2022 May 28.

Saint-Martin Willer, A., Montani, D., Capuano, V., & Antigny, F. (2024). Orai1/STIMs modulators in pulmonary vascular diseases. Cell calcium, 121, 102892.

Sammels, E., Parys, J. B., Missiaen, L., De Smedt, H., & Bultynck, G. (2010). Intracellular Ca2+ storage in health and disease: a dynamic equilibrium. Cell calcium, 47(4), 297–314.

Sassano ML, Felipe-Abrio B, Agostinis P. ER-mitochondria contact sites; a multifaceted factory for Ca2+ signaling and lipid transport. Front Cell Dev Biol. 2022;10:988014. Published 2022 Aug 16.

Schrank, S., Barrington, N., & Stutzmann, G. E. (2020). Calcium-Handling Defects and Neurodegenerative Disease. Cold Spring Harbor perspectives in biology, 12(7), a035212.

Scorrano L, De Matteis MA, Emr S, et al. Coming together to define membrane contact sites. Nat Commun. 2019;10(1):1287. Published 2019 Mar 20.

Sehgal P, Szalai P, Olesen C, et al. Inhibition of the sarco/endoplasmic reticulum (ER) Ca2+-ATPase by thapsigargin analogs induces cell death via ER Ca2+ depletion and the unfolded protein response. J Biol Chem. 2017;292(48):19656-19673.

Sen, T., Gupta, R., Kaiser, H., & Sen, N. (2017). Activation of PERK Elicits Memory Impairment through Inactivation of CREB and Downregulation of PSD95 After Traumatic Brain Injury. The Journal of neuroscience: the official journal of the Society for Neuroscience, 37(24), 5900–5911.

Sharma, J.N.; Al-Omran, A.; Parvathy, S.S. Role of nitric oxide in inflammatory diseases. Inflammopharmacology 2007, 15, 252–259.

Shen, N.; Wang, Z.; Wang, C.; Zhang, J.; Liu, C. Methane Alleviates Inflammation and Apoptosis of Dextran Sulfate Sodium-Induced Inflammatory Bowel Diseases by Inhibiting Toll-Like Receptor 4 (TLR4)/Myeloid Differentiation Factor 88 (MyD88)/Nuclear Translocation of Nuclear Factor-κB (NF-κB) and Endoplasmic Reticulum Stress Pathways in Mice. Med. Sci. Monit. 2020, 26, e922248.

Sheng, W., Wang, G., Tang, J., Shi, X., Cao, R., Sun, J., Lin, Y. H., Jia, C., Chen, C., Zhou, J., & Dong, M. (2020). Calreticulin promotes EMT in pancreatic cancer via mediating Ca2+ dependent acute and chronic endoplasmic reticulum stress. Journal of experimental & clinical cancer research: CR, 39(1), 209.

Shi, M., Chai, Y., Zhang, J., & Chen, X. (2022). Endoplasmic Reticulum Stress-Associated Neuronal Death and Innate Immune Response in Neurological Diseases. Frontiers in immunology, 12, 794580.

Shiga, Y., Rangel Olguin, A. G., El Hajji, S., Belforte, N., Quintero, H., Dotigny, F., Alarcon-Martinez, L., Krishnaswamy, A., & Di Polo, A. (2024). Endoplasmic reticulum stress-related deficits in calcium clearance promote neuronal dysfunction that is prevented by SERCA2 gene augmentation. Cell reports. Medicine, 5(12), 101839.

Shimano, H., & Sato, R. (2017). SREBP-regulated lipid metabolism: convergent physiology - divergent pathophysiology. Nature reviews. Endocrinology, 13(12), 710–730.

Simpson DSA, Oliver PL. ROS Generation in Microglia: Understanding Oxidative Stress and Inflammation in Neurodegenerative Disease. Antioxidants (Basel). 2020;9(8):743. Published 2020 Aug 13.

Singh, R., Kaur, N., Choubey, V., Dhingra, N., & Kaur, T. (2024). Endoplasmic reticulum stress and its role in various neurodegenerative diseases. Brain research, 1826, 148742.

Siwecka, N., Rozpędek-Kamińska, W., Wawrzynkiewicz, A., Pytel, D., Diehl, J. A., & Majsterek, I. (2021). The Structure, Activation and Signaling of IRE1 and Its Role in Determining Cell Fate. Biomedicines, 9(2), 156.

Solt, L.A.; May, M.J. The IkappaB kinase complex: Master regulator of NF-kappaB signaling. Immunol. Res. 2008, 42, 3–18

Sonninen, T.M.; Goldsteins, G.; Laham-Karam, N.; Koistinaho, J.; Lehtonen, Š. Proteostasis Disturbances and Inflammation in Neurodegenerative Diseases. Cells 2020, 9, 2183

Soto C, Pritzkow S. Protein misfolding, aggregation, and conformational strains in neurodegenerative diseases. Nat Neurosci. 2018;21(10):1332-1340.

Torres M, Castillo K, Armisén R, Stutzin A, Soto C, Hetz C. Prion protein misfolding affects calcium homeostasis and sensitizes cells to endoplasmic reticulum stress. PLoS One. 2010;5(12):e15658. Published 2010 Dec 29.

Valdés, P., Mercado, G., Vidal, R. L., Molina, C., Parsons, G., Court, F. A., Martinez, A., Galleguillos, D., Armentano, D., Schneider, B. L., & Hetz, C. (2014). Control of dopaminergic neuron survival by the unfolded protein response transcription factor XBP1. Proceedings of the National Academy of Sciences of the United States of America, 111(18), 6804–6809.

Van Goor, F., Hadida, S., Grootenhuis, P. D., Burton, B., Stack, J. H., Straley, K. S., Decker, C. J., Miller, M., McCartney, J., Olson, E. R., Wine, J. J., Frizzell, R. A., Ashlock, M., & Negulescu, P. A. (2011). Correction of the F508del-CFTR protein processing defect in vitro by the investigational drug VX-809. Proceedings of the National Academy of Sciences of the United States of America, 108(46), 18843–18848.

Van Goor, F., Straley, K. S., Cao, D., González, J., Hadida, S., Hazlewood, A., Joubran, J., Knapp, T., Makings, L. R., Miller, M., Neuberger, T., Olson, E., Panchenko, V., Rader, J., Singh, A., Stack, J. H., Tung, R., Grootenhuis, P. D., & Negulescu, P. (2006). Rescue of DeltaF508-CFTR trafficking and gating in human cystic fibrosis airway primary cultures by small molecules. American journal of physiology. Lung cellular and molecular physiology, 290(6), L1117–L1130.

Veit, G., Da Fonte, D. F., Avramescu, R. G., Premchandar, A., Bagdany, M., Xu, H., Bensinger, D., Stubba, D., Schmidt, B., Matouk, E., & Lukacs, G. L. (2020). Mutation-specific dual potentiators maximize rescue of CFTR gating mutants. Journal of cystic fibrosis: official journal of the European Cystic Fibrosis Society, 19(2), 236–244.

Veit, G., Roldan, A., Hancock, M. A., Da Fonte, D. F., Xu, H., Hussein, M., Frenkiel, S., Matouk, E., Velkov, T., & Lukacs, G. L. (2020). Allosteric folding correction of F508del and rare CFTR mutants by elexacaftor-tezacaftor-ivacaftor (Trikafta) combination. JCI insight, 5(18), e139983.

W, F., Schmid, J., Düssmann, H., Concannon, C. G., & Prehn, J. H. (2015). Imaging of single cell responses to ER stress indicates that the relative dynamics of IRE1/XBP1 and PERK/ATF4 signalling rather than a switch between signalling branches determine cell survival. Cell death and differentiation, 22(9), 1502–1516.

Walter NS, Gorki V, Bhardwaj R, Punnakkal P. Endoplasmic Reticulum Stress: Implications in Diseases. Protein J. 2025 Apr;44(2):147-161. Epub 2025 Mar 13. PMID: 40082380.

Wang F, Liu DZ, Xu H, et al. Thapsigargin induces apoptosis by impairing cytoskeleton dynamics in human lung adenocarcinoma cells. ScientificWorldJournal. 2014;2014:619050. Published 2014 Jan 28.

Wang, B., Zhao, Z., Xiong, M., Yan, R., & Xu, K. (2022). The endoplasmic reticulum adopts two distinct tubule forms. Proceedings of the National Academy of Sciences of the United States of America, 119(18), e2117559119.

Wang, L., Popko, B., & Roos, R. P. (2014). An enhanced integrated stress response ameliorates mutant SOD1-induced ALS. Human molecular genetics, 23(10), 2629–2638.

Wang, W. A., Agellon, L. B., & Michalak, M. (2019). Organellar Calcium Handling in the Cellular Reticular Network. Cold Spring Harbor perspectives in biology, 11(12), a038265.

Wang, X., Tse, C., & Singh, A. (2025). Discovery and Development of CFTR Modulators for the Treatment of Cystic Fibrosis. Journal of medicinal chemistry, 68(3), 2255–2300.

Wang, Z., Jiao, P., Zhong, Y., Ji, H., Zhang, Y., Song, H., Du, H., Ding, X., & Wu, H. (2022). The Endoplasmic Reticulum-Stressed Head and Neck Squamous Cell Carcinoma Cells Induced Exosomal miR-424-5p Inhibits Angiogenesis and Migration of Humanumbilical Vein Endothelial Cells Through LAMC1-Mediated Wnt/β-Catenin Signaling Pathway. Cell transplantation, 31, 9636897221083549.

Wang, Z., Li, Q., Kolls, B. J., Mace, B., Yu, S., Li, X., Liu, W., Chaparro, E., Shen, Y., Dang, L., Del Águila, Á., Bernstock, J. D., Johnson, K. R., Yao, J., Wetsel, W. C., Moore, S. D., Turner, D. A., & Yang, W. (2023). Sustained overexpression of spliced X-box-binding protein-1 in neurons leads to spontaneous seizures and sudden death in mice. Communications biology, 6(1), 252.

Watanabe, S., & Yamanaka, K. (2025). Mitochondria and Endoplasmic Reticulum Contact Site as a Regulator of Proteostatic Stress Responses in Neurodegenerative Diseases. BioEssays: news and reviews in molecular, cellular and developmental biology, 47(7), e70016.

Wu H, Carvalho P, Voeltz GK. Here, there, and everywhere: The importance of ER membrane contact sites. Science. 2018;361(6401):eaan5835.

Wu, C. H., Silvers, C. R., Messing, E. M., & Lee, Y. F. (2019). Bladder cancer extracellular vesicles drive tumorigenesis by inducing the unfolded protein response in endoplasmic reticulum of nonmalignant cells. The Journal of biological chemistry, 294(9), 3207–3218.

Xu X, Pang Y, Fan X. Mitochondria in oxidative stress, inflammation and aging: from mechanisms to therapeutic advances. Signal Transduct Target Ther. 2025;10(1):190. Published 2025 Jun 11.

Yan, C., Liu, J., Gao, J., Sun, Y., Zhang, L., Song, H., Xue, L., Zhan, L., Gao, G., Ke, Z., Liu, Y., & Liu, J. (2019). IRE1 promotes neurodegeneration through autophagy-dependent neuron death in the Drosophila model of Parkinson's disease. Cell death & disease, 10(11), 800.

Zhang IX, Raghavan M, Satin LS. The Endoplasmic Reticulum and Calcium Homeostasis in Pancreatic Beta Cells. Endocrinology. 2020;161(2):bqz028.

Zhang, W., Shi, Y., Oyang, L., Cui, S., Li, S., Li, J., Liu, L., Li, Y., Peng, M., Tan, S., Xia, L., Lin, J., Xu, X., Wu, N., Peng, Q., Tang, Y., Luo, X., Liao, Q., Jiang, X., & Zhou, Y. (2024). Endoplasmic reticulum stress-a key guardian in cancer. Cell death discovery, 10(1), 343.

Zhang, Y., Yang, X., Qiu, C., Liu, F., Liu, P., & Liu, Z. (2018). Matrine suppresses AGE-induced HAEC injury by inhibiting ROS-mediated NRLP3 inflammasome activation. European journal of pharmacology, 822, 207–211.

Zhang, Z., Liu, F., & Chen, J. (2018). Molecular structure of the ATP-bound, phosphorylated human CFTR. Proceedings of the National Academy of Sciences of the United States of America, 115(50), 12757–12762.

Zhao Y, Wang Y, Zhang L, Wang W, Fahey TJ, Yao K. BRAF inhibition promotes ER stress-mediated cell death in uveal melanoma. Neoplasma. 2022;69:1070–8.

Zhao, N., Cao, J., Xu, L., Tang, Q., Dobrolecki, L. E., Lv, X., Talukdar, M., Lu, Y., Wang, X., Hu, D. Z., Shi, Q., Xiang, Y., Wang, Y., Liu, X., Bu, W., Jiang, Y., Li, M., Gong, Y., Sun, Z., Ying, H., … Chen, X. (2018). Pharmacological targeting of MYC-regulated IRE1/XBP1 pathway suppresses MYC-driven breast cancer. The Journal of clinical investigation, 128(4), 1283–1299.

Zhao, R. Z., Jiang, S., Zhang, L., & Yu, Z. B. (2019). Mitochondrial electron transport chain, ROS generation and uncoupling (Review). International journal of molecular medicine, 44(1), 3–15.

Zhao, R., Lv, Y., Feng, T., Zhang, R., Ge, L., Pan, J., Han, B., Song, G., & Wang, L. (2022). ATF6α promotes prostate cancer progression by enhancing PLA2G4A-mediated arachidonic acid metabolism and protecting tumor cells against ferroptosis. The Prostate, 82(5), 617–629.

Zhu, P., Li, T., Li, Q., Gu, Y., Shu, Y., Hu, K., Chen, L., Peng, X., Peng, J., & Hao, L. (2022). Mechanism and Role of Endoplasmic Reticulum Stress in Osteosarcoma. Biomolecules, 12(12), 1882.

Zimmermann, J.S.M.; Linxweiler, J.; Radosa, J.C.; Linxweiler, M.; Zimmermann, R. The endoplasmic reticulum membrane protein Sec62 as potential therapeutic target in SEC62 overexpressing tumors. Front. Physiol. 2022, 13, 1014271

Zou, L., Collins, H. E., Young, M. E., Zhang, J., Wende, A. R., Darley-Usmar, V. M., & Chatham, J. C. (2021). The Identification of a Novel Calcium-Dependent Link Between NAD+ and Glucose Deprivation-Induced Increases in Protein O-GlcNAcylation and ER Stress. Frontiers in molecular biosciences, 8, 780865.